DYNAMICS OF A SINGLE-PHASE SQUARE NATURAL CIRCULATION LOOP SUBJECTED TO AN EXTERNAL PULSATING POWER INPUT

Thesis Submitted in Partial Fulfilment of the Requirements for the Degree of

MASTER OF NUCLEAR ENGINEERING

By

ARNAB GHOSH MAZUMDER

UNIVERSITY REGISTRATION NUMBER: 141074 OF 2017-2018

EXAMINATION ROLL NUMBER: M4NUE19013

UNDER THE SUPERVISION OF

PROF. ACHINTYA MUKHOPADHYAY

DEPARTMENT OF MECHANICAL ENGINEERING

JADAVPUR UNIVERSITY

KOLKATA 700032

SCHOOL OF NUCLEAR STUDIES & APPLICATION

FACULTY OF INTERDISCIPLINARY STUDIES, LAW AND MANAGEMENT

JADAVPUR UNIVERSITY

KOLKATA 700032

MAY 2019

JADAVPUR UNIVERSITY

FACULTY OF INTERDISCIPLINARY STUDIES, LAW AND MANAGEMENT

SCHOOL OF NUCLEAR STUDIES AND APPLICATION

CERTIFICATE OF RECOMMENDATION

*This is to certify that the thesis entitled "***Dynamics of a single-phase square Natural Circulation Loop subjected to an external pulsating power input***", which is being submitted by* ***Arnab Ghosh Mazumder*** *in partial fulfilment of the requirements for the award of the degree of "****Master of Nuclear Engineering"*** *at the School of Nuclear Studies and Application, Jadavpur University, Kolkata 700032, during the academic year 2018-2019, is the record of the student's own work carried out by him under our supervision.*

Thesis Guide
Prof. Achintya Mukhopadhyay
Department of Mechanical Engineering
Jadavpur University, Kolkata 700032

Prof. (Dr.) Amitava Gupta
Director
School of Nuclear Studies and Application
Jadavpur University Kolkata 700032

Dr. Pankaj Kumar Roy
Dean
Faculty of Interdisciplinary Studies,
Law and Management
Jadavpur University Kolkata700032

JADAVPUR UNIVERSITY

FACULTY OF INTERDISCIPLINARY STUDIES, LAW AND MANAGEMENT

SCHOOL OF NUCLEAR STUDIES AND APPLICATION

CERTIFICATE OF APPROVAL

*The foregoing thesis entitled "***Dynamics of a single-phase square Natural Circulation Loop subjected to an external pulsating power input***" is hereby approved as a credible study of an engineering subject carried out and presented in a satisfactory manner to warrant its acceptance as a prerequisite for the degree of "****Master of Nuclear Engineering"*** *at the School of Nuclear Studies and Application, Jadavpur University, Kolkata 700032, for which it has been submitted. It is understood that by this approval the undersigned do not necessarily endorse or approve any statement made, opinion expressed or conclusion drawn there in but approve the thesis only for the purpose for which it is submitted.*

Committee on Final Examination
For Evaluation of the Thesis

Signature of Examiners

*Only in case the recommendation is concurred in

JADAVPUR UNIVERSITY

FACULTY OF INTERDISCIPLINARY STUDIES, LAW AND MANAGEMENT

SCHOOL OF NUCLEAR STUDIES AND APPLICATION

DECLARATION OF ORIGINALITY AND COMPLIANCE OF ACADEMIC ETHICS

*It is hereby declared that the thesis entitled "***Dynamics of a single-phase square Natural Circulation Loop subjected to an external pulsating power input***" contains literature survey and original research work by the undersigned candidate, as part of his degree of "**Master of Nuclear Engineering"** at the School of Nuclear Studies and Application, Jadavpur University, Kolkata 700032.*

All information in this document has been obtained and presented in accordance with academic rules and ethical conduct.

It is also declared that all materials and results, not original to this work have been fully cited and referred throughout this thesis, according to rules of ethical conduct.

Name: **ARNAB GHOSH MAZUMDER**

Registration Number: 141074 of 2017-2018

Examination Roll Number: M4NUE19013

Dated: 29-05-2019

(Signature)

ARNAB GHOSH MAZUMDER

Master of Nuclear Engineering

School of Nuclear Studies and Application

Jadavpur University, Kolkata700032

ACKNOWLEDGEMENT

I am deeply grateful to my guide Prof. Achintya Mukhopadhyay for his unparalleled support and guidance, which has helped me in the successful completion of this thesis. Without his wise and valuable advice it wouldn't have been possible to prepare this thesis successfully.

I would also like to thank Prof. (Dr.) Amitava Gupta, Director, School of Nuclear Studies and Applications, Jadavpur University, without, whose initiative and support, it would not have been possible to carry out the project.

I am also thankful to all the faculty of Project Neptune Lab of Mechanical Engineering department Jadavpur University for their sincere support during the preparation of the work.

I would also like to express my profound gratitude to Dr. Sirshendu Mondal, Assistant Professor, Dept. of Mechanical Engineering, National Institute of Technology Durgapur with whom I had the privilege to work with during my thesis. His guidance and suggestions have proved to be highly resourceful.

I also owe my deepest gratitude to Ritabrata Saha, Priyankan Datta and Somnath De, PhD scholars of Mechanical Engineering department Jadavpur University and o all my wonderful classmates of Nuclear engineering department for their regular help in completing this thesis.

Finally, I would like to thank my mother and my sister and everyone in my family for their constant support and encouragement throughout my journey and helping me completing this thesis.

Dt: 29-05-2019 ARNAB GHOSH MAZUMDER

ABSTRACT

The Natural Circulation Loop (NCL) plays an important role as a modern and efficient heat extraction mechanism in numerous new age engineering applications one of which is in the nuclear energy industry. A single-phase natural circulation system, under constant heater power, exhibits various dynamical states such as steady, periodic and chaotic behaviour with increasing level of heater power. In the present study, a systematic investigation on the effect of a time-dependent fluctuating power on a single-phase square NCL has been done. To that end, numerical simulations have been carried out on a MATLAB based Simulink model of a single phase square NCL. In the model, a sinusoidal oscillation of the heater power is implemented over a range of forcing frequencies and amplitudes on the system in order to study the effect of the fluctuating power on the response dynamics of the system. It has been observed under the current study that the application of the pulsating power influences the dynamics of the NCL at specified values of amplitude and frequency in accordance with the principles of synchronization of two pulsating oscillators.

CONTENTS

LIST OF FIGURES

NOMENCLATURE

A	Area of cross section (m^2)
C_p	Specific heat of fluid at constant pressure (J/kg K)
C_{pex}	Specific heat of coolant at constant pressure (J/kg K)
C_{pw}	Specific heat of wall material (J/kg K)
d_{in}	Internal loop diameter (mm)
dz	Increment in length (m)
f_{in}	Friction factor
Gr	Grashof number
h_i	Heat transfer coefficient between fluid and wall (W/m^2K)
h_o	Heat transfer coefficient between wall and surrounding (W/m^2K)
h_{rad}	Radiation heat transfer coefficient (W/m^2K)
h_{hex}	Heat transfer coefficient between wall and coolant (W/m^2K)
k_f	Thermal conductivity of fluid (W/mK)
k_w	Thermal conductivity of wall (W/mK)
k_{hex}	Thermal conductivity of heat exchanger (W/mK)
L_{loop}	Total loop length (m)
Re_d	Reynold's number
Nu	Nusselt number
Pr	Prandlt number
P	Power (W)
Ra	Rayleigh number
t	Time (s)
T_a	Ambient temperature (°C)
T_f	Fluid temperature (°C)
T_w	Wall temperature (°C)

T_{hex}	Coolant temperature (°C)
T_{ref}	Reference temperature (°C)
v_f	Fluid velocity (m/s)
V_w	Wall volume (m^3)
V_{hex}	Heat exchanger fluid volume (m^3)
B_{av}	Thermal volumetric expansion coefficient (K^{-1})
ε	emissivity
μ_f	Dynamic viscosity of fluid (kg/ms)
ν_f	Kinematic viscosity of fluid (m^2/s)
ν_{hex}	Kinematic viscosity of coolant (m^2/s)
ρ_f	Fluid density (kg/m^3)
ρ_w	Density of wall material (kg/m^3)
ρ_{hex}	Coolant density (kg/m^3)
σ	Stefan-Boltzmann constant (W/m^2K^{-4})
f_n	Natural frequency of system

INTRODUCTION CHAPTER 1

Natural circulation system are considered to be one of the most important and attractive options of the heat extraction mechanism in various thermal engineering applications like solar water heaters, cooling of gas turbine blades, internal combustion engines and nuclear reactor core, transformer cooling geothermal power extraction and several others.

The natural circulation loop (NCL) primarily works by the combined effects of buoyancy and frictional forces acting within the working fluid by exploiting the density gradient established within the working fluid. A study by Misale [1] presents a detailed overview on the physical working principles of a single phase NCL. In general, a natural circulation system predominantly consists of a heat source, a heat sink and connecting pipes through which the heated and cooled fluid flows. The fluid flow in the system starts spontaneously under the action of gravitational body force when the heat source is turned on. A time lag exists between the switching on of the heat source and the initiation of the fluid flow. This is equal to the time taken by the system to achieve the minimum density difference within the hotter and cooler sections of the fluid required for the buoyancy forces to start working and establish the mass flow. If the operating conditions of the heater and the sink and also the ambient conditions are kept constant, then a stable flow of the fluid within the loop can be achieved.

Due to the uneven heating and cooling, we get a density variation between the two vertical arms of the loop. This results in a hydrostatic pressure difference within the system due to to the buoyant forces developed. If for example ρ_A and ρ_B are the values of density achieved within the riser and the downcomer of the loop where ($\rho_B > \rho_A$), the hydrostatic pressure difference between the point A and point B of the loop, as shown in Fig:1, would be

$$P = gH(\rho_B - \rho_A).$$

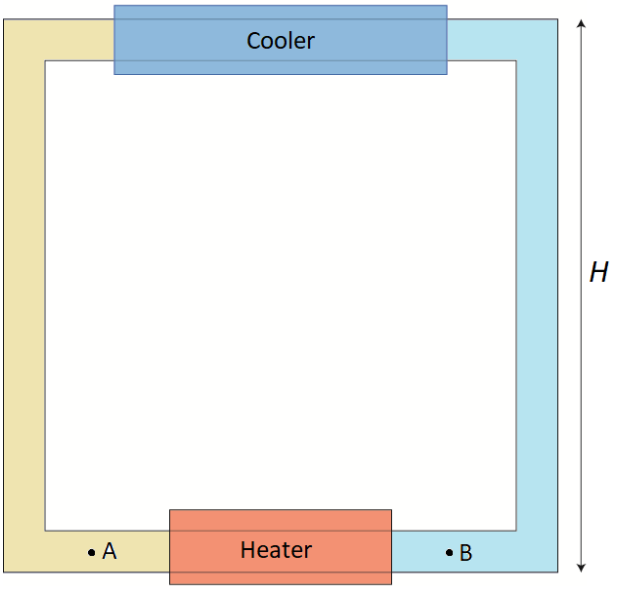

Figure 1: *A Natural Circulation Loop*

At steady state, the pressure difference would be balance by acceleration and frictional forces within the system and can be approximated as

$$gH(\rho_B - \rho_A) = \frac{R(mf)^2}{2\rho}$$

Where *R* denotes the frictional resistance and *mf* denotes the mass flow rate.

This shows that, as the heat supplied in increased, the density difference of the fluid $(\rho_B - \rho_A)$ increases which inturn leads to higher mass flow rate of the fluid within the loop. Hence the flow rate is dependant on the heat supplied and also on the loop height *H*.

Therefore, the heat source placed at the lower arm of the loop heats the fluid thereby making it less dense which rises up due to the action of the buoyant forces and the heat exchanger placed at a higher elevation cools the fluid and the denser cooler fluid moves down the loop and the combined effect of the pressure difference between the two vertical arms and the internal frictional forces maintain a stable flow within the loop. This motion helps to extract heat from a source placed at a lower elevation in a continuous manner without

The elimination of any kind of intervention mechanical or electrical feedback device from the cycle of heat extraction in order to safely shut down the reactor in an

event of an emergency has made NCLs much more reliable and safer than the conventional methods of reactor cooling system and emergency core cooling system of nuclear reactors. Post Three Miles island incident era NCLs have always been encouraged be a suggestive alternative due to their inbred and improved passive safety. Thus natural circulation systems has gained a lot of popularity in applications as a passive safety system. The absence of mechanical or electrical components from safety systems have made them much simpler and robust in nature and have reduced operation and maintenance cost as well.

In the nuclear industry, an extensive use of natural circulation systems is found in Pressurized Water Reactors, Pressurized Heavy Water Reactors, and VVERs and are commonly employed in steam generators of ratings around 1000 MW_t or higher. Removal of decay heat, which is one of the major challenges in nuclear reactor operation also uses NCL and also for cooling of post-accident containment and radioactive waste storage facilities. Nuclear reactors continue to produce heat even after being shut down due to radioactive fission product decay and the removal of this heat is crucial to maintain the fuel temperature within safety limits for the safe operation of a nuclear power plant. Thus application of NCL in shut down heat removal systems is also very common in recent days. Use of NCL in nuclear or fossil-fuelled power plants have seen the elimination of maldistribution of pressure causing unequal flow in the parallel heated channels due to the usage of pumps. In forced circulation, there is a requirement for variable speed drives because of the fact that the steam production rate are not constant. However, using NCL allows the system to operate with non-uniform power distribution without causing critical heat flux. Finally, since NCL operates on natural physical laws, the chances of it to fail like mechanically driven fluid is negligible and so it is able to provide a continuous uninterrupted flow for which it is actively used as back up for removal of decay heat in the event of pumping power failure.

However, the absence of any external signal operated the mechanism to control the flow rate of the fluid results in the formation of instabilities within the loop It has been observed that since the entire fluid flow depends on the forces developed within the fluid, the loop is susceptible to various instabilities due to changes in operating parameters. These instabilities, as compared to forced circulation, are more unstable because of low driving force and non-linear behaviour of natural convection within the

fluid. Even in cases where a stable flow is expected, the fact that the buoyancy and frictional forces are not coherent or in phase with each other will cause oscillatory motion of the flow due to any disturbance in the driving force which in turn will affect the driving force itself. Hence due to the strong interdependency between the flow and the driving force, a regenerative feedback is imminent in the mechanism, which results in the instabilities. The thermal hydraulic behaviours which can be observed in a single phase NCL include stable behaviour, where across the heat sink there is steady temperature difference, neutral stable where the temperature difference across the heat sink oscillates without amplification, neutral unstable where the temperature difference oscillation across the heat sink occurs in both positive and negative without amplification, and unstable where temperature difference across the heater is amplified and the loop dynamics experiences flow reversals.

The instabilities with the natural circulation system depends on the relation between the friction within the loop and the buoyancy forces generated due to density variation. Any change in flow rate of the system in steady motion is opposed by viscous and thermal dissipation. An increase in heat supplied results in increase in the flow rate due to higher density difference within the fluid. However higher flow rates lead to increase in friction which reduces the overall effect of the buoyancy forces thereby reducing mass flow rate. These two opposing effects often are not in phase and eventually result in oscillations in the flow due to overpassing each other.

Sometimes a localized region of hot fluid might appear from the heated section due to thermal disturbances which can be hotter than the normal steady state temperature of the system. This hot pocket, while rising to a higher elevation through the hot leg of the loop, accelerates the flow due to large buoyancy force acting on it. A reverse phenomenon occurs when a relatively cooler pocket of fluid emerges from the heater. As it rises along the hot leg and descends along the cold leg, the flow rate decelerates and the even hotter localized pockets of fluid emerge from the heat source and colder pockets of fluid from the cooler as they get more time to exchange heat at their respective heat source and sink due to reduced flow rate. This results in a oscillatory motion within the loop. This periodic effect amplifies with every passing cycle till the point the buoyant forces cause a flow reversal within the loop. The same phenomena repeats in the reverse direction of flow causing the flow to reverse its flow

directions repeatedly in clockwise or anti-clockwise direction. Thus the creation of localized pockets of hot and cold fluid is the main cause for flow oscillations in NCL.

Such problems also find their way when natural circulation system is applied as the heat extraction mechanism of a system. There are several challenges in the application of NCL specifically in the nuclear industry. The operating parameters in a nuclear power plant are so crucial that addressing the problems of NCL often becomes very challenging. One of its major drawbacks is its low driving force. The only way to increase driving force is increasing the loop height which might result in a clumsy and uneconomic design and susceptible to accidents. Hence the maximum working height of a natural circulation system is limited to 10 m. These systems also face the challenge of obtaining low system pressure loss. The only simple way to reduce pressure losses is to increase the diameter of working components however, in doing so would make the system transients sluggish and also add to the overall construction and maintenance cost. Apart from the above problems natural circulation systems are inherently prone to instabilities as those discussed above which makes the functioning even more challenging.

Despite such challenges, researchers and engineers are hoping to improve the shortcomings and drawbacks in the operation and uses of NCL in its various applications. Over the course of years, NCL has been a subject of investigation and study to try and understand its fundamentals and behaviour under various operating conditions and parameters.

Seyyadi et al. [2] carried out an experimental numerical and investigation of a single-phase rectangular NCL with asymmetric heater position. They considered heater to be located at a distance equally from both left and right vertical arms, in other words, a centrally placed heater in the loop, especially in the experimental setup. A horizontal heater and a horizontal cooler rectangular single-phase NCL with asymmetric heater position both was investigated both experimentally and numerically, at different heater power and loop inclination angles. It was observed that on increasing the inclination angle, there was a rise in the average loop temperature heater power was increased and the rate of rising of Reynold's number was reduced thereby indicating that with increase in the angle of inclination of the loop, the flow characteristics of the working fluid was tending towards laminar flow. Along with that, the reduction in the modified Grashof number and increase in the value of the modified Stanton number with the increase in

inclination angle indicated a reduction in buoyant forces operating within the fluid and enhancement in the performance of the heat exchanger of the loop respectively.

A study by Wu et al. [3] was conducted on a flow resistance performance of the single-phase NCL with necessary verification by experiments. The study focussed on the innovative resistance flow, considering the effect of the frictional resistance and local resistance in the NCL and the analytical relations between the NCL mass flow rate and the heating power and the temperature rise of the heating section and the heating power were all obtained by using the approximation and fitting approach. The study showed the flow rate heating power characteristic number has a close relationship with the flow regime and the flow resistance in the NCL. It is the function of Reynold's number and the ratio of the local pressure loss coefficient and friction coefficient and decreased with the increase of friction coefficient of the system.

An investigation of the numerical and analytical models based on data obtained from experiments was conducted by Luzzi et al. [4]. In this study, a numerical and semi-analytical model namely Object-Oriented (O-O) one-dimensional model and a three-dimensional Computational Fluid Dynamics (CFD) model are developed by the authors to study the behaviour of the natural convection dynamics against data collected from a single phase NCL setup using water as the operating fluid.

Vijayan et al. [5] developed a non-loop specific scaling laws by using a simple one-dimensional theory and compared it with experimental results of three NCLs of rectangular orientation. The basis of the analysis was on simple assumptions like viscous heating, negligible axial conduction effects and heat loss and compressible liquid. It was found for a case, the model and prototype use similar fluid in both the secondary as well as the primary side of the heat exchanger. It was concluded that the scaling laws of power to volume, used in the study accurately replicates the steady-state behaviour and the modified Stanton number and loop diameter significantly affects the transient and stability behaviour. Therefore the scaled test facilities which are made on the basis of scaling principles of power to volume do not necessarily replicate the prototype plant's expected stability behaviour expected in. A two-point effect on the stability behaviour of loop diameter is also concluded in the study. It directly stabilizes the natural circulation flow due to increase in the value of the ratio of length to diameter ratio and indirectly due to its effect in increasing the value of modified Stanton number.

An investigation by Vijayan et al. [6] was done on a generalized flow equation for single-phase NCLs following multiple friction laws. The enlisted generalized flow equations for single-phase NCL which existed was only applicable for a single friction law where the entire flow would be either laminar or turbulent not addressing partially laminar or partially turbulent flow. The proposed steady-state flow equation for a single-phase NCL was formulated on a one-dimensional theory by considering the fluid flow to be partly laminar and partly turbulent. The results were tested against experimental data obtained from four orientations with Horizontal Heater and Horizontal Cooler (HHHC), Horizontal Heater and Vertical Cooler (HHVC), Vertical Heater and Horizontal Cooler (VHHC), Vertical Heater and Vertical Cooler (VHVC) and was found that the same general correlation is in agreement with all given orientations.

A study on the response of the dynamics of a single phase rectangular NCL to various excitations of input power was done by Basu et. al. [7]. The study focuses on the transient behaviour of NCLs when subjected to convective cooling and direct heat supply where three basic signals with step, ramp and exponential profiles are applied to the input power increase and decrease. The results showed that step and exponential signal input contributed to instability during increase in applied power due to the involuntary nature of the transition and the system took a high amount of time to reach steady state for the power to decrease to a stable state after a step change. For a continuous power supply change, the system dynamics with time gradient of increasing nature was found to have better performance while the exponential profile showed inferior performance as compared to the stepped increase in power due to the sharp gradient in the initial stages of transition.

The effects of geometric operating parameters on the steady performance of a single-phase NCL with loss of heat to the surrounding was investigated in a study by Basu et al. [8]. The study aimed to develop a theoretical model to replicate the steady-state functioning of a rectangular single-phase NCL to study the role of different geometric conditions on the behaviour of the dynamics of the system. The system is considered as an associated problem with the wall interacting with loop fluid, cooling stream and surrounding along with different parts of the loop. The overall outcome of the study indicated that having loops with small height and small diameter achieved higher effectiveness although the given conditions result in reduced flow rate. Having

longer heater length increases the heat transfer between the walls to fluid and avoids rapid alterations in rate of fluid flow during fluctuations. Uninsulated parts of the loop in the horizontal arms have no other use other than increasing the surface area exposed to heat loss to the surroundings and must be kept as minimum as possible and using highly conductive wall material decreases the temperature gradient within the fluid thereby increasing the loop effectiveness due to increased heat transfer on coolant side.

The existence of dynamical regions of the mass flow behaviour of a single-phase NCL was established by Saha et.al. [9] in a study conducting the classification of the nature of the dynamics of a single phase square NCL. The study concludes that the flow characteristics of the mass flow of the loop can be categorized into steady, oscillating with periodic oscillations and chaotic flow regime with flow reversal achieved by varying the heater power which provided valuable insight for the current study.

An investigation on the ability of heat removal depending on various orientations of a single phase NCL based on Entransy dissipation method was done by Talebi et. al. [10]. The Entransy dissipation study is known to be a very efficient way to calculate the heat transfer capacity of such systems. The investigation on stability of the system was done by non-linear study of stability and an attempt was done to improve the performance of a rectangular single-phase NCL and repeated by changing the cooler and heat source alignment. The effect of diameter of the loop, and the dimensions of the heat source and cooler and also the amount of heat supplied was studied based on the Entransy dissipation and also the heat extraction capability of the various alignment of the loops.

Cheng et al. [11] used a simple mathematical model of a single phase NCL having fluids for heating and cooling purposed to study the nature of heat transfer of the model. The loop used water as the primary and the secondary. It was observed that the modified Grashof number, Reynold's number and rate of transfer of heat increased as the operating temperature of the system was increased. An existence of laminar flow in the system was established based on the value of the Reynold's number and the increase in the heat transfer rate and Reynold's number was observed with increment in the diameter of the loop.

Misale [12] conducted a study based on experiments to determine the significance of stepped input of power on the performance of a single-phase natural circulation system. The study also includes the investigation of the amplitude of stepped power and also the periodic oscillations of the system. The power applied to the loop varied from 500 W to 3000 W with amplitude of steps equal to 20% or 50%. The tests showed a chaotic nature for both steady and time-varying power with amplitude and frequency of the periodic nature of the systems increased with increment in applied power.

A simulation to study the unstable nature of a single phase NCL circulation with reiterative reversal of flows in a rectangular loop was done by Vijayan et al. [13]. Loops of rectangular orientation having with differing diameter were experimentally studied to establish that the one with the greatest diameter showed the highest instabilities and repeated flow reversals with erratic frequency of occurrence with increase in power. The Reynold's number varied from a range of +10000 to -10000 owing to the reversal in flow dynamics which made the flow to go through laminar and turbulent behaviour in repetition. However, the computer simulation done using ATHLET code failed to show instabilities in the system under course nodalisation whereas on gradually refining the nodal structure revealed the instabilities in its behaviour and all other characteristic nature observed in the experiments.

MOTIVATION

NCL fundamentally is a highly efficient mechanism for heat extraction from a heat source without the help of any external agents, solely depending on the natural forces and dynamics of the system due to variation in heating and orientation of the loop structure. This has made it very popular in various engineering applications due to its inherent simplicity and advantages.

However, the challenges faced while working with NCL is also known and so researchers have embarked on several studies and investigation to understand the dynamics of NCL systems in a better manner. A characteristic problem with natural circulation systems is the existence of instabilities which result in fluctuations in mass flow resulting in a periodic oscillations and also flow reversal during extreme operating conditions leading to a chaotic behaviour of the system.

Oscillatory motion or flow reversal are both detrimental to the smooth working of the loop and must be minimised as much as possible. This study is motivated by an attempt to understand the periodic oscillatory behaviour of the natural circulation dynamics when subjected to an external periodic oscillator and to see if such an action sheds some light on how these systems behave when faced with unwanted external fluctuations within the operating parameter or even into the uncharted possibilities of controlling these oscillations via external forcing influence to reduce or control them as per requirement.

OBJECTIVE

This study is an attempt to analyse the effect of a time-dependent fluctuating heater power on the dynamics of a single phase square NCL. A MATLAB based Simulink model of a single phase square shaped NCL, developed previously by Saha et al [8] and the non-linear dynamics of the mass flux of the system when subjected to the power perturbation, is studied. The variation in the nature of the mass flux of the loop under the different operating parameters of the pulsating power presents a detailed view of the way the dynamics of a single phase NCL behave. The power applied to the loop is sinusoidal in nature and is applied in addition to a base power of the heater with variation in the frequency and the amplitude of the pulsating power.

The MATLAB based Simulink model used for the current study was previously developed by Saha et al. [8] for numerical and experimental study of a single phase square NCL. The model is modified for the current study to accommodate the pulsating sinusoidal power source of the heater and to include the effects of heat transfer to the surroundings due to radiation heat transfer.

NUMERICAL MODELLING CHAPTER 2

In the present study, we have considered a natural circulation system as an oscillator when subjected to a specific range of input power. This system is subjected to an external pulsating power input of sinusoidal nature and the both these two oscillators are expected to interact with each other in accordance with the principle of synchronization.

An oscillator is an active system and contains a sustained energy source which is transformed into an oscillatory motion with a characteristic natural frequency of the system. If isolated, the oscillator continues to exhibit a constant periodic behaviour until the source of energy expires. The nature and features of the oscillations is determined by the operating parameters of the system. When such an oscillator is subjected to an external perturbation, the later influences the dynamics of the oscillator and we see a departure from its natural behaviour. This effect is seen mainly manifested by a change in the frequency and amplitude of the system. The oscillator often tends to synchronize itself with the external perturbation when the forcing parameters reach optimum values due to their weak interactions.

Synchronization is one of the most rudimentary phenomena associated with oscillations. It is the direct and most common consequence of the interaction of various systems with each other. In general terms synchronization means that different systems influence each other to adjust their time scales of oscillations however, there is a large variety of its visible actualization. Synchronization phenomenon in a large group of coupled systems often manifests themselves as collective coherent systems appearing via the non-equilibrium phase transition.

Forced synchronization focuses on the fact that one system engages another system but the former system does not experience any influence from the former system in return. One system readjusts its own frequency and amplitude due to the influence of the other system instead of both the systems changing their dynamics mutually together which is the case in mutual synchronization.

It has been observed that for a given magnitude of forcing amplitude, the frequency of the driven oscillator is dependent on the detuning or the difference

between the frequencies of the two oscillators. For sufficiently minor detuning, the external action engages and modifies the phase of the other oscillator so that the frequency of the driven oscillator is ultimately equal to the frequency of the driving system. The onset of a certain relationship where the natural state frequency of the driven self-sustained oscillator is modified by the external signal to a condition of equal operating frequency between the systems is referred to as phase locking. The synchrony in phase locking is a result of either systematic phase advancement or ascent, or phase retardation of the self-sustained oscillation as a result of the action of the external forcing oscillator on it. For example, if the natural frequency of the driven oscillator is greater than the forcing external frequency during synchronism, the external force, will slow down the self-sustained oscillation by reducing the internal rate of phase change of the oscillator by means of periodic phase detainment. The reverse happens in case of the forcing external frequency being higher than the natural frequency of the driven system, where the frequency of the latter would have to be moved up.

If the frequencies f_2 and f_1 of two oscillators are commensurate or proportional over some range of control parameter values, that is if $f_2 / f_1 = p / q$ (p and q integers) over this parameter range, then we can say that the two oscillators are frequency locked or equivalently, mode-locked or phase locked. One frequency is locked into being a rational number multiple of the other frequency. For a non-linear oscillator, in general, the actual oscillation frequency depends on the oscillator's amplitude of motion. Thus, under normal conditions, we would expect the frequency of a non-linear oscillator to change if some parameter of the system changes, because this change in parameter will cause the amplitude of the oscillation to change. On this account, we might expect that a very precise setting of parameter values is required to get a particular frequency ratio, say p / q. However, in frequency locking the same ratio p / q holds over some range of parameter value.

For a set of parameter values, the temporal behaviour of an oscillator can be characterized by a Fourier series of sinusoidal oscillation. For oscillator number 1 we can write

$$x_1(t) = \sum_{k=1}^{\infty} B_k \sin(2\pi k f_1 t + \phi_k)$$

Where k is a positive integer. B_k is the amplitude associated with the harmonic kf_1 and $_k$ is the phase for that frequency. The crucial point here is that the motion can be thought of as being made up of periodic motion with frequencies $2f_1$, $3f_1$ and so on and amplitudes B_1, B_2, B_3 etc. Similarly, oscillator 2 can be described as

$$x_2(t) = \sum_{j=1}^{\infty} C_j \sin\left(2\pi j f_2 t + \psi_j\right)$$

Now if the two frequencies f_1 and f_2 are commensurate with the frequency ratio $f_2/f_1 = p / q$, then the p th harmonic of f_1, that is $p\ f_1$ is the same as the qth of f_2. Since these two oscillators are interacting, this equality means that the q th harmonic of f_2 can interfere with the motion associated with the pth harmonic of f_1 to generate a kind of resonance effect. If $q\ f_2 = p\ f_1$, then there will be an infinite number of overlapping frequencies with $n\ q\ f_2 = n\ p\ f_1$ and n=1,2,3… If the frequencies were incommensurate or incoherent, then none of the harmonics would coincide and the mutual resonance would not occur. These notions allow us to say that frequency locking occurs whenever the resonance interaction of harmonics due to nonlinearities, win out over the tendency of the oscillators' frequencies to change. Based on this, we would expect that as one of the frequencies is changed, say f_1, which might be the frequency of the oscillator driving the system, with the strength of the nonlinearities, held fixed, the frequencies would lock for some range of f_1 values, but then would either unlock (become incommensurate) or jump to another integer ratio for the new value of f_1.

Apart from synchronicity, two interacting oscillators also influence each other in other ways. When external oscillation with a forcing frequency f_1 is applied to an oscillator with the internal frequency f_2, no interaction between the two oscillations take place if f_1 is much lower than f_2. But when f_1 approaches f_2, the latter is pulled towards the former because of a non-linear interaction between both oscillators. So the oscillator now oscillates with a corrected internal frequency f_2' instead of f_2 or $f_1<f_2'<f_2$ or $f_1>f_2'>f_2$. Integer multiples of $|f_2'-f_1|$ appear in the spectrum near f_2' and also amplitude modification on the time scale of $1/|f_2'-f_1|$ can be observed. This is known as frequency pulling which is a universal feature of a forced oscillator. Frequency pulling tends to reduce $|f_1-f_2|$ resulting in a proportionate reduction in the beating frequency.

Another classic feature of forced self-excited flows is that when the forcing amplitude is insufficient to cause total synchronization and when f_1 is incoherent with

f_2, that is when the two frequencies are not rational multiples of each other, the system simultaneously oscillates at multiple different frequencies. This behaviour is known as quasiperiodicity. Quasiperiodicity appears as sharp peaks at linear combinations of f_1 and f_2 in the frequency spectrum

The quasiperiodic scenario involves competition between two or more independent frequencies characterizing the dynamics of the system. Quasiperiodicity is often shown by a non-linear system with a natural frequency, driven by an external periodic force. Now as explained earlier, if individual frequencies of two oscillators, f_1 and f_2 have the ratio equal to p/q where p and q are two integers, then we can say the frequencies are commensurate or in other words, the frequency ratio is rational. If there are no integers which satisfy the given condition, then the frequencies are incommensurate or, equivalently the frequency ratio is irrational. If the ratio is rational then we can conclude that the system's behaviour is periodic. However, if the ratio is irrational, then we say the behaviour is quasiperiodic in nature. The term quasiperiodic is used to describe the behaviour when the two frequencies are incommensurate because in such a case, the system's behaviour never exactly repeats itself and the temporal behaviour of a quasiperiodic system can look quite irregular in nature.

Several study on the synchronous behaviour of multiple oscillators have been done previously by several researchers. A study on the experiments and modelling of quasiperiodic behaviour and phase locking in hydro-dynamically self-excited flames was done by Li et al. [14] where an acoustic forcing is applied to a spectrum of jet diffusion flames. The flames have regions of instability near their bases and hence, oscillations are observed at discrete natural frequencies and around these frequencies, at different amplitudes, the forcing oscillator is applied and the response tending to phase locked condition is measured.

Dewan et al. [15] conducted a study on asynchronous quenching harmonic engagement of Van der Pol oscillations and phase locking. It showed that there are three physically different ways which can cause synchronism which are termed as phase locking, passive and active asynchronous quenching. The purpose was to show the mentioned physical interpretation and to derive a basis of distinguishing the three above mentioned processes. It was concluded that phase locking occurs when self-sustained oscillations stay during entrainment and are detected by the saddle point effect on the transients during the obtainment or recovery from phase perturbation. The two forms

of asynchronous quenching result from the powerful force driving effects which eliminates the self-sustained oscillation or reducing it substantially.

Cercek et al. [16] conducted a study on non-linear dynamics of instability in front of a positively biased electrode in a magnetized plasma. Here, non-linear dynamics of instability that is triggered by a positive electrode in a weakly magnetized discharge plasma column is studied. Two characteristics non-linear phenomenon which is synchronization and frequency pulling or periodic pulling are demonstrated and explained by the model of Van der Pol oscillator.

Guan et al. [17] conducted low order modelling along with experiments in a synchronous framework on open loop control of periodic thermoacoustic oscillation. In this study, the authors examined the nature of synchronization of a laminar conical premixed flame in a tube combustor under the influence of a periodic acoustic forcing by experiments and compared the response of this forced oscillating system with that of Duffing-Van der Pol oscillator under forcing. This study has three main conclusions which are, that it demonstrates that studying open loop control from a synchronization viewpoint can give important insight into the best effective forcing conditions and also shows that for weak thermoacoustic oscillations, the most effective forcing condition is that which causes lock-in via a torus death bifurcation as it is most favourable for asynchronous quenching. Lastly, it also demonstrates that the dynamics of synchronization of a real combustor can be qualitatively simulated with a low order universal oscillator.

Murugesan et al. [18] published a study on a hydro-dynamically self-excited jet's complex network investigation under forcing synchronization. In this study, a complex network is used to study and predict the two ways to establish synchronization in a prototype self-excited flow of a low-density jet of axisymmetric orientation, at a working condition close to its first Hopf point using visible algorithm and recurrence condition. It was found that the assortativity coefficient, indicates by which to differentiate between Saddle node and Torus death routes to synchronization. The topological features for creating the networks with recurrence conditions, varied between two routes to synchronization. Finally, this study established that the routes to synchronization can be differentiated using complex networks.

Guan et al. [19] conducted a study on the effects of external forcing on self-excited thermoacoustic oscillator and strange non-chaotic and chaotic attractors within. The synchronization dynamics beyond the phase locking condition of a self-excited thermoacoustic system was studied via experiments. Periodic acoustic forcing was applied to the system consisting of a laminar premixed flame within a tube combustor. On the increment of forcing amplitude above that required for phase locking, it was seen that the system moves out of phase locking and enter into chaos. The study sheds light on the fact that when an attempt is made to regulate periodic thermoacoustic oscillations with the help of external periodic forcing, the forcing frequency must be carefully selected along with the forcing amplitude.

A study on the periodic and non-periodic thermoacoustic oscillation on lock-in under forced synchronization, bifurcation and open loop control was done by Kashinath et al. [20] The study aims to investigate the effect harmonic acoustic forcing of open loop on three types of thermoacoustic oscillations of self-excited nature which are chaotic, quasi-periodic and periodic in nature to represent the synchronization dynamics leading up to and above lock-in, including scrutinizing the bifurcation that causes lock-in and lastly to explore the accessibility of operating open loop forcing to weaken non-periodic thermoacoustic oscillations. The study establishes that the exacting forcing amplitude needed for lock-in is dependent on the fact if the forcing frequency is beyond or less the natural self-excited frequency and the proximity of the forcing frequency with the natural frequency. At particular values of forcing frequencies, even weak forcing is enough to reduce the strength of the self-excited oscillations to amplitudes value almost 90% less than that if the system is not forced. Also, it may be possible to reduce the strength of non-periodic thermoacoustic oscillations by carefully choosing the two forcing frequencies and amplitude, applied sequentially.

An experimental and theoretical investigation was done by Mondal et al. [21] to study the nature of interaction of a thermoacoustic system's oscillatory mode with external harmonic excitation by varying the excitation amplitude along with the forcing frequency. The synchronization states between the external signal and the response dynamics were identified and maximum suppression in amplitude of the response dynamics were recorded.

GOVERNING EQUATIONS

The model of a single phase square shaped NCL under investigation in this given study is developed using MATLAB based Simulink platform. The continuity and the mass momentum along with the energy equation for the entire loop is solved considering the following assumptions

1. Any variation in operating parameters or property of the loop is neglected in the radial direction.
2. The density variation, in case of the loop momentum equation, is only considered for the body force term, in accordance with the Boussinesq approximation.
3. Appropriate correlation for pressure drop due to friction and heat transfer correlation is used for determining the heat transfer coefficient for wall to loop fluid and wall to air heat transfer.
4. Pressure loss at pipe bends is considered to be negligible.
5. The viscous dissipation term in the energy equation has been neglected.
6. Loss of heat from the tube wall to the surroundings in the form of radiation heat is considered in evaluating the energy equation for the tube walls.
7. Constant property of the wall material.

The total length of the square loop under investigation is 4000 mm long with the loop height and width equal to 1000 mm each. The heater section, placed at the lower horizontal arm of the loop is taken to be 400 mm in length with 300 mm of the non-heater section on either side consisting of tube walls. The heat exchanger or the cooler is situated at the upper horizontal arm of the loop and is 600 mm long with 200 mm of the tube wall on either side. The loop's internal diameter is equal to 30 mm with a thickness of 1 mm and the external diameter is equal to 32 mm. Apart from that, the diameter of the heat exchanger placed at the cooler section is equal to 50 mm.

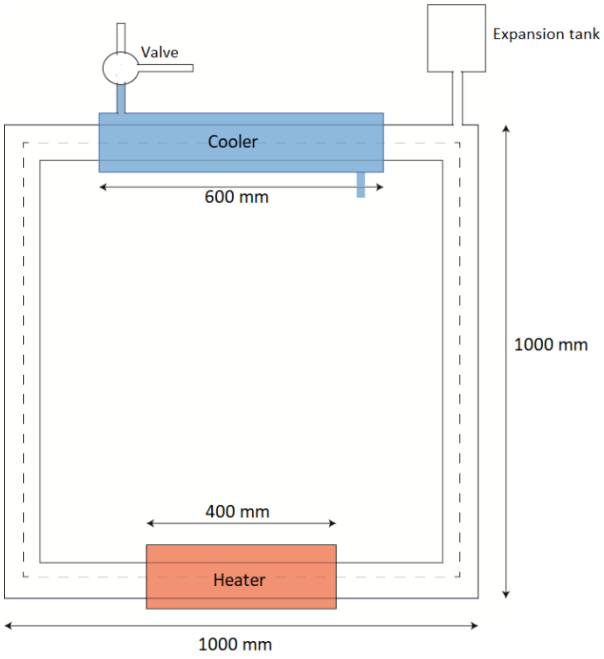

Figure 2*: Schematic diagram of square natural circulation loop*

For calculation, the entire loop is divided into 802 number of elements of 5 mm grid size each and the loop governing equations are solved over the entire loop for a time step of 0.005 seconds to obtain a converged solution. The measure of the optimum grid size of 5 mm and a time step of 0.005 seconds was obtained by an extensive grid independent study conducted by Saha et. al. [21] for the given model. For small temperature change, the subsequent change in the density of the loop fluid is low and hence the Boussinesq approximation is maintained as mentioned earlier. Therefore, the density in inertia terms is considered as a constant with reference temperature, whereas the buoyancy term is considered with the first-order change of density and temperature.

The governing equations of the NCL:

The continuity equation for Loop fluid:

$$\frac{\partial \rho_f}{\partial t} + \frac{\partial (\rho_f v_f)}{\partial z} = 0$$

The momentum equation for Loop fluid:

$$\frac{\partial (\rho_f v_f)}{\partial t} L_{loop} = -\frac{f_{in} (\rho_f v_f)^2 L_{loop}}{2 \rho_f d_{in}} + \oint \rho_0 g \beta_{av} (T_f - T_{ref}) dz$$

The energy equation for Loop fluid:

$$\frac{\partial(\rho_f C_p T_f)}{\partial t} + \frac{\partial[(\rho_f v_f) C_p T_f]}{\partial z} = \frac{\partial\left(k_f \frac{\partial T_f}{\partial z}\right)}{\partial z} - \frac{4h_i(T_f - T_w)}{d_{in}}$$

The energy equation for coolant:

$$\frac{\partial(\rho_{hex} C_{p_{hex}} T_{hex})}{\partial t} + \frac{\partial[(\rho_{hex} v_{hex}) C_{p_{hex}} T_{hex}]}{\partial z} = \frac{\partial\left(k_{hex} \frac{\partial T_{hex}}{\partial z}\right)}{\partial z} + \frac{h_{hex} A_0 (T_w - T_{hex})}{V_{hex}}$$

The equation for momentum is integrated over the entire Loop to obtain the given equation which denotes the various forces acting within the loop. The fluid inertia term is denoted by the term on the left-hand side while the first term and the second term on the right-hand side signifies the friction term and the buoyancy term respectively. As mentioned earlier, the motion of the loop fluid established within the loop when subjected to the heater power is due to the combined effect of the friction term and the buoyancy term. The negative sign of the friction term shows that the buoyancy effect is actually the driving force behind the loop fluid motion while the friction term is actually the resistive term.

The energy equations have transient and convective terms on the left-hand side, while on the right-hand side of the equations include the conduction and heat exchange due to convection respectively in both the energy equations for loop fluid and heat exchanger coolant.

The heat conduction equation for the heater tube wall:

$$\frac{\partial(\rho_w C_{p_w} T_w)}{\partial t} = \frac{\partial\left(k_w \frac{\partial T_w}{\partial z}\right)}{\partial z} + \frac{h_i A_i (T_f - T_w)}{V_w} - \frac{h_{rad} A_0 (T_w - T_a)}{V_w} + \frac{P}{V_w}$$

The heat conduction equation for the non-heater tube wall:

$$\frac{\partial(\rho_w C_{p_w} T_w)}{\partial t} = \frac{\partial\left(k_w \frac{\partial T_w}{\partial z}\right)}{\partial z} + \frac{h_i A_i (T_f - T_w)}{V_w} - \frac{(h_0 + h_{rad}) A_0 (T_w - T_a)}{V_w}$$

The heat conduction equation for heat exchanger:

$$\frac{\partial(\rho_w C_{p_w} T_w)}{\partial t} = \frac{\partial\left(k_w \frac{\partial T_w}{\partial z}\right)}{\partial z} + \frac{h_i A_i (T_f - T_w)}{V_w} - \frac{(h_{ex+} h_{rad}) A_0 (T_w - T_a)}{V_w}$$

where, $h_{rad} = 4\varepsilon\sigma T_a^3$

In addition to the steady heater power, a periodic perturbation in heater power is applied to the tube wall at the heater region is applied. Heat exchange takes place through convective heat transfer at the cooler region and via convective and radiation heat loss to the ambient for other uninsulated parts of the tube including the horizontal tubes, riser and downcomer.

Along the entire length of the loop, the tube wall also exchanges heat with the loop fluid via convection. This amount to a substantial amount of heat loss by the loop fluid but when the tube wall temperature exceeds the loop fluid temperature, heat transfer takes place from the tube wall to the fluid which results in further anomalies in the mass flow of the fluid.

The analysis of the MATLAB based Simulink model of the NCL in this study require certain correlations to determine friction factor (*f*), heat transfer coefficient between wall and loop fluid, heat coefficient between wall and coolant in the heat exchanger and the heat transfer coefficient between the tube wall and ambient to evaluate the heat loss.

Correlation for determining friction factor for the loop fluid:

- for laminar flow, $Re_d < 2300$ $\quad f_{in} = \frac{64}{Re_d}$
- for turbulent flow, $Re_d > 2300$ $\quad f_{in} = (0.79 \ln Re_d - 1.64)^{-2}$

Where Re_d is Reynold's number given by

$$Re_d = \frac{\rho_f v_f d_{in}}{\mu_f}$$

The correlations for the fluid to wall heat transfer:

- for laminar flow,

$$f_{in} = \frac{64}{Re_d} \quad , \quad Nu = \frac{0.086\left\{Re_d Pr\left(\frac{d_{in}}{L}\right)\right\}^{1.33}}{0.1Pr\left(Re_d\left(\frac{d_{in}}{L}\right)\right)^{0.83}+1} + 4.364$$

- for transition or turbulent flow,

$$f_{in} = (0.79 \ln Re_d - 1.64)^{-2}\,, \quad Nu = \frac{\left(\frac{f_{in}}{8}\right)(Re_d - 1000)Pr}{1+12.7\left(\frac{f_{in}}{8}\right)^{0.5}(Pr^{0.66}-1)}$$

Correlation for the wall to ambient heat transfer:

$$Ra = Gr.Pr = \frac{g\beta L^3(T_w - T_\infty)}{\upsilon^2}.\frac{\upsilon}{\alpha}$$

- for vertical cylinders, riser and downcomers,

$$Nu_{l,cyl} = CF.Nu_l$$

where $Nu_l = \frac{2.8}{\ln\left(1+\frac{2.8}{C_l Ra^{1/4}}\right)}$, $CF = \frac{1.8\phi}{\ln(1+1.8\phi)}$

$\phi = \frac{L/d_0}{\left(C_l Ra^{1/4}\right)}$, for constant wall temperature

$\phi = \frac{L/D}{\left(C_l Ra^{1/4}\right)}$, for constant heat flux

- for bare tube wall,

$$Nu_l = \left(0.60 + \frac{0.387Ra^{1/6}}{\left[1+\left(\frac{0.559}{Pr}\right)^{9/16}\right]^{8/27}}\right)^2 \quad \text{for } 10^{-5} < \text{Ra} < 10^{12}$$

The mass, momentum and energy equations of the loop fluid and heat exchanger coolant and the tube wall heat transfer equation are discretized while solving in MATLAB using the given conditions. The diffusion terms of the above equations are discretized by the central difference scheme and the convective terms with the help of the upwind scheme along with an explicit scheme.

- The energy equation for loop fluid:

$$T_f(i,j+1) = T_f(i,j) + \frac{k_f dt}{\rho_f C_p dz^2}\{T_f(i+1,j) - 2T_f(i,j) + \quad T_f(i-1,j)\} - \frac{MFdt\{T_f(i,j) - T_f(i-1,j)\}}{\rho_f dz} + \frac{4h_i dt}{\rho_f C_p d_{in}}\{T_w(i,j) - T_f(i,j)\}$$

- The energy equation for heat exchanger coolant:

$$T_{hex}(i,j+1) = T_{hex}(i,j) + \frac{k_{hex} dt}{\rho_{hex} C_{p_{hex}} dz^2}\{T_{hex}(i+1,j) - \quad 2T_{hex}(i,j) + T_{hex}(i-1,j)\} - \frac{MF_{hex} dt\{T_{hex}(i,j) - T_{hex}(i-1,j)\}}{\rho_{hex} dz} + \quad \frac{h_{hex} A_{out} dt}{V_{hex} \rho_{hex} C_{p_{hex}}}\{T_w(i,j) - T_{hex}(i,j)\}$$

- The tube wall heat conduction equation are:

1. *Bare tube section:*

$$T_w(i,j+1) = T_w(i,j) + \frac{k_w dt}{\rho_w C_{p_w} dz^2}\{T_w(i+1,j) - 2T_w(i,j) + T_w(i-1,j)\} - \frac{h_i A_{in} dt}{V_w \rho_w C_{p_w}}\{T_w(i,j) - T_f(i,j)\} + \frac{(h_o + h_{rad}) A_{out} dt}{V_w \rho_w C_{p_w}}\{T_w(i,j) - T_a\}$$

2. *Heater section:*

$$T_w(i,j+1) = T_w(i,j) + \frac{k_w dt}{\rho_w C_{p_w} dz^2}\{T_w(i+1,j) - 2T_w(i,j) + T_w(i-1,j)\} - \frac{h_i A_{in} dt}{V_w \rho_w C_{p_w}}\{T_w(i,j) - T_f(i,j)\} + \frac{P dt}{V_w C_{p_w} \rho_w}$$

3. *Riser and Downcomer section:*

$$T_w(i,j+1) = T_w(i,j) + \frac{k_w dt}{\rho_w C_{p_w} dz^2}\{T_w(i+1,j) - \quad 2T_w(i,j) + T_w(i-1,j)\} - \frac{h_i A_{in} dt}{V_w \rho_w C_{p_w}}\{T_w(i,j) - T_f(i,j)\} - \frac{(h_o + h_{rad}) A_{out} dt}{V_w \rho_w C_{p_w}}\{T_w(i,j) - T_a\}$$

4. *Cooler section:*

$$T_w(i,j+1) = T_w(i,j) + \frac{k_w dt}{\rho_w C_{p_w} dz^2}\{T_w(i+1,j) - 2T_w(i,j) + T_w(i-1,j)\} - \frac{h_i A_{in} dt}{V_w \rho_w C_{p_w}}\{T_w(i,j) - T_f(i,j)\} - \frac{h_{hex} A_{out} dt}{V_w \rho_w C_{p_w}}\{T_w(i,j) - T_{hex}(i,j)\}$$

The power input to the heater section of the loop was modified to suit the current requirements of the study. The original model of the loop under investigation, developed by Saha et al. [9] had a constant power supply. An additional sinusoidal power fluctuation was added to the system to create a time-varying pulsating power supply to be supplied to the system.

If the base power level applied be P , then the fluctuation in power is equal to

$$\Delta P = \frac{P.A}{100}\sin(2\pi F dt)$$

Where A is the amplitude percentage, F is the pulsating frequency and dt is the time step. The forcing frequency F of the pulsating power is equal to

$$F = n.f_n$$

where f_n is the natural frequency of the system at a given base power level. Therefore, the power supplied to the system is obtained by,

$$P_p = P + \Delta P \text{ , or}$$

$$P_p = P + \frac{P.A}{100}\sin(2\pi F dt) \text{ , or}$$

$$P_p = P + \frac{P.A}{100}\sin(2\pi.n.f_{n.}dt)$$

The initial operating conditions of the loop under investigations are as follows:

- System temperature for region before heat exchanger is taken to be 23°C.
- System temperature for region after heat exchanger is taken to be 22°C.
- Heat exchanger temperature is considered to be 20°C.
- Ambient temperature is taken to be 20°C.
- Heat exchanger mass flow rate is equal to 40 kg/m^2.s

The present study discusses the effects of the presence of an external power perturbation on a periodic natural circulation system and the resulting response dynamics of the system to such an external forcing.

The dynamic characteristics of a single-phase natural circulation system is a function of the input heater power supplied. We observe different nature of the response when the power levels of such a system is varied. The system moves from a stable steady state at low power levels to a periodic behaviour where the mass flow of the operating undergoes oscillations when the power levels are increased. On increasing the input power further, the oscillation amplitude amplifies and eventually, the system undergoes flow reversals and becomes chaotic in nature.

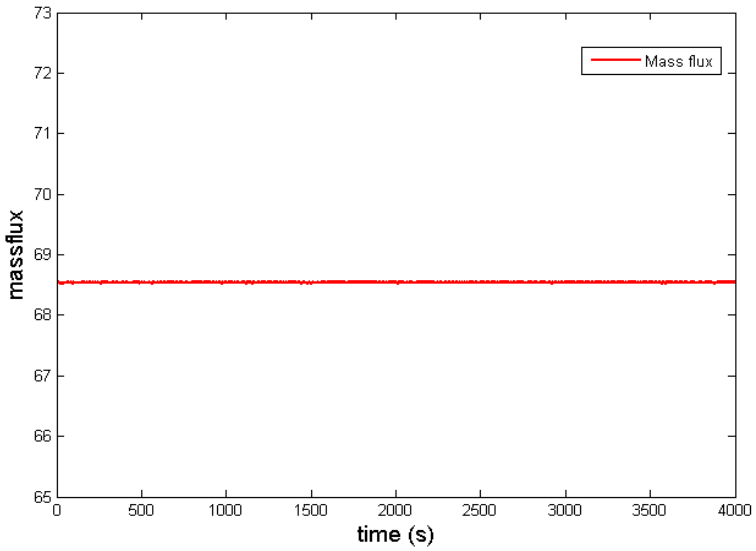

Figure 3*: Mass flux at 600 W steady power*

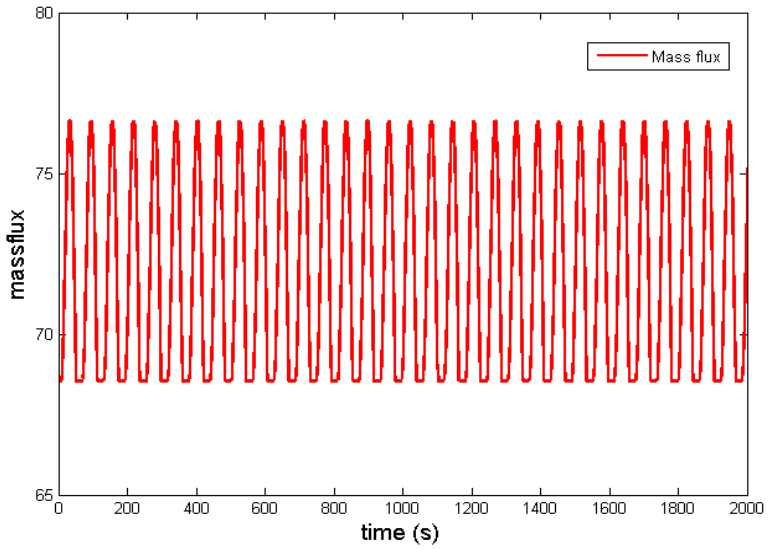

Figure 4*: Mass flux at 700 W steady power*

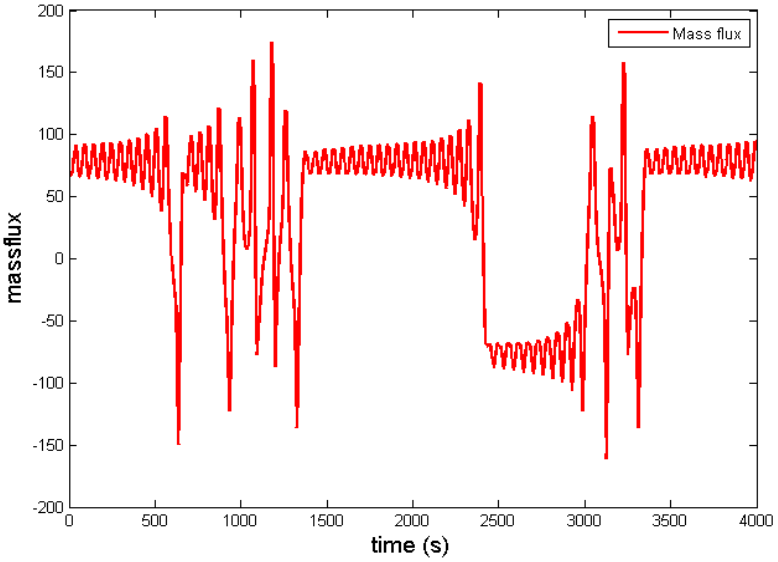

Figure 5*: Mass flux at 800 W steady power*

In this study, a periodically oscillating NCL is taken at two different power levels and a fluctuation in the input power is introduced. The applied amplitude of the pulsating input power includes 1%, 3%, 5%, 7% and 10% of the base input powers equal to 675 W and 700 W, all of which result in periodic oscillations in the system and the frequency ratio of the forcing frequency to the natural frequency of the system ranges from 0.45 to 1.5 with a greater number of steps of frequency ratio for higher amplitudes of the external perturbation. The MATLAB based Simulink model is used to determine the dynamics of the system, especially the mass flux of the natural circulating system under the pulsating power for a time period of 5000 s and the data

obtained, is analysed and plotted after eliminating the initial transient part of the system response.

The time series of the mass flux under pulsating power is plotted along with the mass flux of the same operating conditions under steady power to show the amplification or suppression of the mass flux oscillation as compared to that under constant power for a sample time of 2000 s. The nature of the pulsating power and the resulting mass flux is also plotted in terms of their normalized values and a Fast Fourier Transform is also done to determine the system frequency in response to the external forcing of the pulsating power. At lower amplitudes of 1% and 3% of the input powers of 675 W and 700 W, the external forcing reveals the following results.

From the figures (Fig. 6 - 13) for 1% and 3% amplitude of the base input power, the effect on the system dynamics of the loop is almost negligible irrespective of the value of the external forcing frequency. The dominant frequency of system under the external perturbation continues to be equal to the natural frequency of the system as indicated by the black peaks of the FFT plots. The forcing frequency and amplitude of the external pulsating power appears to be too weak to affect the system in any way or in any way influence the system. The fundamental dynamics of the system in its natural state appear to be far too robust in comparison to the external oscillator with low amplitude and frequency, to be influenced by it.

The external forcing at 3% amplitude and forcing frequency of 1.50, appears to have a minor effect on the system at 675 W. In Fig 8-9, we see secondary frequency of mass flux oscillations appear within the system when the forcing amplitude is equal to 3% of the input power. We also see an increase in oscillation amplitude of the system but the amplification reduces when the forcing frequency ratio is increased to 1.50 as seen in Fig 9. However, it is too negligible to consider. The same parameters of pulsating power, when applied to the power level of 700 W, has no observable effect on the system indicating that an external forcing with a given value of operating amplitude and frequency finds it easier to interact with the system operating at low power levels. However, from the observations, we can say that the system shows the possibility of demonstrating response dynamics much more influenced by the external perturbation with higher forcing amplitude and frequency.

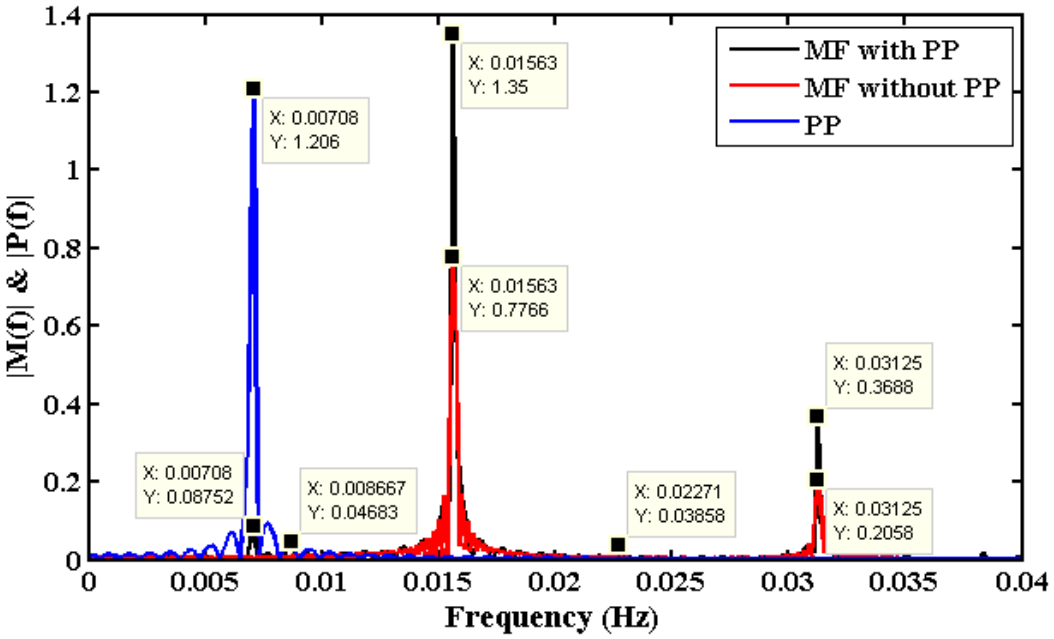

(A)

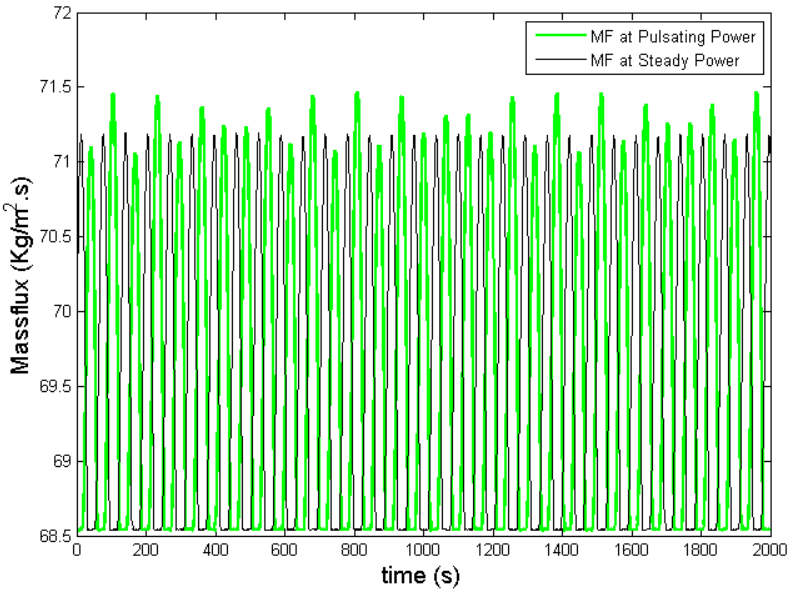

(B)

Figure 6*: System dynamics for base input power of 675W at 1% amplitude and frequency ratio 0.45*

(A) Fast Fourier Transform plot

(B) Time series plot of mass flux at steady power vs pulsating power

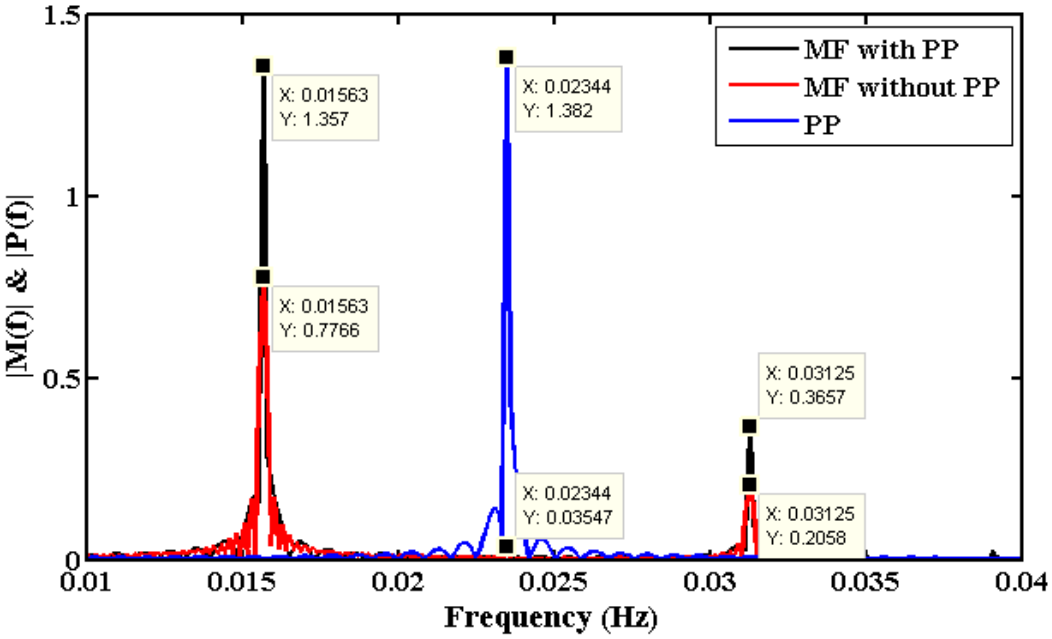

(A)

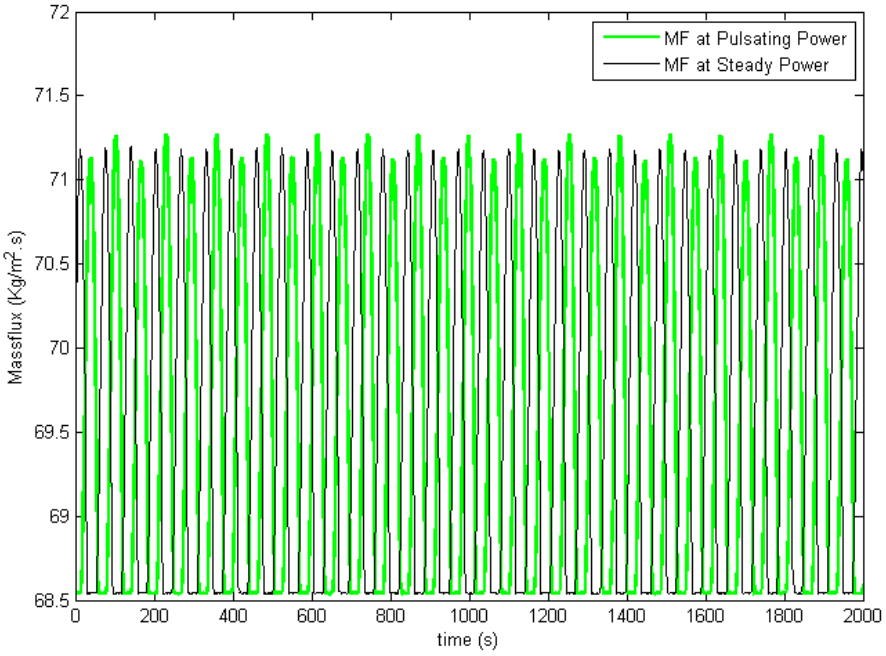

(B)

Figure 7*: System dynamics for base input power of 675W at 1% amplitude and frequency ratio 1.50*

(A) Fast Fourier Transform plot

(B) Time series plot of mass flux at steady power vs pulsating power

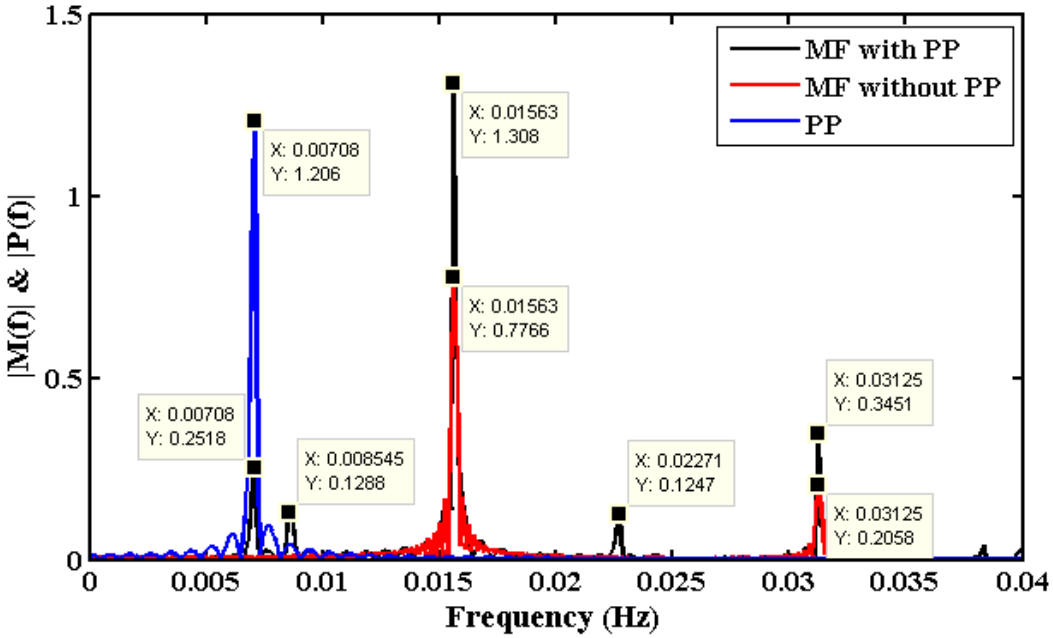

(A)

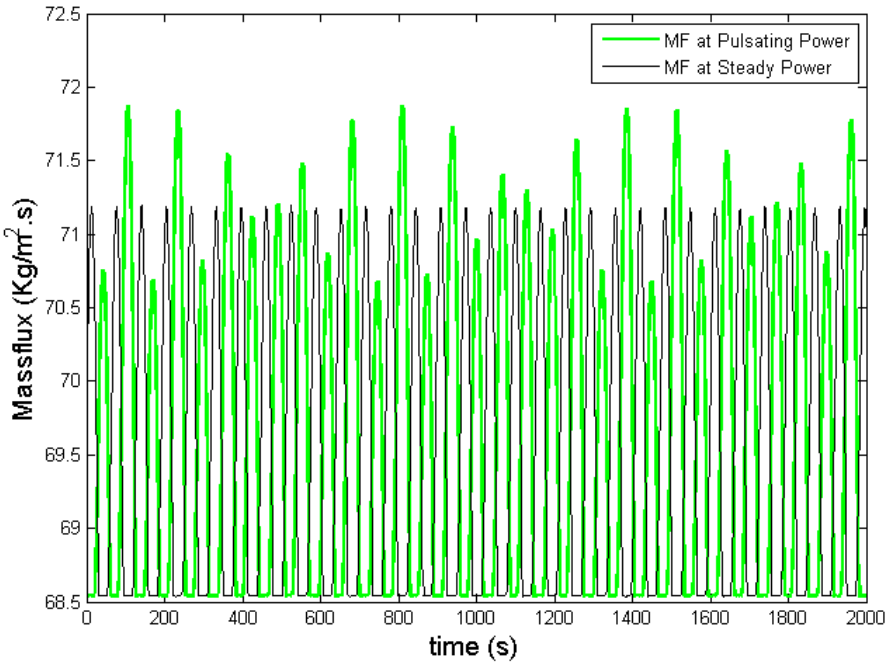

(B)

Figure 8*: System dynamics for base input power of 675W at 3% amplitude and frequency ratio 0.45*

(A) Fast Fourier Transform plot

(B) Time series plot of mass flux at steady power vs pulsating power

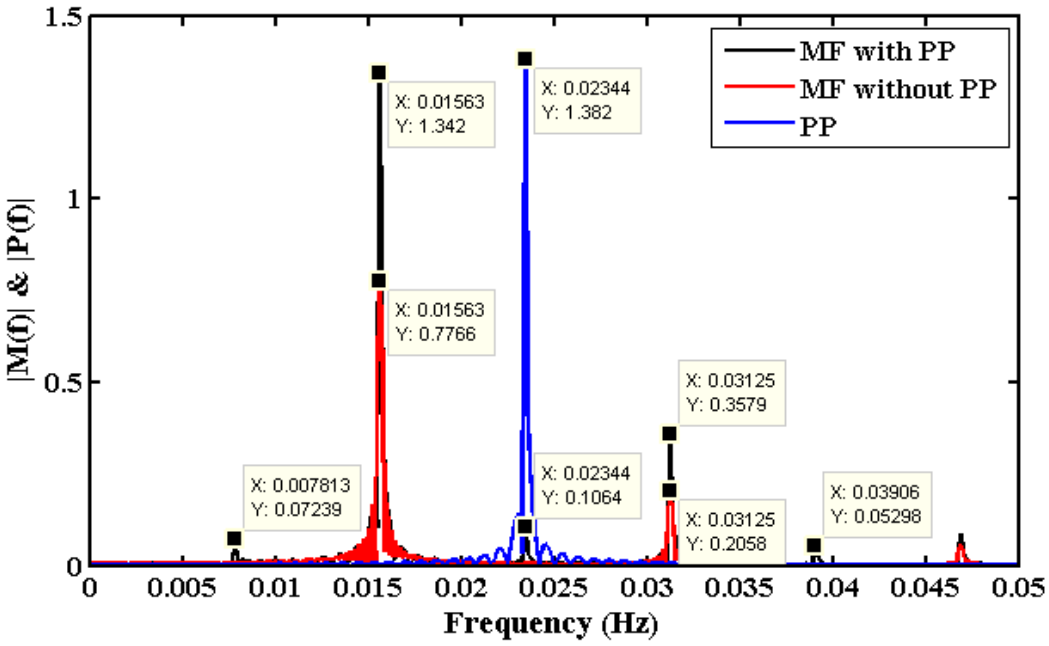

(A)

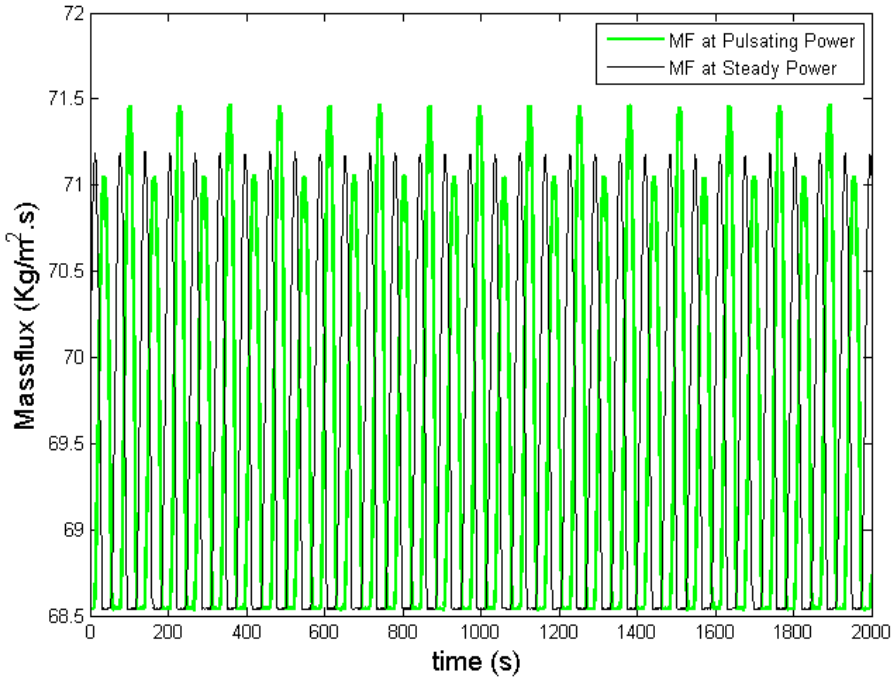

(B)

Figure 9*: System dynamics for base input power of 675W at 3% amplitude and frequency ratio 1.50*

(A) Fast Fourier Transform plot

(B) Time series plot of mass flux at steady power vs pulsating power

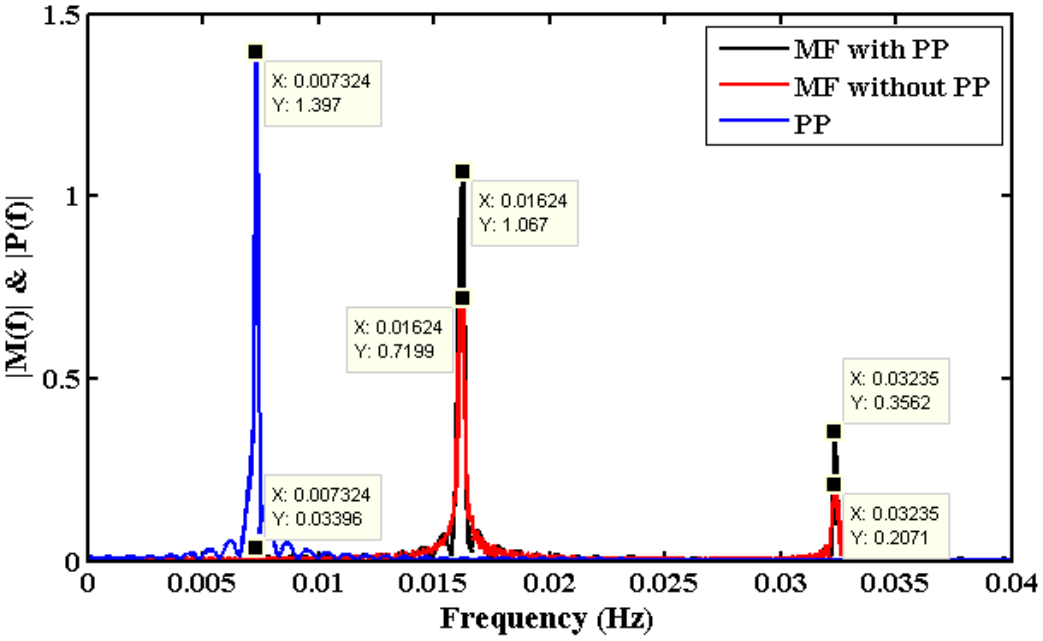

(A)

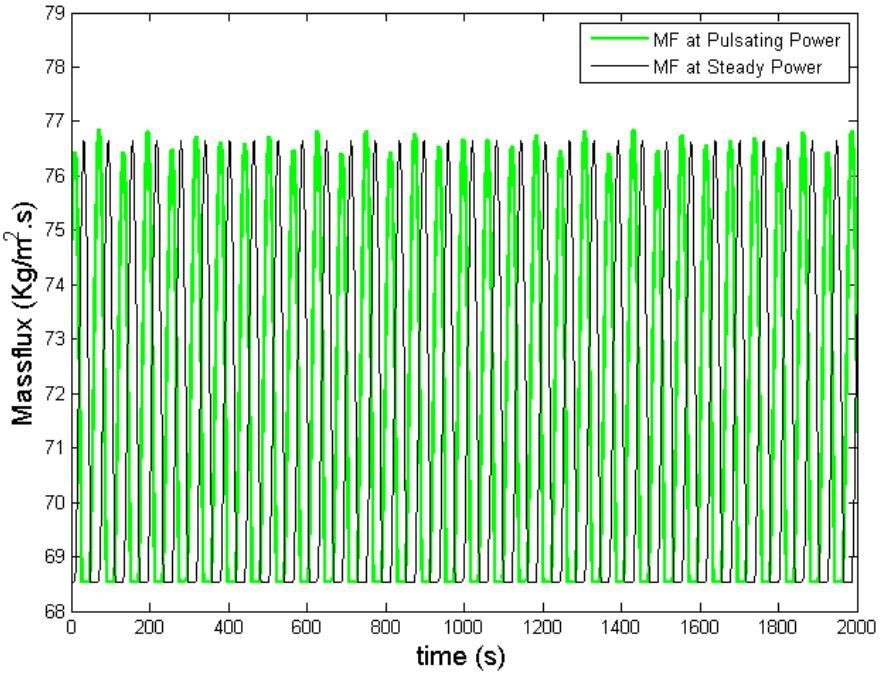

(B)

Figure 10*: System dynamics for base input power of 700W at 1% amplitude and frequency ratio 0.45*

(A) Fast Fourier Transform plot

(B) Time series plot of mass flux at steady power vs pulsating power

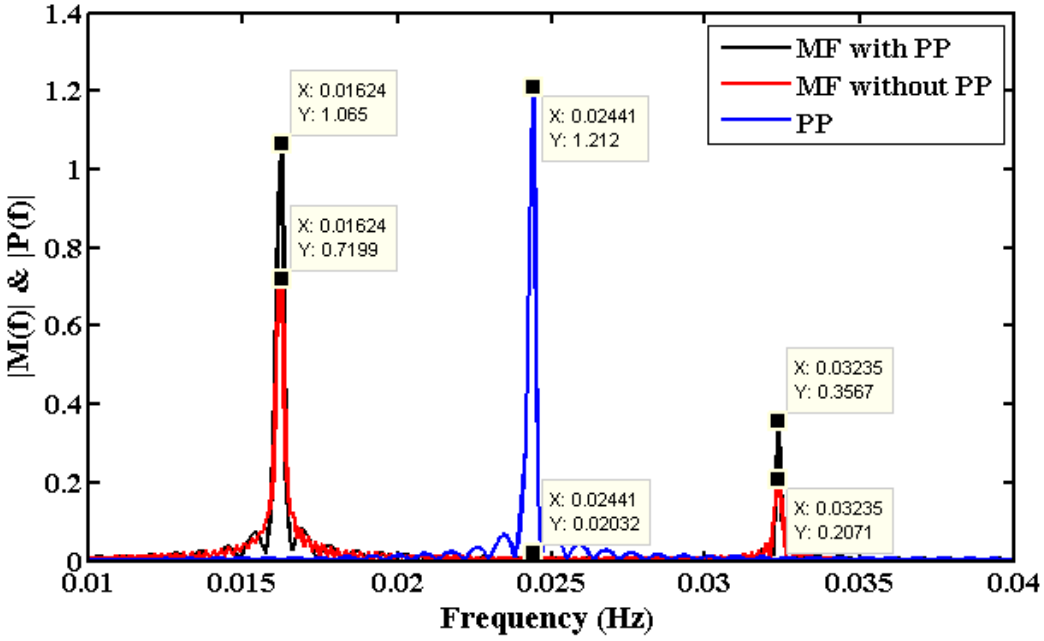

(A)

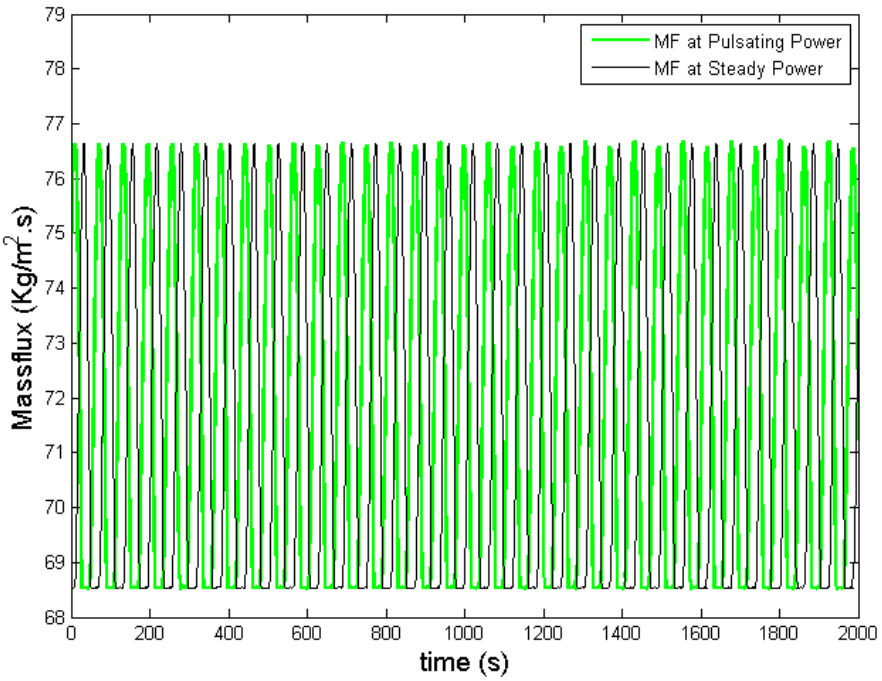

(B)

Figure 11*: System dynamics for base input power of 700W at 1% amplitude and frequency ratio 1.50*

(A) Fast Fourier Transform plot

(B) Time series plot of mass flux at steady power vs pulsating power

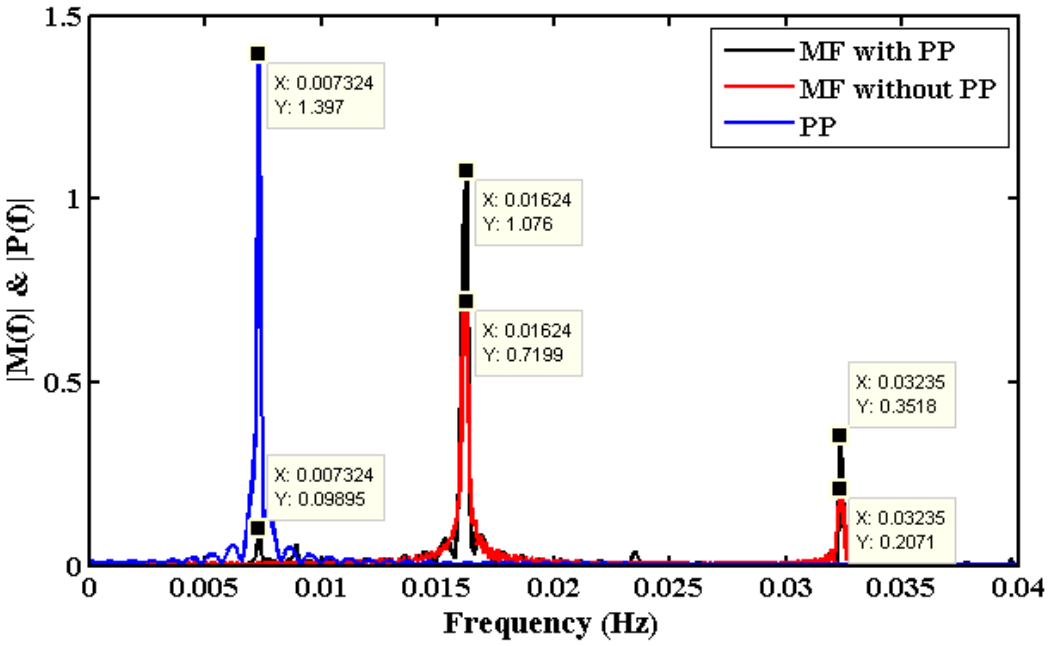

(A)

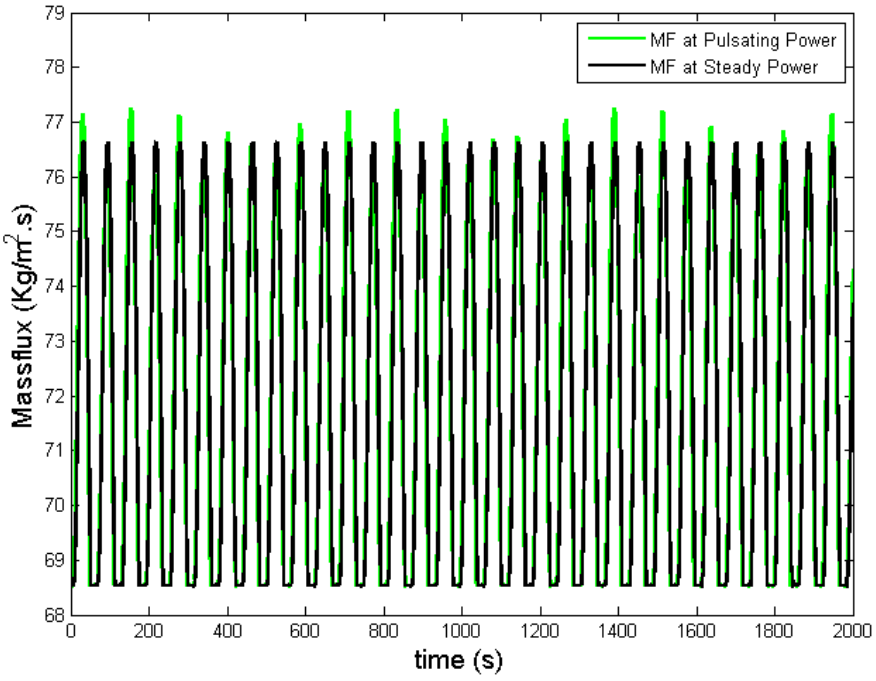

(B)

Figure 12: *System dynamics for base input power of 700W at 3% amplitude and frequency ratio 0.45*

(A) Fast Fourier Transform plot

(B) Time series plot of mass flux at steady power vs pulsating power

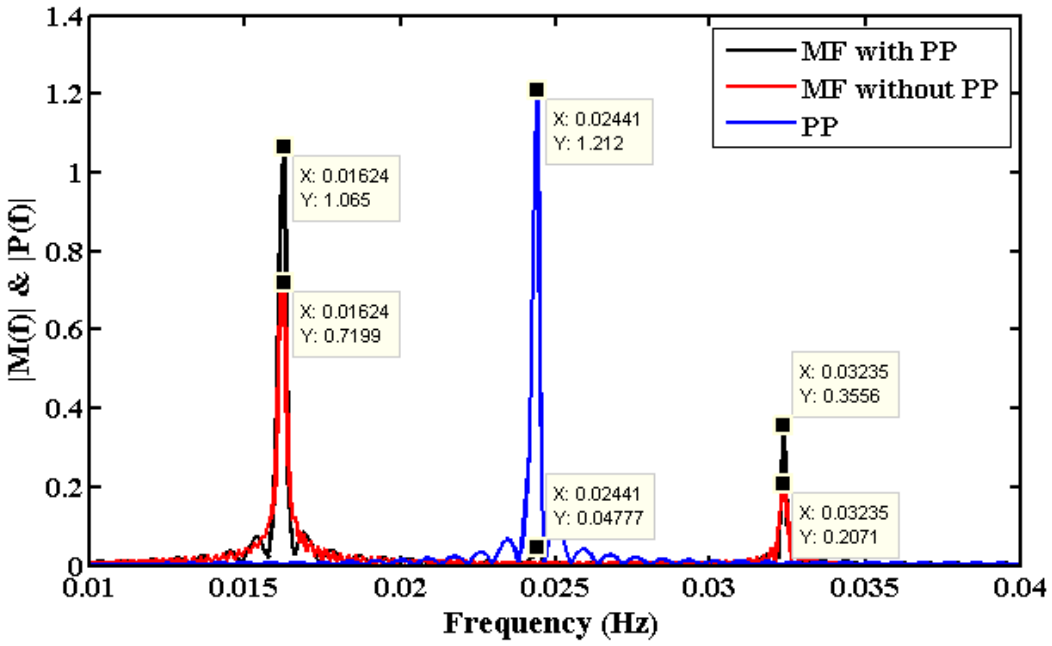

(A)

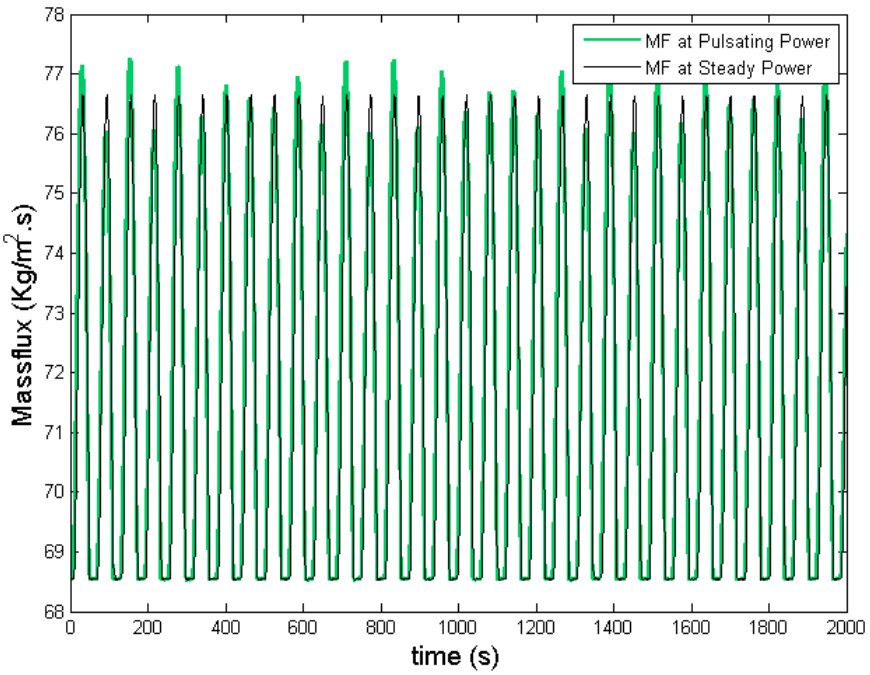

(B)

Figure 13*: System dynamics for base input power of 700W at 3% amplitude and frequency ratio 1.50*

(A) Fast Fourier Transform plot

(B) Time series plot of mass flux at steady power vs pulsating power

However, on increasing the amplitude of the power perturbation and with fine-tuned forcing frequency, the system starts to react to the external forcing and we can observe the system interacting with the system even more strongly.

On increasing the forcing amplitude to 5%, 7% and 10% and frequency of the pulsating power for 675 W and 700 W reveals the following results. The observations of the response dynamics of the natural circulation system, when subjected to an external pulsating power at 5%, 7% and 10% fluctuating amplitude for input power of 675 W and 700 W show almost identical behaviour of the system's response dynamics. It was observed that at low forcing frequency, the mass flux of the system is not sinusoidal in nature like the forcing signal, as can be seen in Fig 13 and Fig 27 for forcing frequency ratio of 0.45. Although the system does show signs of influence from the external power perturbation, the absence of sinusoidal nature of the response dynamics indicates a non-linear nature of interaction between the forced and natural oscillations.

When the forcing frequency attains a critical value, the dominant frequency of the system gets entrained and locked on to the frequency of the external oscillator as seen here. When the power perturbation is applied at a frequency which is incommensurate with the natural frequency of the natural circulation system, the mass flux starts to oscillates at a single dominant frequency equal to the forcing frequency. On increasing the forcing frequency further results in desynchronise of the oscillators and they do not remain phase-locked anymore, although the power perturbation continues to influence the response dynamics.

For a given external perturbation amplitude, on increasing the forcing frequency outside the phase-locked regime, the impact of the presence of secondary frequency of the mass flux oscillation equal to the forcing frequency can be observed. The response dynamics of the system oscillates with a combined frequency of the dominant natural frequency of the system and the secondary frequency equal to the forcing parameter. However, within the phase-locked regime, for all the forcing amplitudes, we observe a pronounced amplification of the mass-flux oscillation when the forcing frequency ratio is very close to 1. At both values of 0.95 and 1.2, there is an increase in the oscillations which is further suppressed at higher value of forcing frequency. This might be due to the increased proximity of the forcing frequency to the natural frequency of the system.

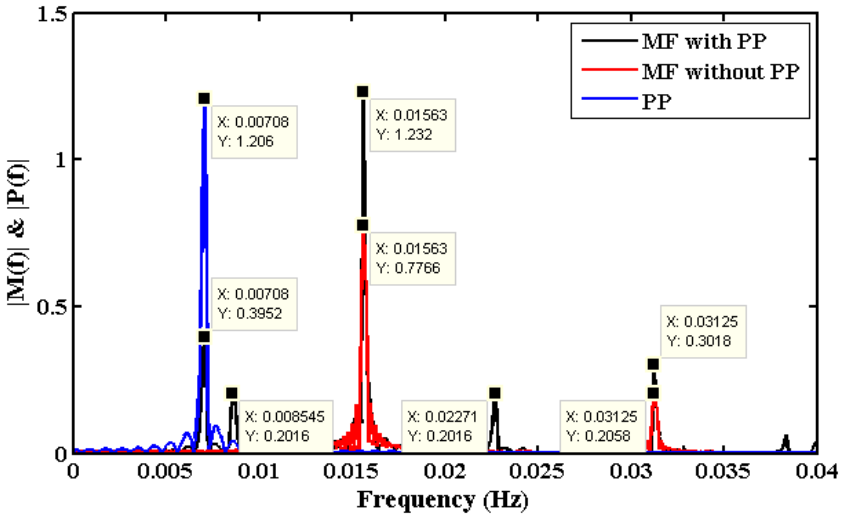

(A) FFT Plot

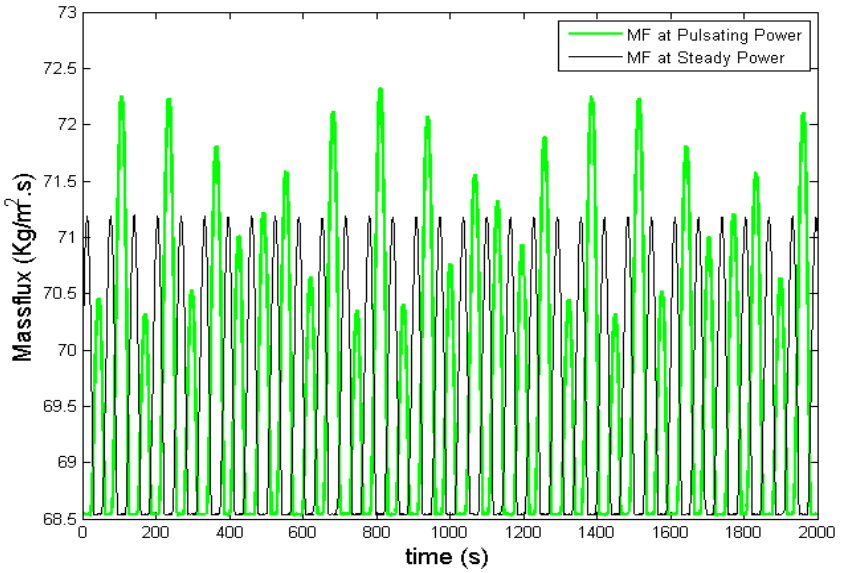

(B) Time series of mass flux under constant power vs pulsating power

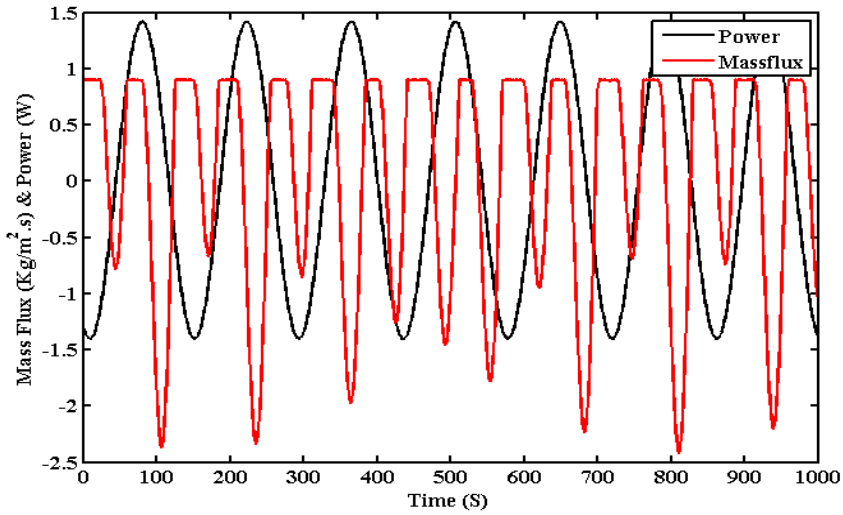

(C) Time series of mass flux and pulsating power

Figure 14: *System dynamics for base input power of 675W at 5% amplitude and frequency ratio 0.45*

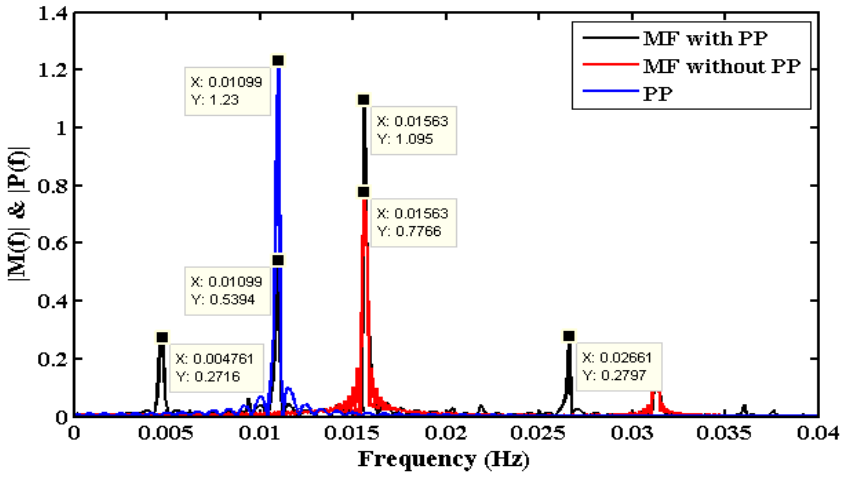

(A) FFT Plot

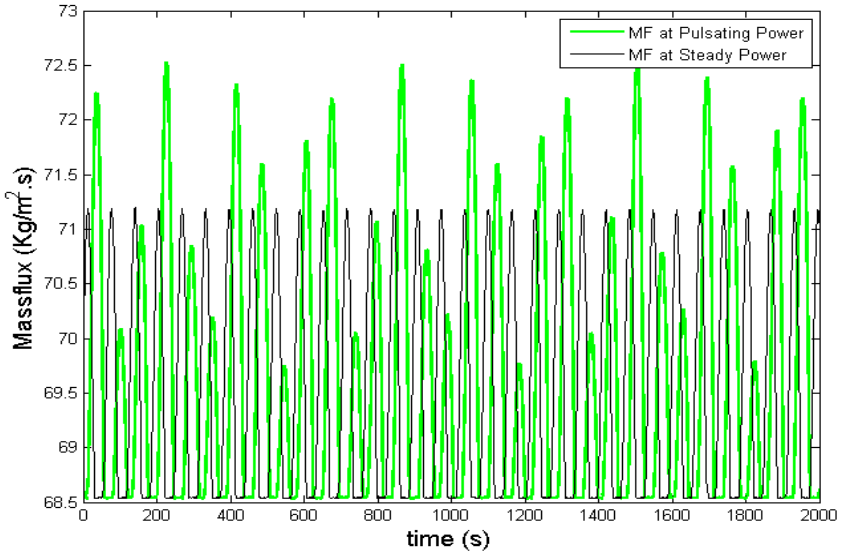

(B) Time series of mass flux under constant power vs pulsating power

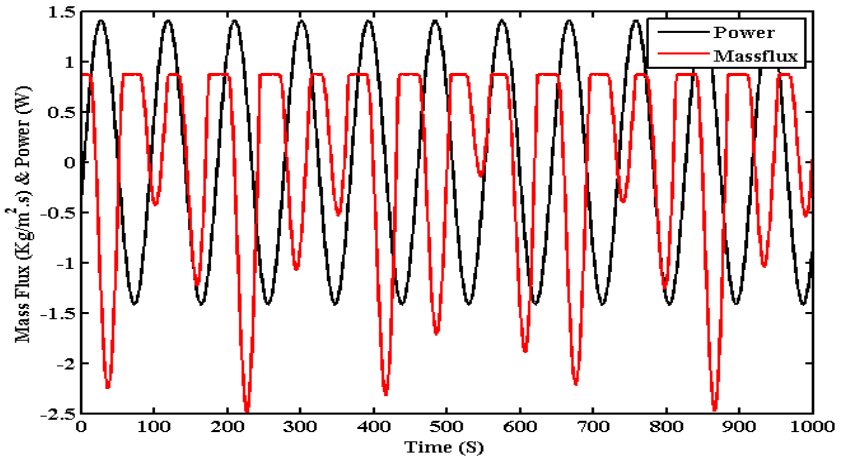

(C) Time series of mass flux and pulsating power

Figure 15: *System dynamics for base input power of 675W at 5% amplitude and frequency ratio 0.70*

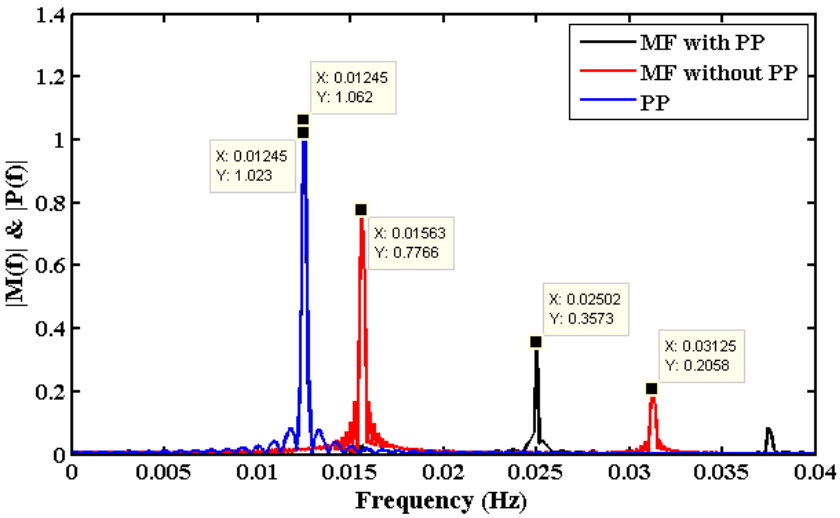

(A) FFT Plot

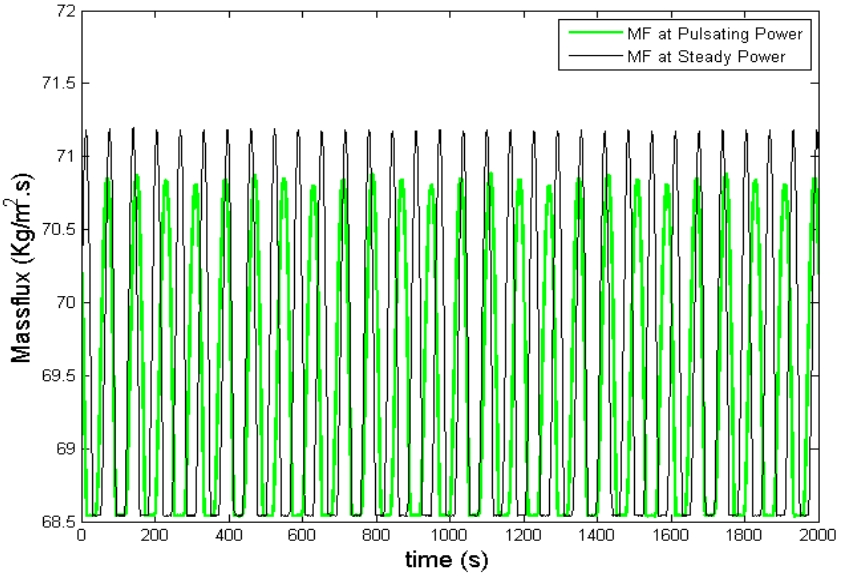

(B) Time series of mass flux under constant power vs pulsating power

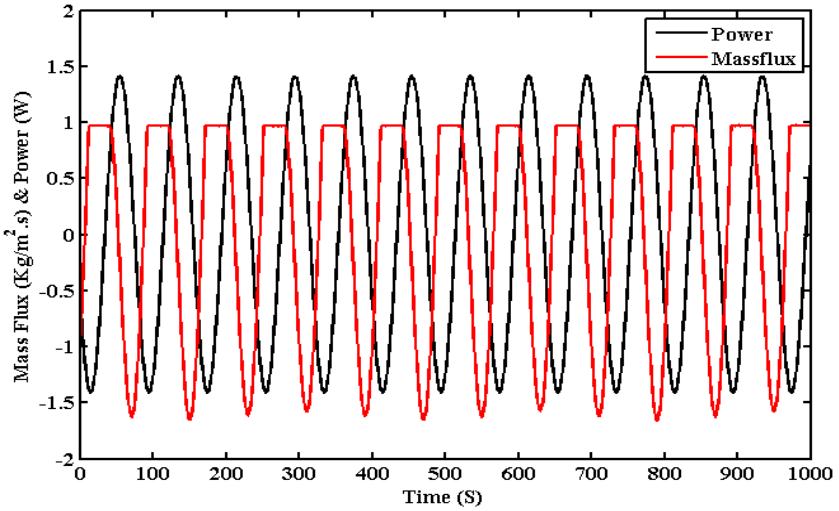

(C) Time series of mass flux and pulsating power

Figure 16: *System dynamics for base input power of 675W at 5% amplitude and frequency ratio 0.80*

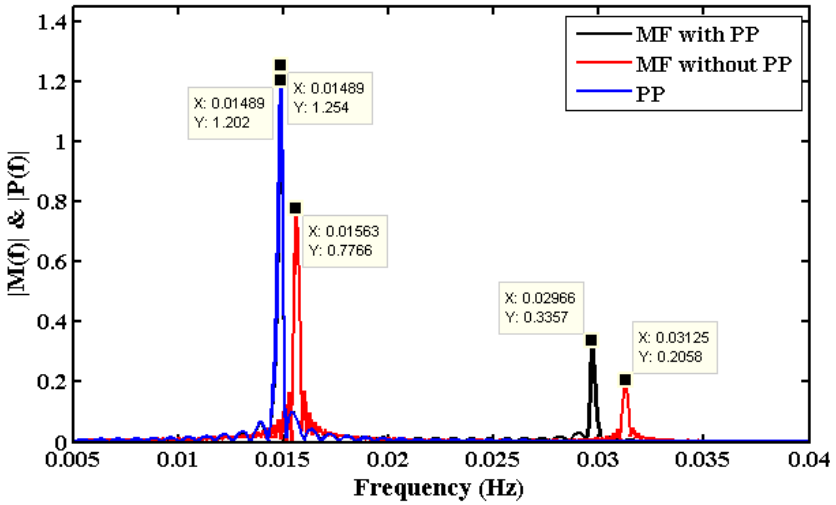

(A) FFT Plot

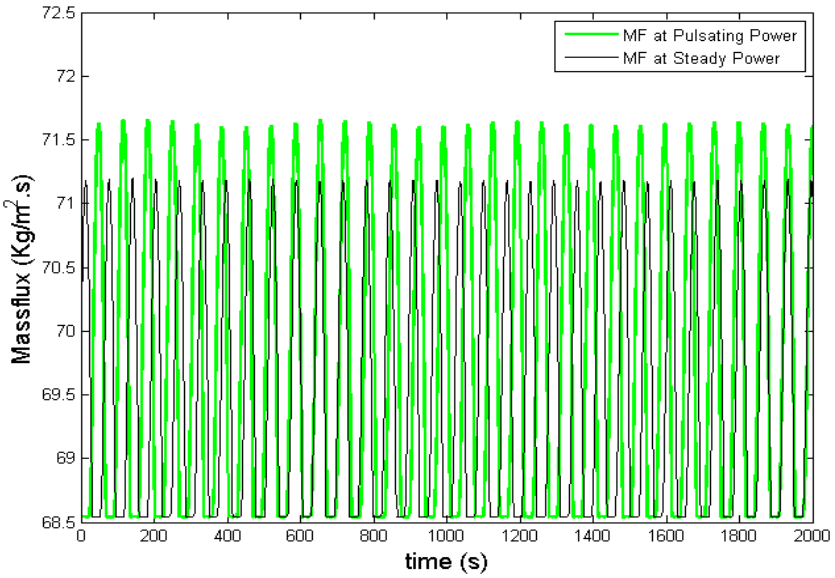

(B) Time series of mass flux under constant power vs pulsating power

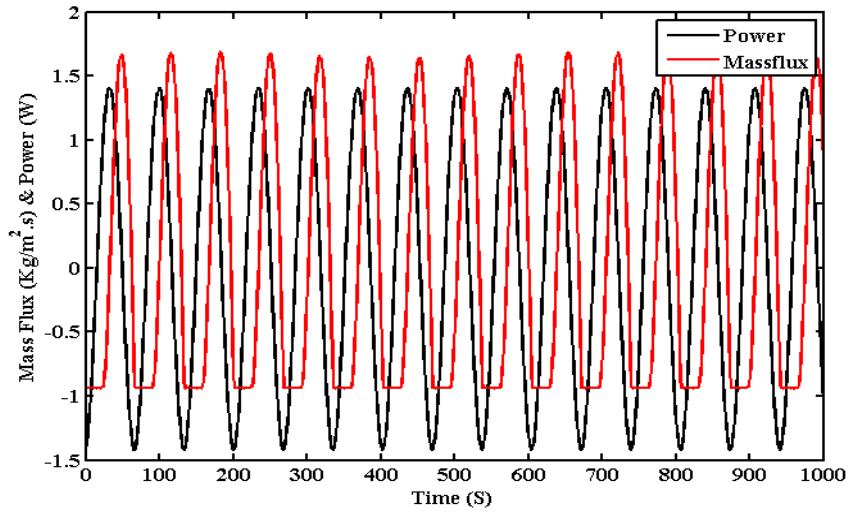

(C) Time series of mass flux and pulsating power

Figure 17*: System dynamics for base input power of 675W at 5% amplitude and frequency ratio 0.95*

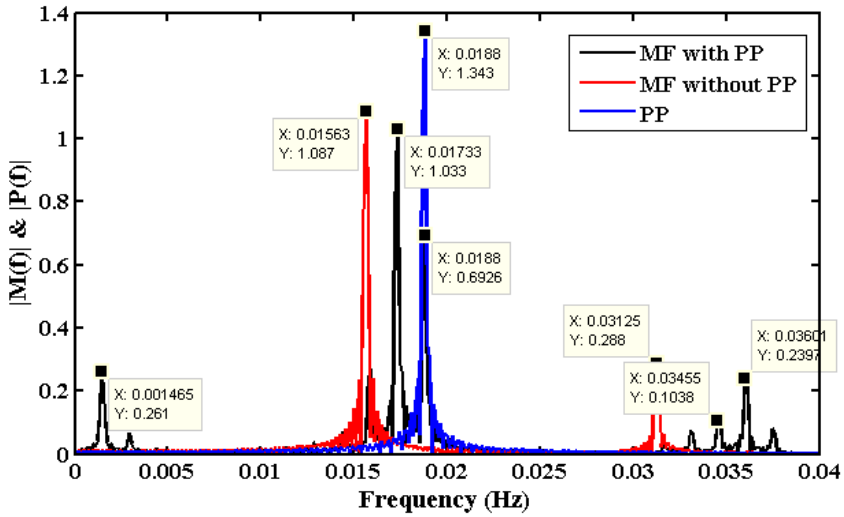

(A) FFT Plot

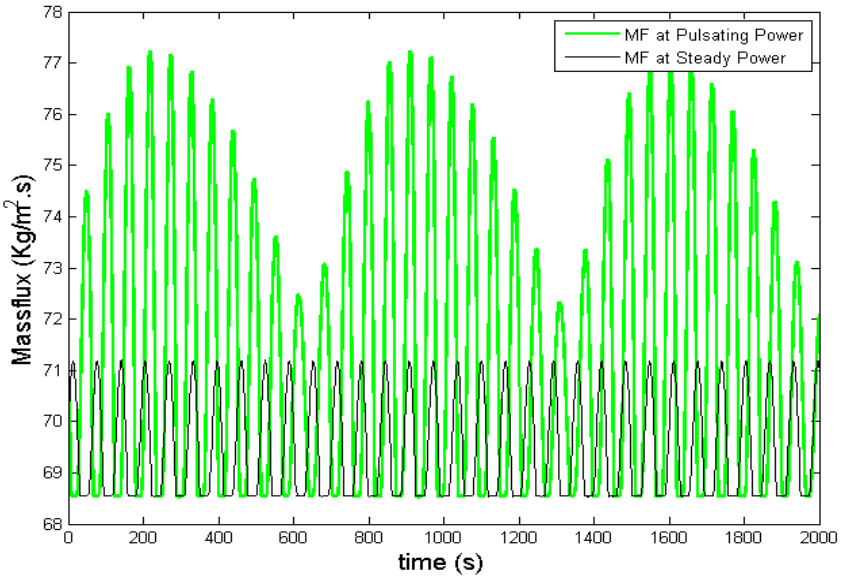

(B) Time series of mass flux under constant power vs pulsating power

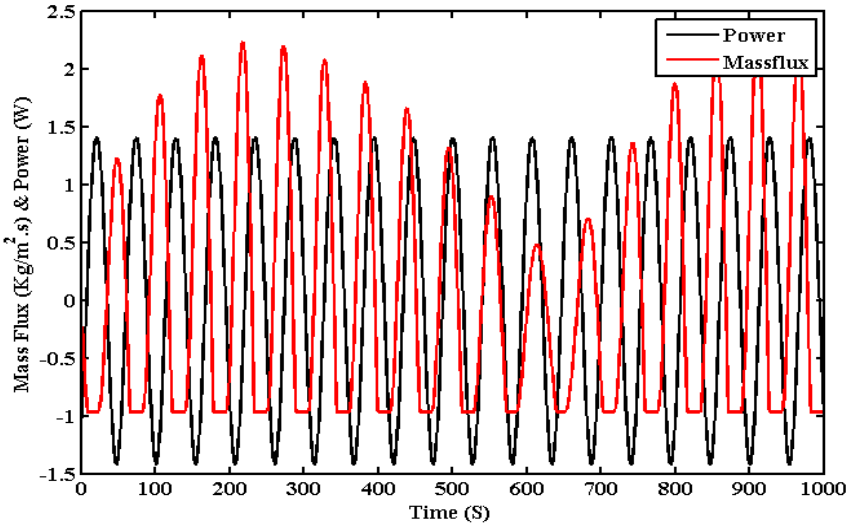

(C) Time series of mass flux and pulsating power

Figure 18*: System dynamics for base input power of 675W at 5% amplitude and frequency ratio 1.20*

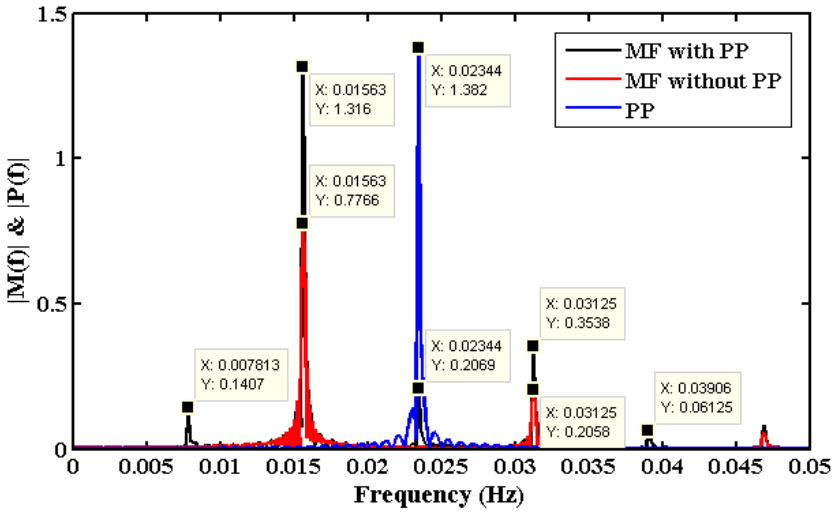

(A) FFT Plot

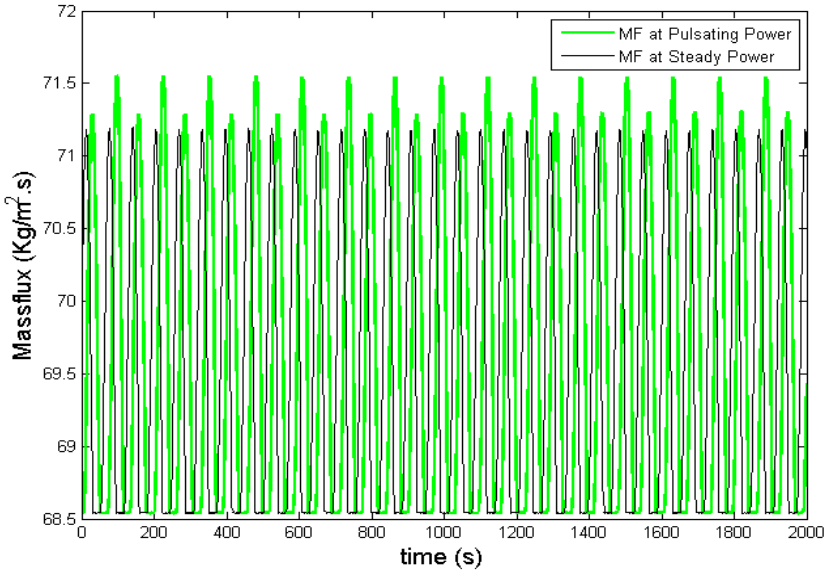

(B) Time series of mass flux under constant power vs pulsating power

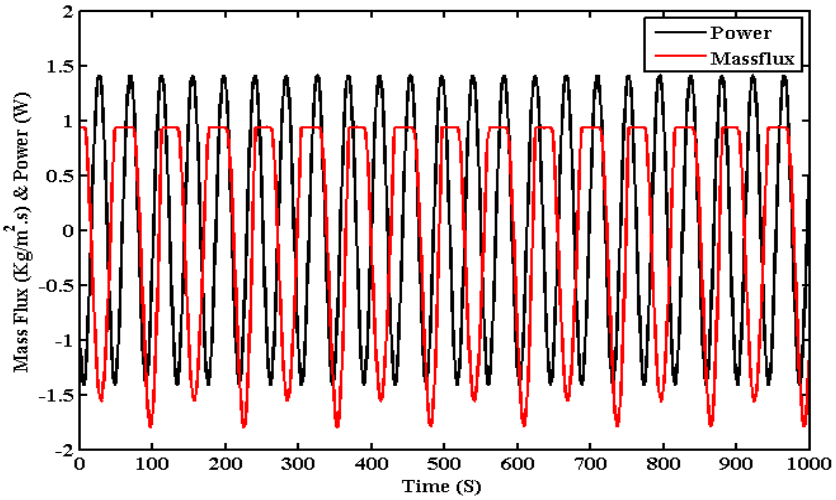

(C) Time series of mass flux and pulsating power

Figure 19: *System dynamics for base input power of 675W at 5% amplitude and frequency ratio 1.50*

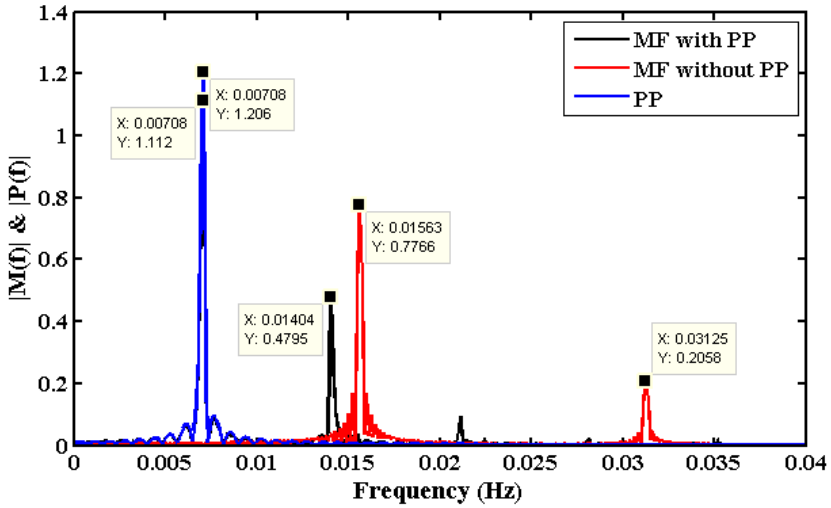

(A) FFT Plot

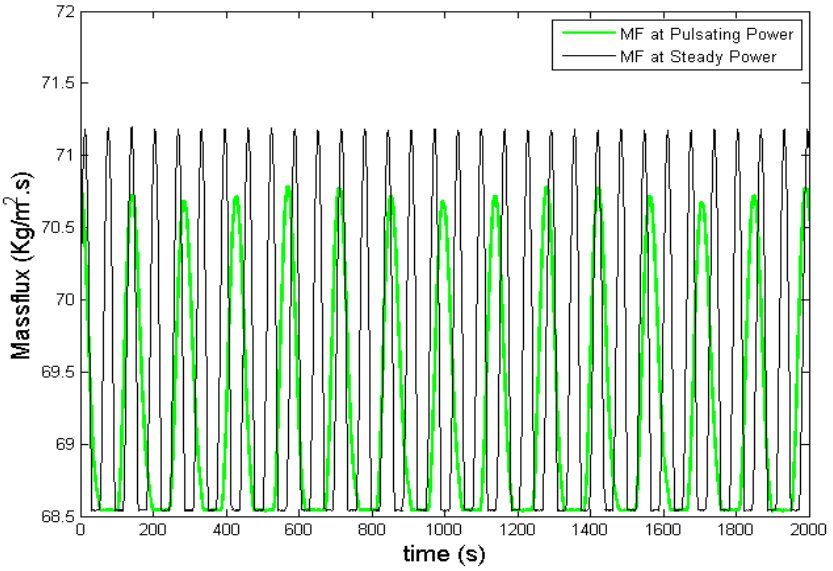

(B) Time series of mass flux under constant power vs pulsating power

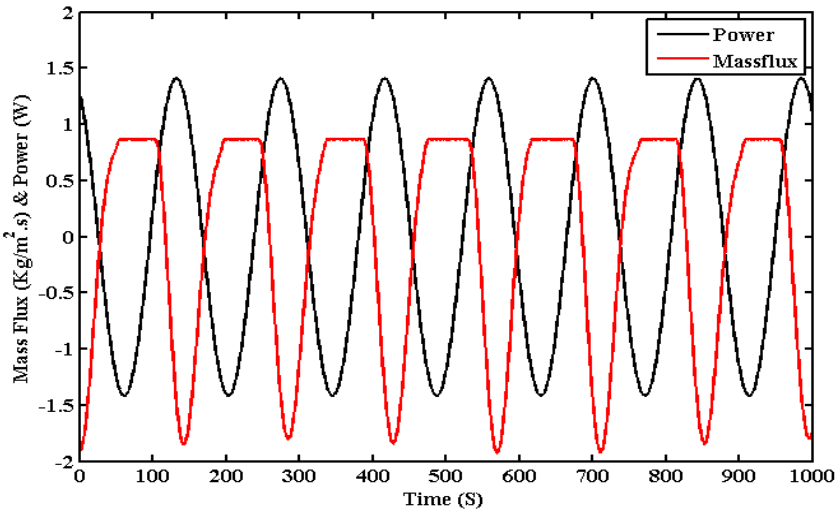

(C) Time series of mass flux and pulsating power

Figure 20: *System dynamics for base input power of 675W at 7% amplitude and frequency ratio 0.45*

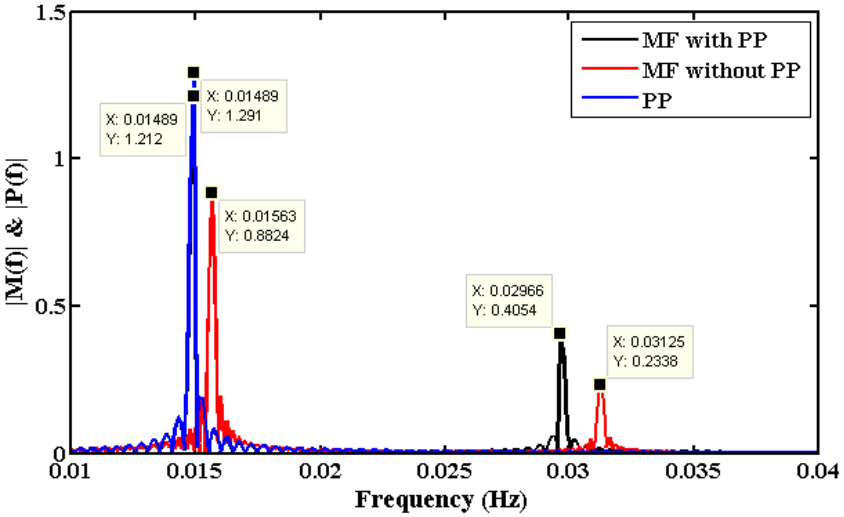

(A) FFT Plot

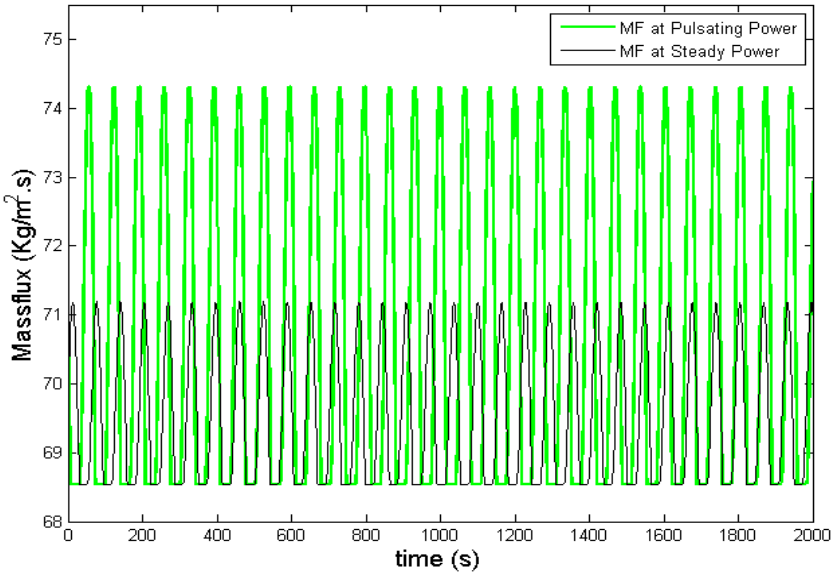

(B) Time series of mass flux under constant power vs pulsating power

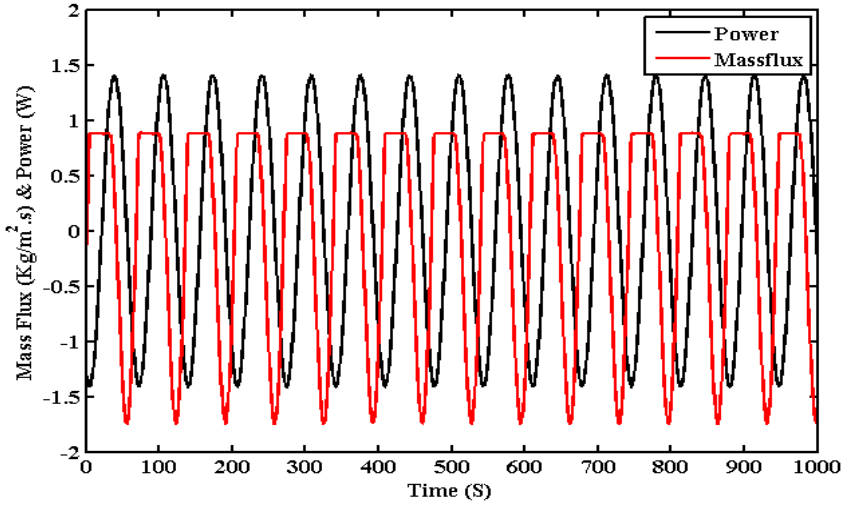

(C) Time series of mass flux and pulsating power

Figure 21: *System dynamics for base input power of 675W at 7% amplitude and frequency ratio 0.95*

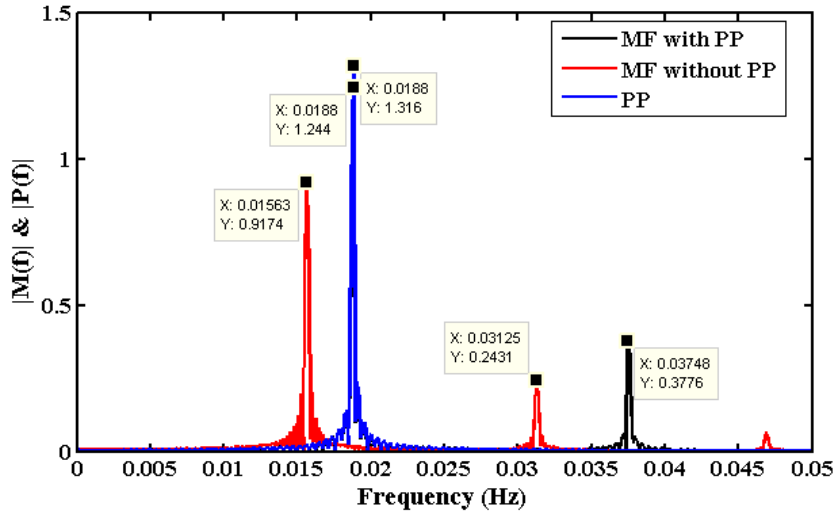

(A) FFT Plot

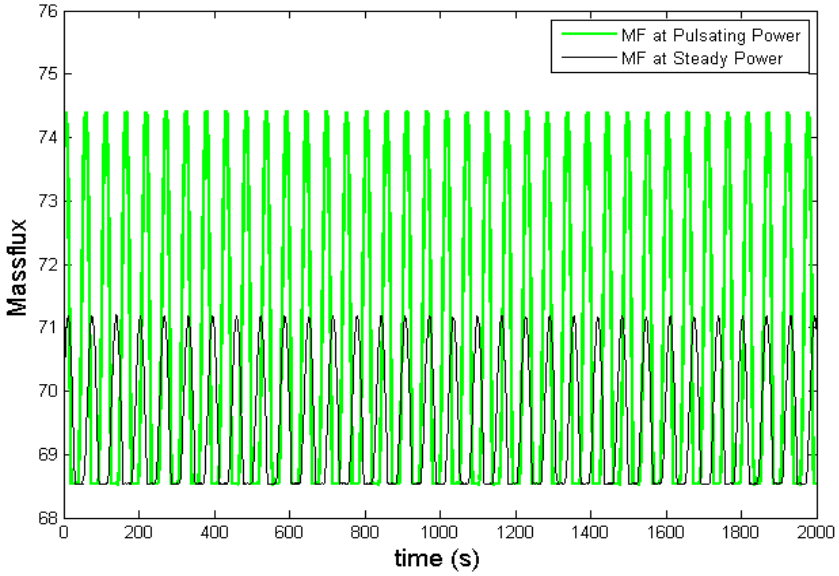

(B) Time series of mass flux under constant power vs pulsating power

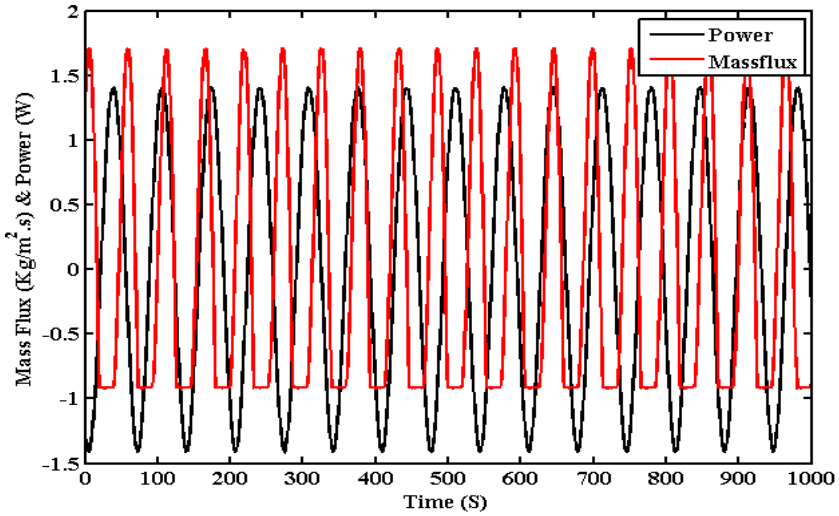

(C) Time series of mass flux and pulsating power

Figure 22: *System dynamics for base input power of 675W at 7% amplitude and frequency ratio 1.20*

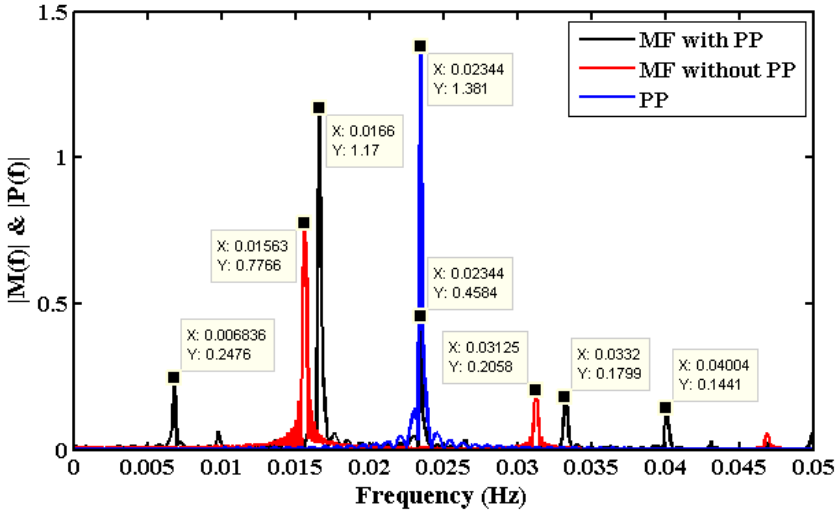

(A) FFT Plot

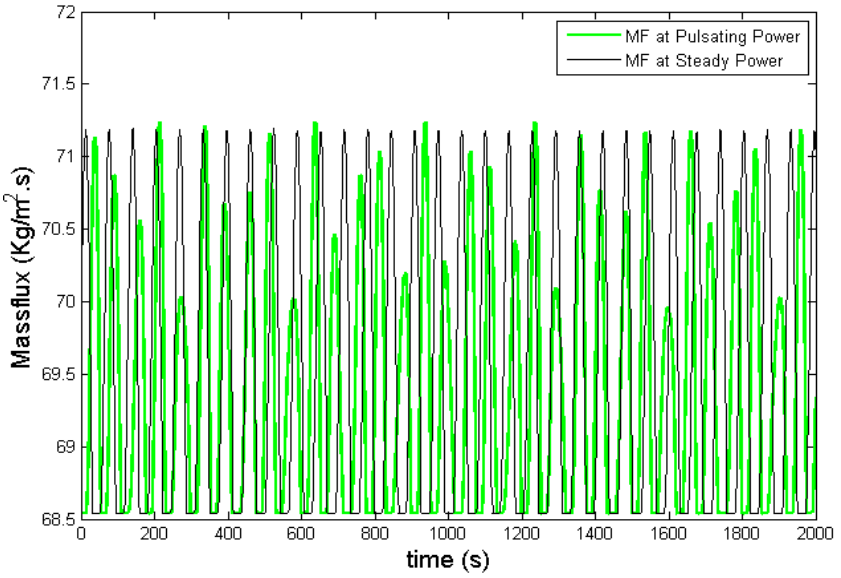

(B) Time series of mass flux under constant power vs pulsating power

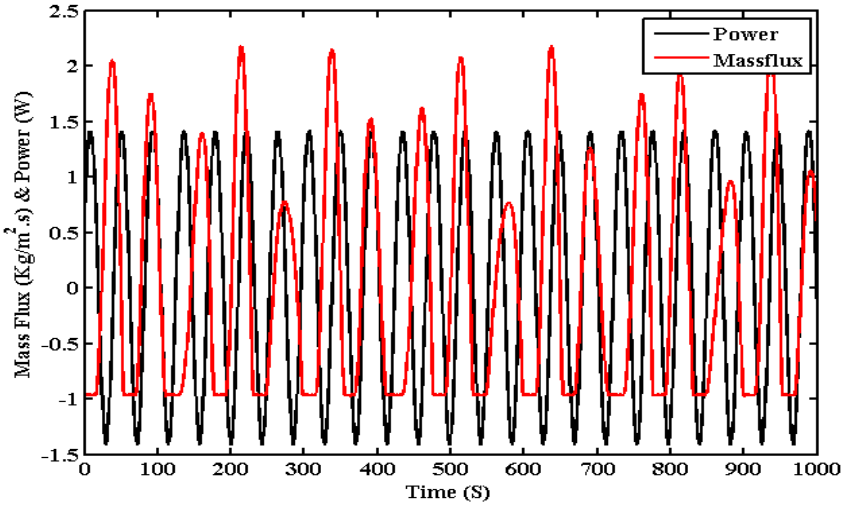

(C) Time series of mass flux and pulsating power

Figure 23: *System dynamics for base input power of 675W at 7% amplitude and frequency ratio 1.50*

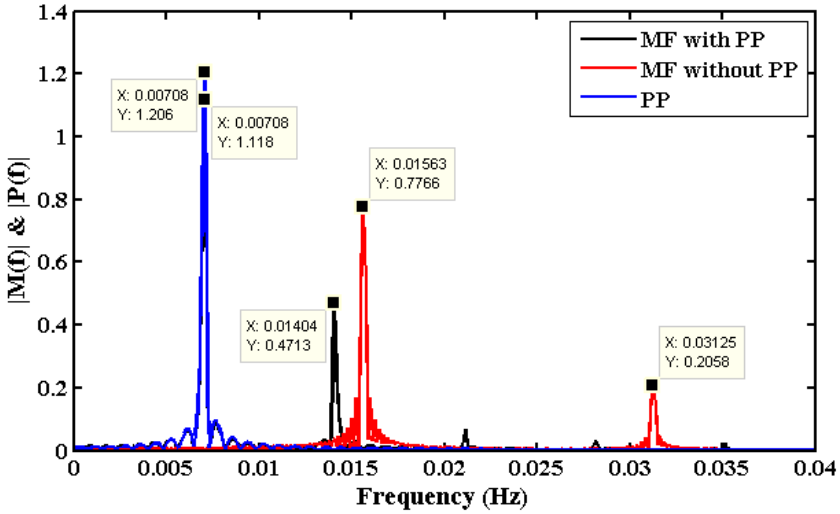

(A) FFT Plot

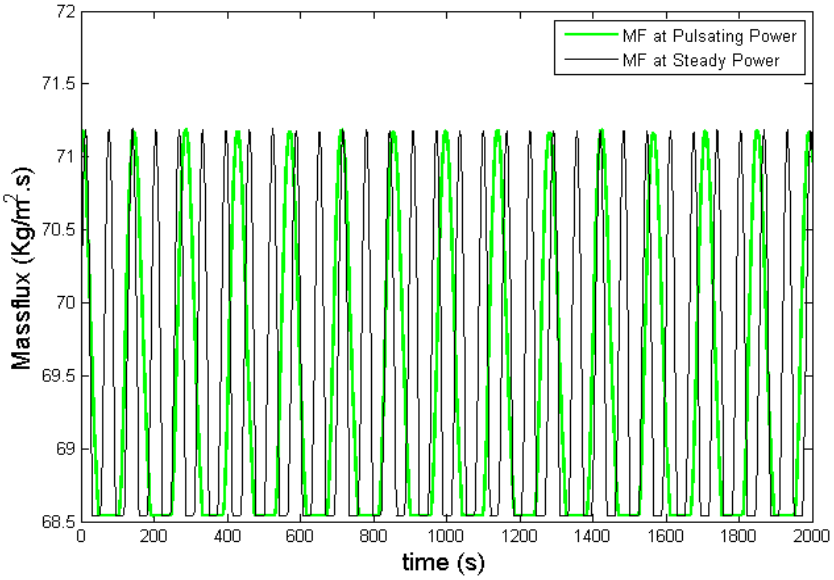

(B) Time series of mass flux under constant power vs pulsating power

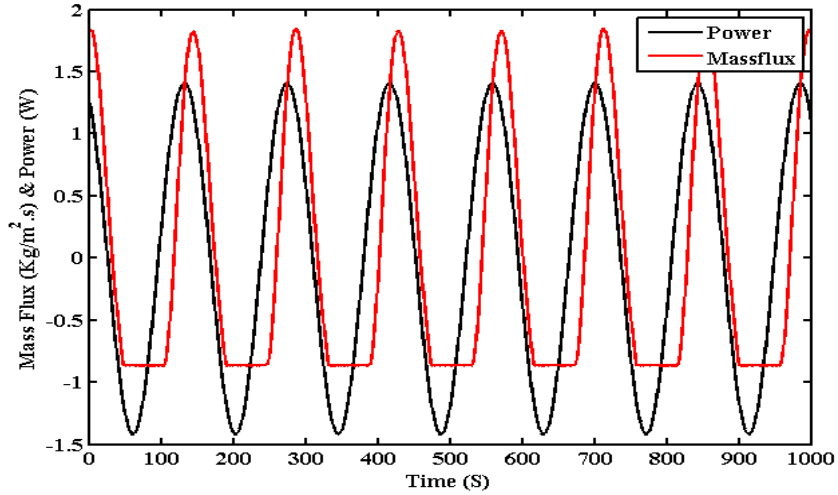

(C) Time series of mass flux and pulsating power

Figure 24*: System dynamics for base input power of 675W at 10% amplitude and frequency ratio 0.45*

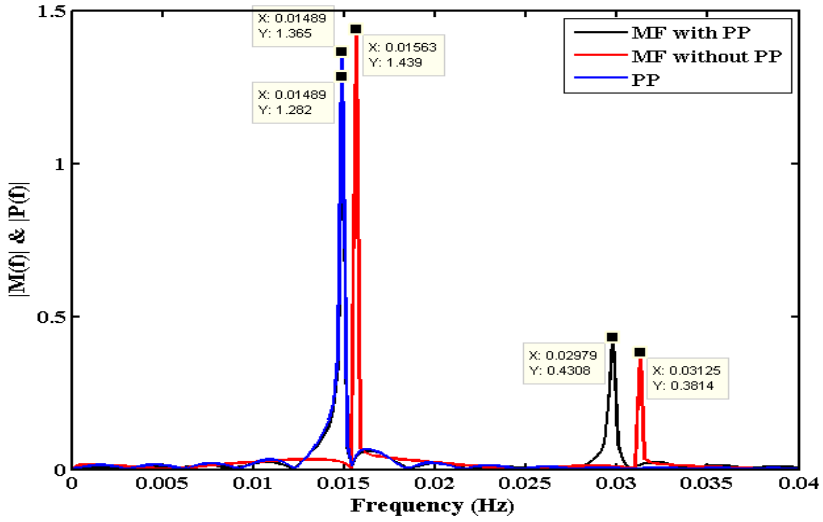

(A) FFT Plot

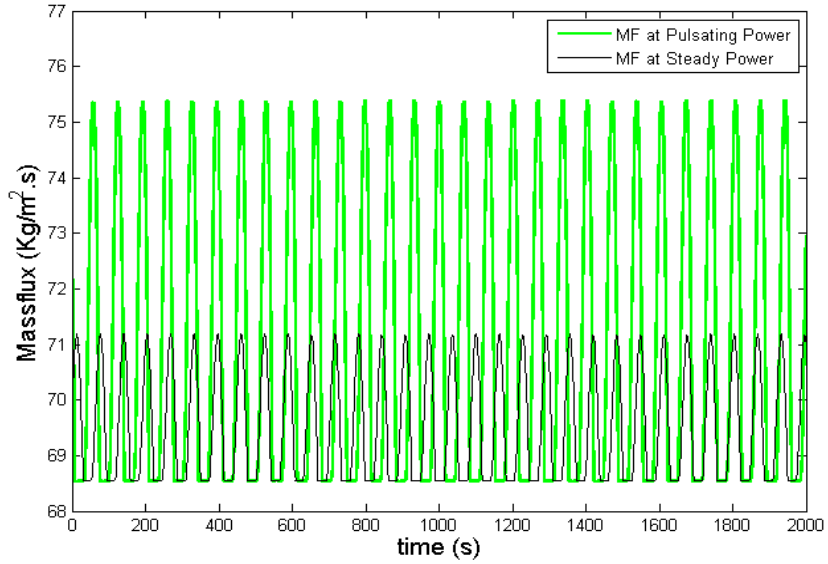

(B) Time series of mass flux under constant power vs pulsating power

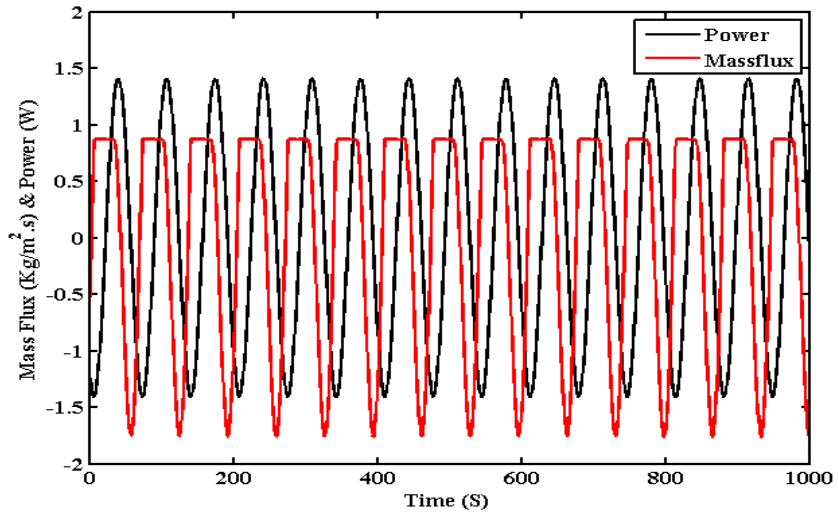

(C) Time series of mass flux and pulsating power

Figure 25*: System dynamics for base input power of 675W at 10% amplitude and frequency ratio 0.95*

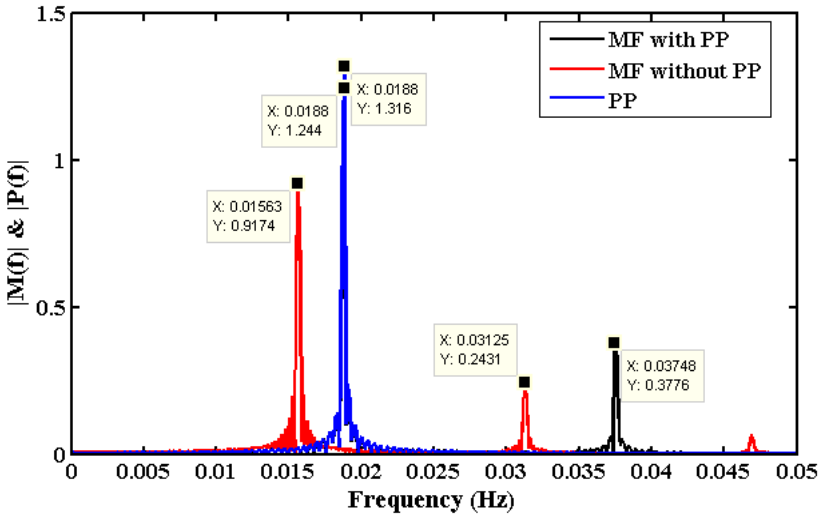

(A) FFT Plot

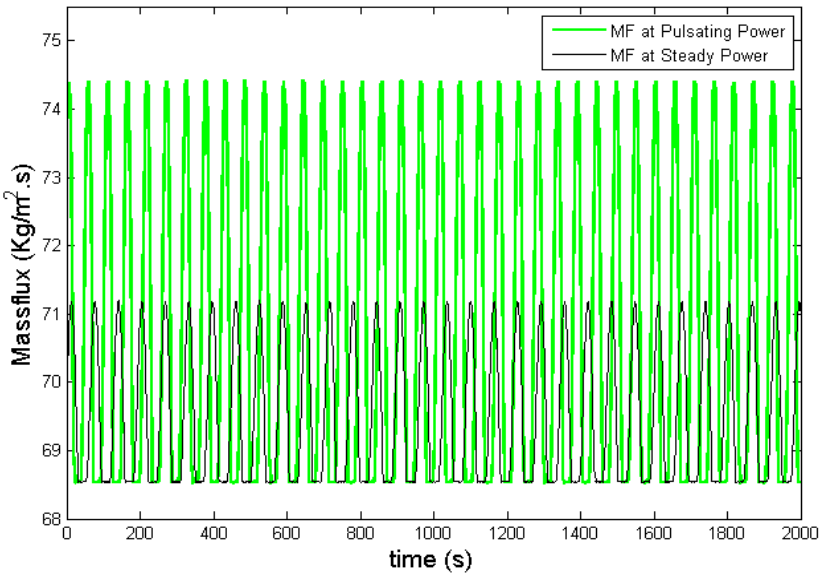

(B) Time series of mass flux under constant power vs pulsating power

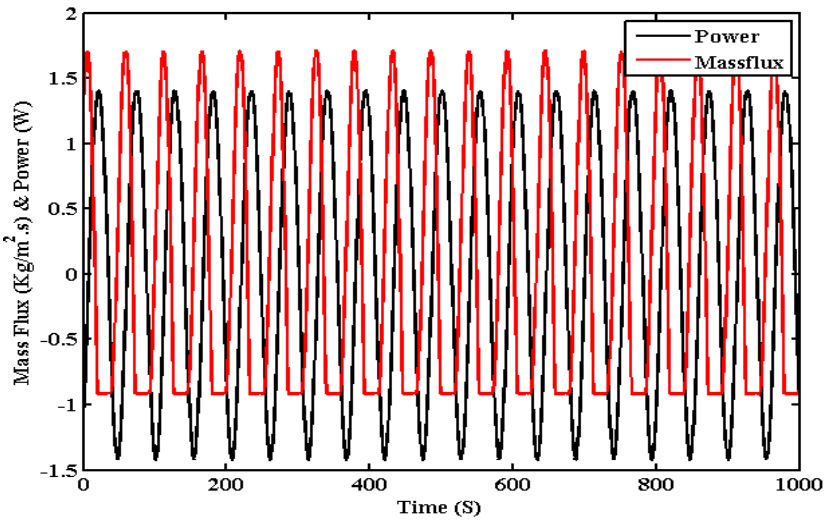

(C) Time series of mass flux and pulsating power

Figure 26*: System dynamics for base input power of 675W at 10% amplitude and frequency ratio 1.20*

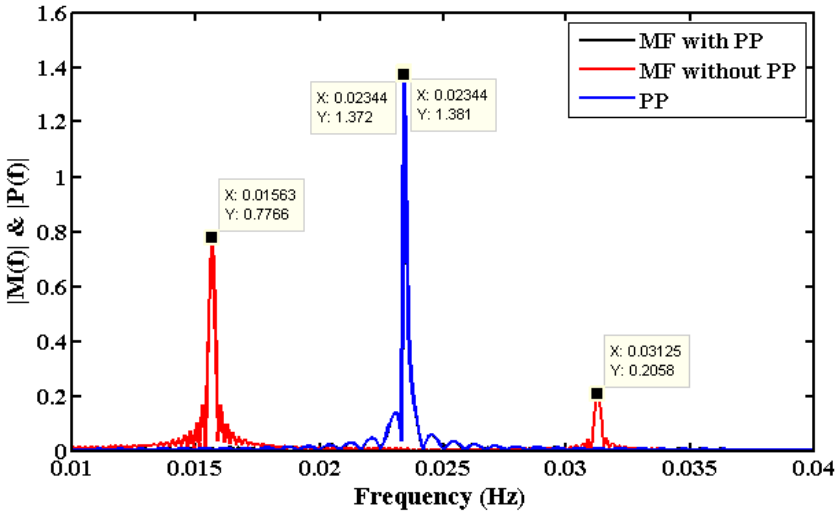

(A) FFT Plot

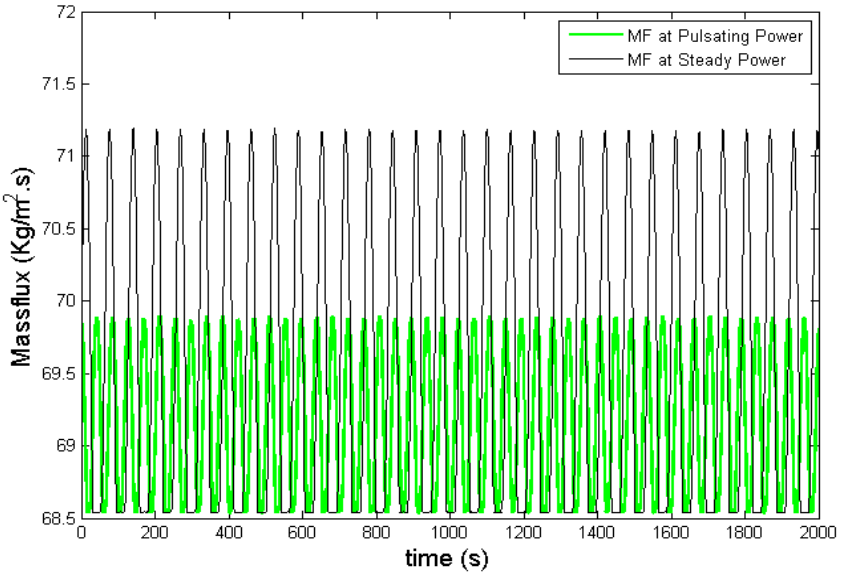

(B) Time series of mass flux under constant power vs pulsating power

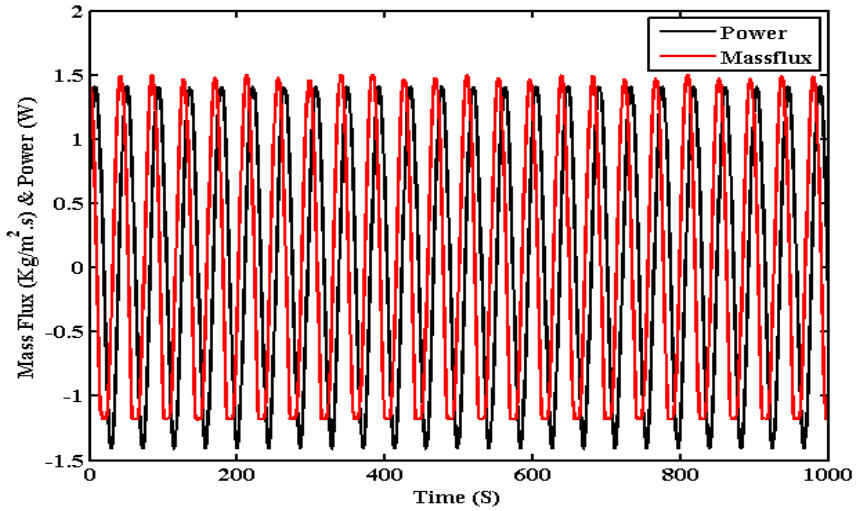

(C) Time series of mass flux and pulsating power

Figure 27: *System dynamics for base input power of 675W at 10% amplitude and frequency ratio 1.50*

The observations of the response dynamics of the natural circulation system, when subjected to an external pulsating power at 5%, 7% and 10% fluctuating amplitude for input power of 700 W show almost identical behaviour of the system's response dynamics as seen before for 675 W.

However, the for a given forcing amplitude, the frequency required for the system to entrain and enter into a phase locked condition with the power perturbation is higher as compared to that for input power equal to 675 W. For 7% and 10 % fluctuating amplitude, phase locking for a input power of 675 W takes place for a forcing frequency ratio value as low as 0.45. But to achieve the same at 700 W input power, the minimum frequency ratio value must be 0.90. also the frequency lock-in regime for 700 W at a given amplitude, is less than the same for 675 W. Apart from this, the amplification of the mass flux oscillation for the same parameters of external forcing, when applied to 700 W input power, is less than that observed for 675 W. the amplification of the oscillations for forcing frequency ratio close to 1 are not as much as that achieved for lower power. This might tell us that to achieve similar effect on two similar systems operating at different input power, the input parameters for the external forcing must be higher for higher input power level.

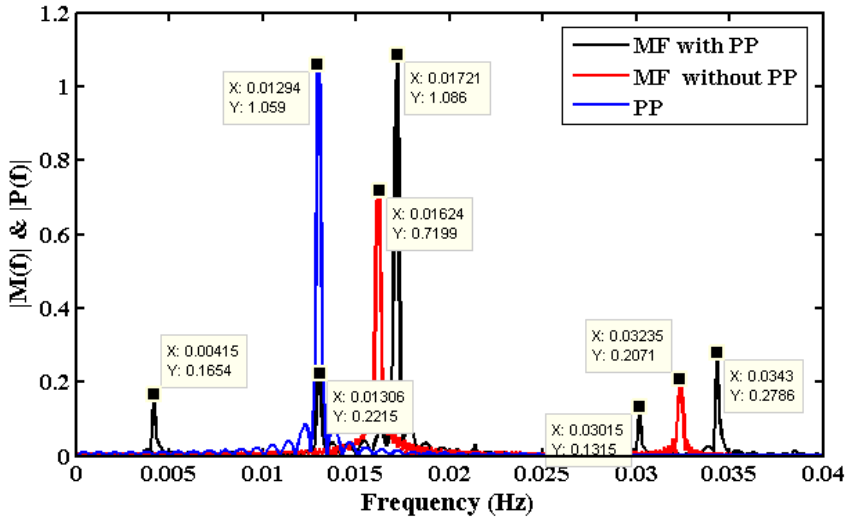

(A) FFT plot

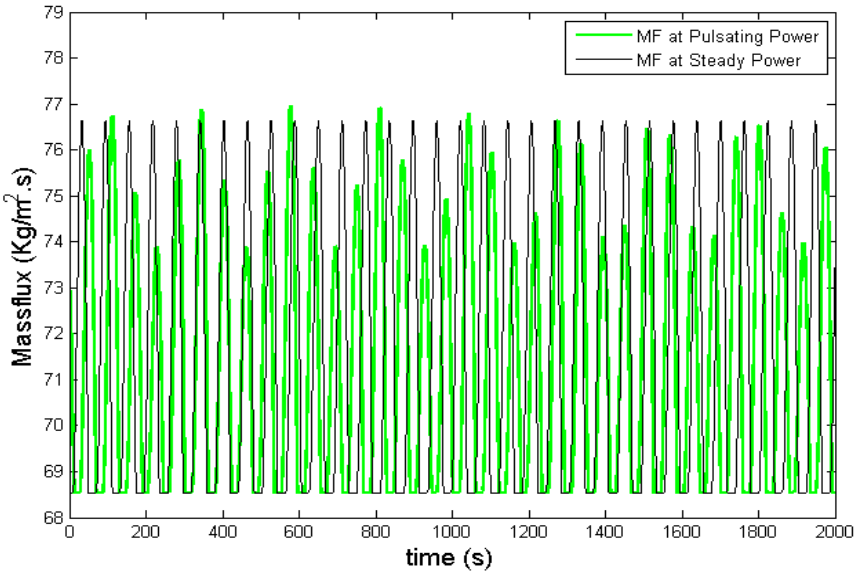

(B) Time series of mass flux under constant power vs pulsating power

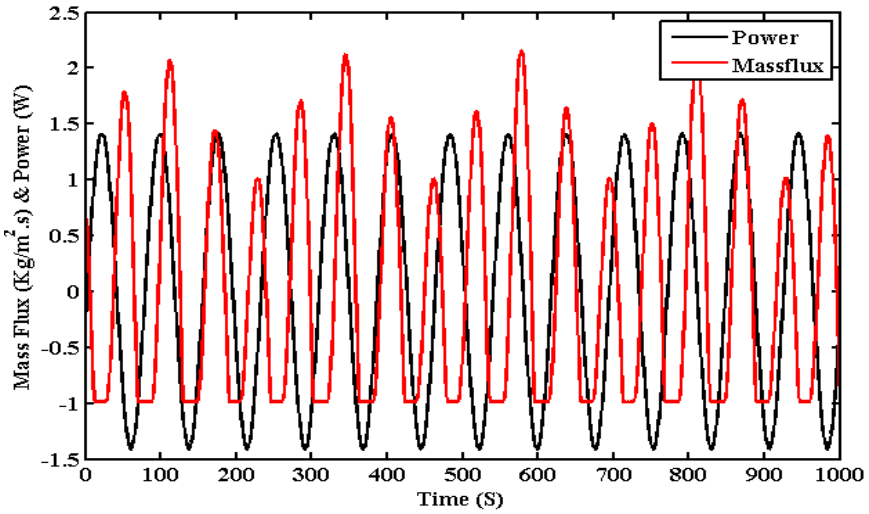

(C) Time series of mass flux and pulsating power

Figure 28: *System dynamics for base input power of 700W at 5% amplitude and frequency ratio 0.80*

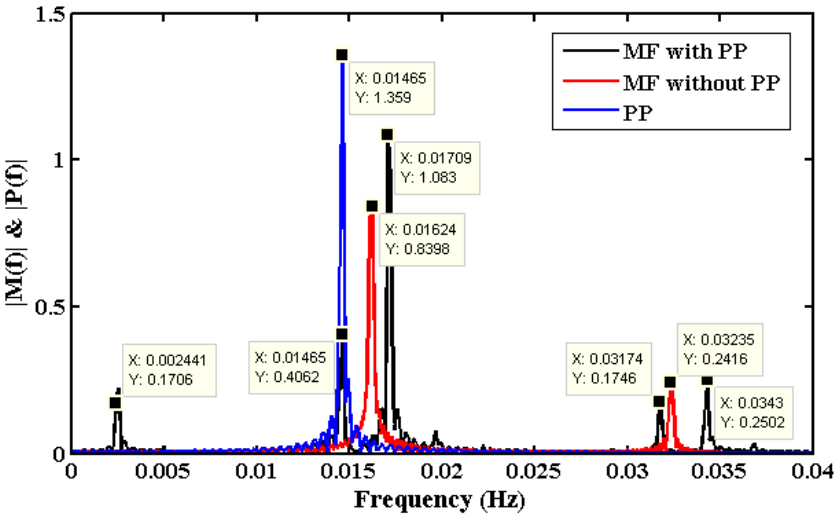

(A) FFT plot

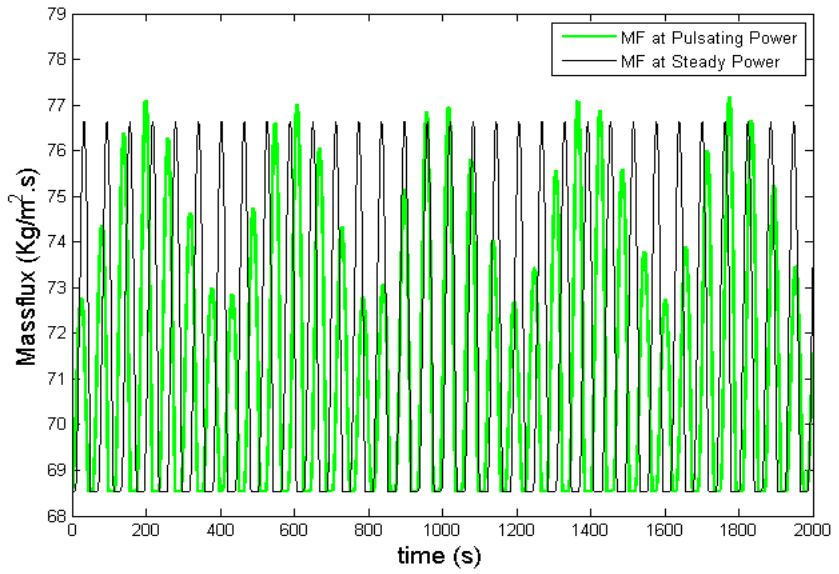

(B) Time series of mass flux under constant power vs pulsating power

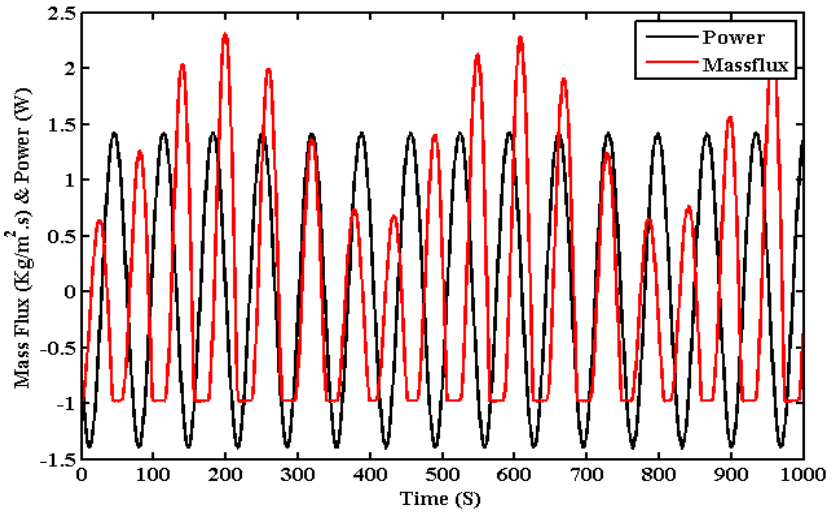

(C) Time series of mass flux and pulsating power

Figure 29: *System dynamics for base input power of 700W at 5% amplitude and frequency ratio 0.90*

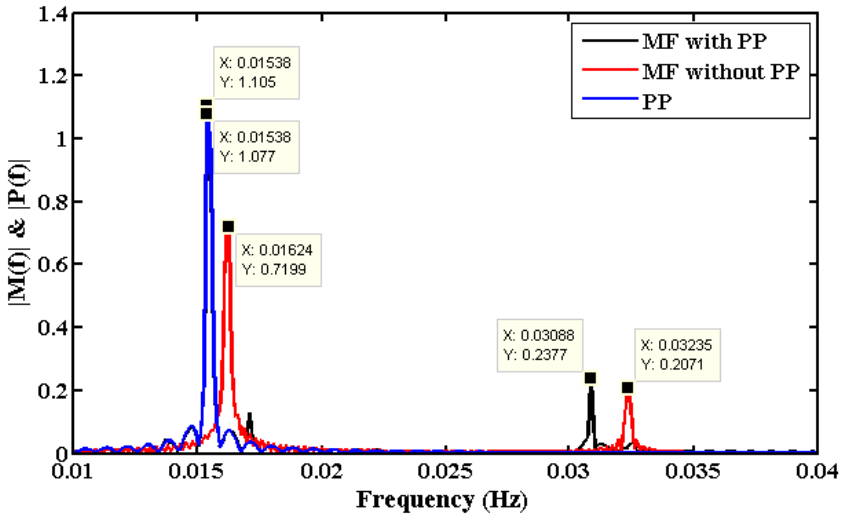

(A) FFT plot

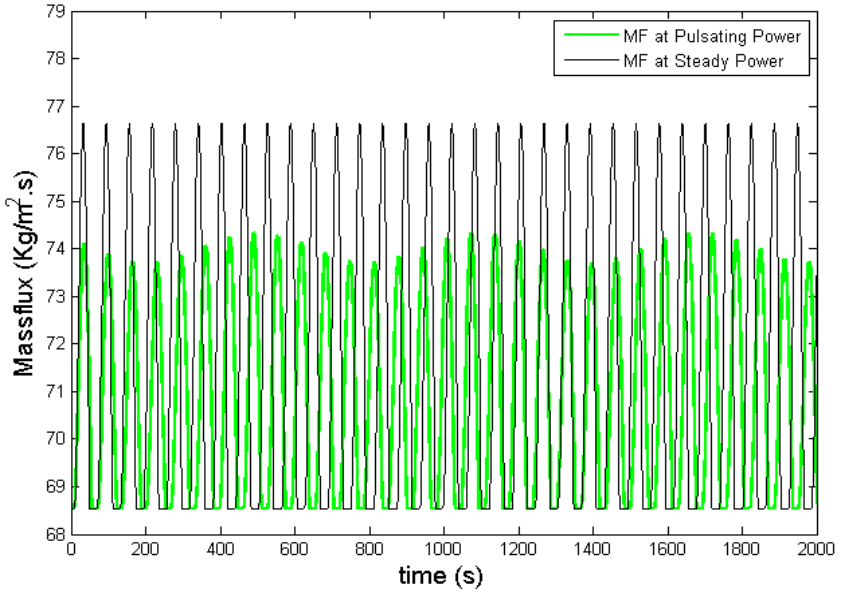

(B) Time series of mass flux under constant power vs pulsating power

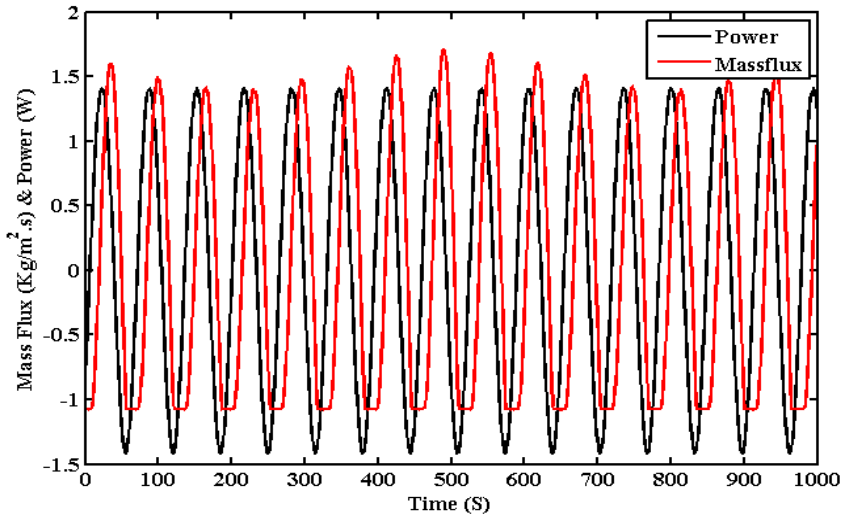

(C) Time series of mass flux and pulsating power

Figure 30: *System dynamics for base input power of 700W at 5% amplitude and frequency ratio 0.95*

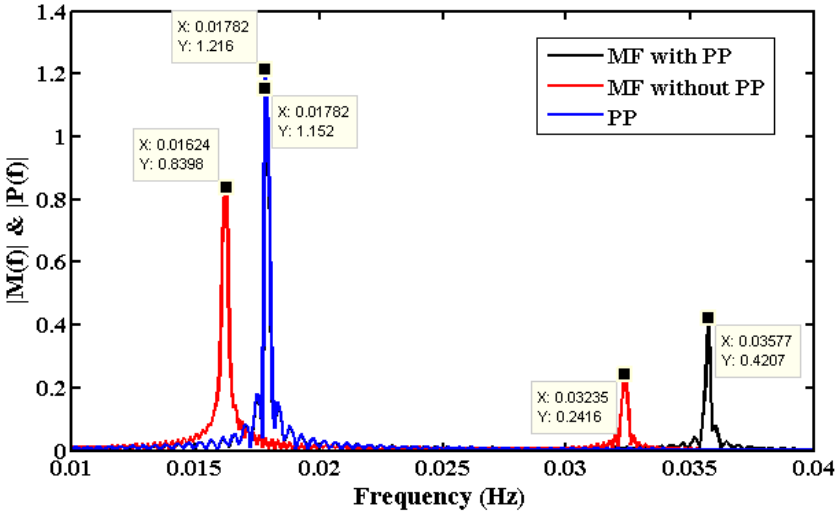

(A) FFT plot

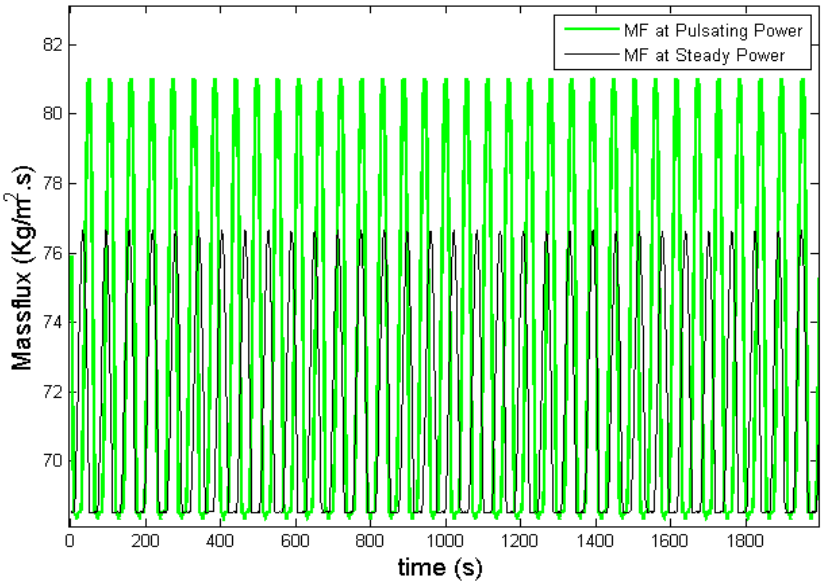

(B) Time series of mass flux under constant power vs pulsating power

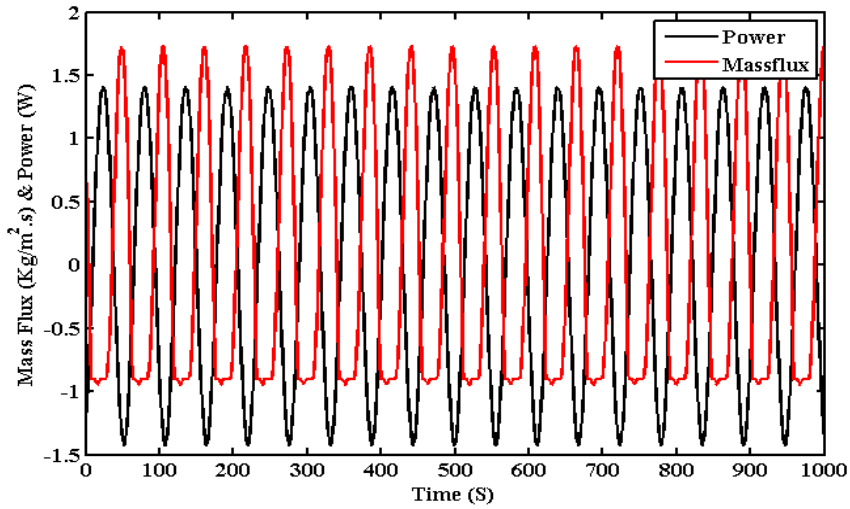

(C) Time series of mass flux and pulsating power

Figure 31: *System dynamics for base input power of 700W at 5% amplitude and frequency ratio 1.1*

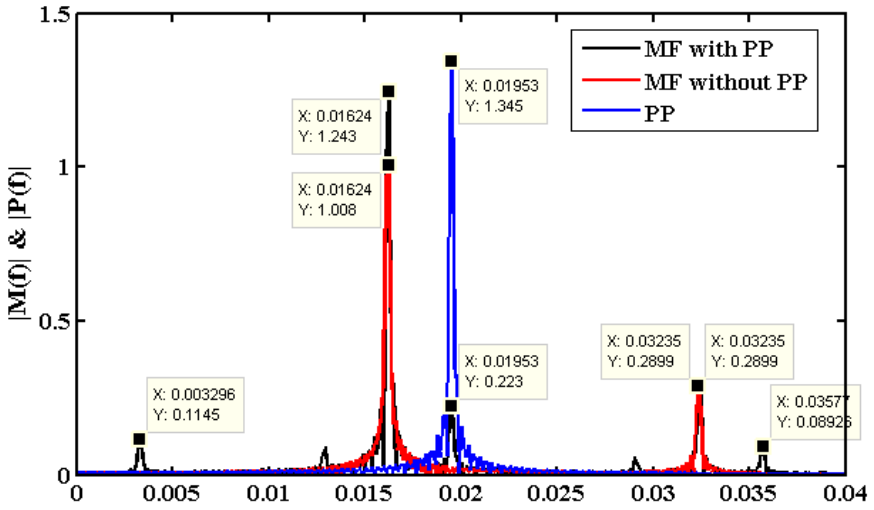

(A) FFT plot

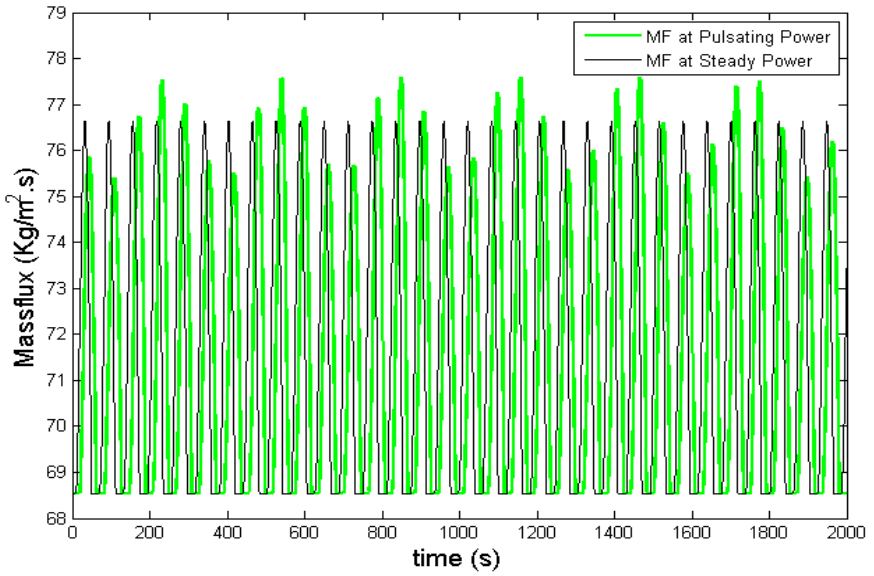

(B) Time series of mass flux under constant power vs pulsating power

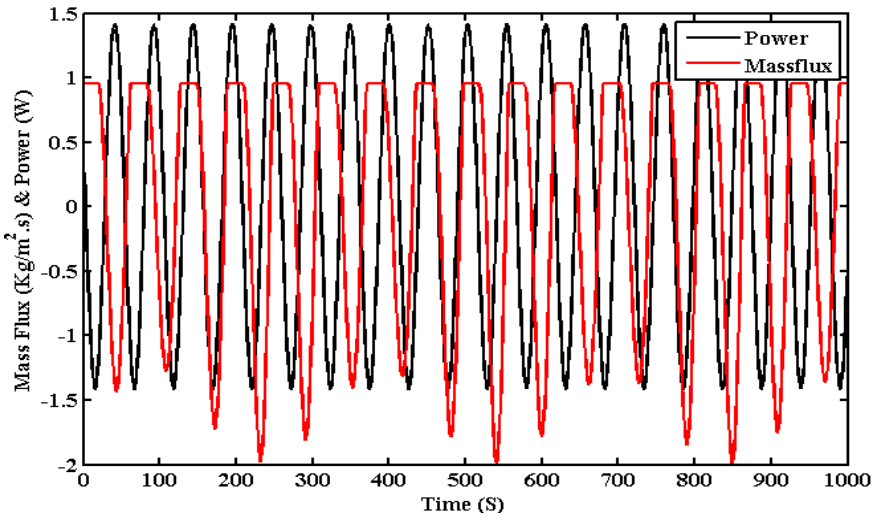

(C) Time series of mass flux and pulsating power

Figure 32: *System dynamics for base input power of 700W at 5% amplitude and frequency ratio 1.2*

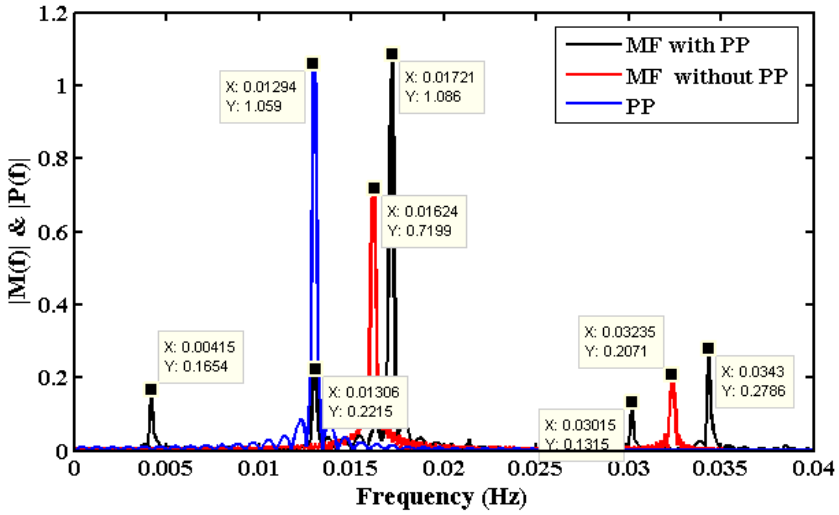

(A) FFT plot

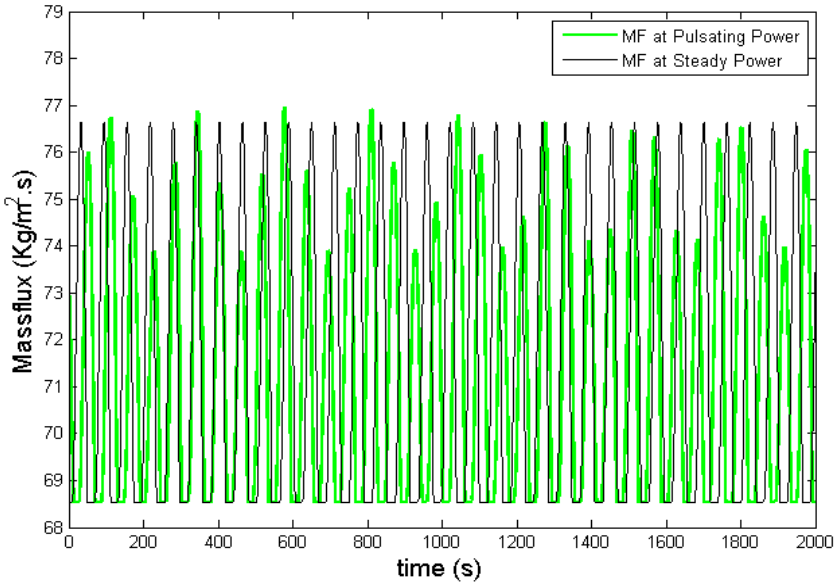

(B) Time series of mass flux under constant power vs pulsating power

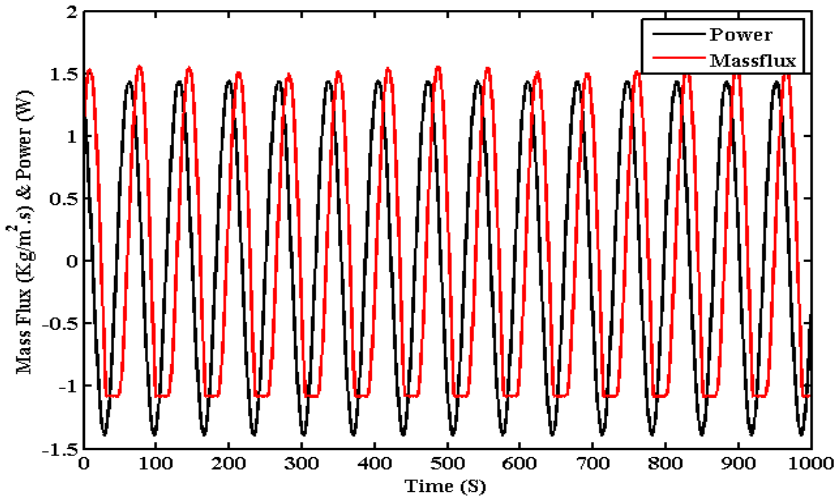

(C) Time series of mass flux and pulsating power

Figure 33: *System dynamics for base input power of 700W at 7% amplitude and frequency ratio 0.80*

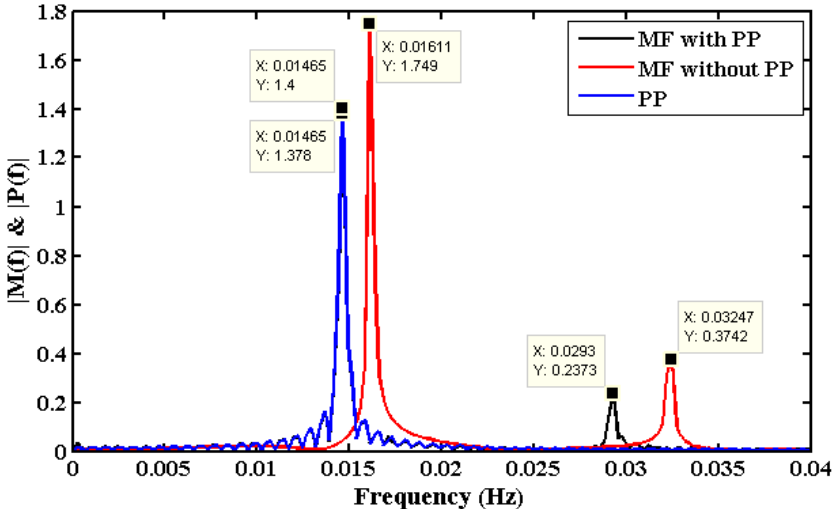

(A) FFT plot

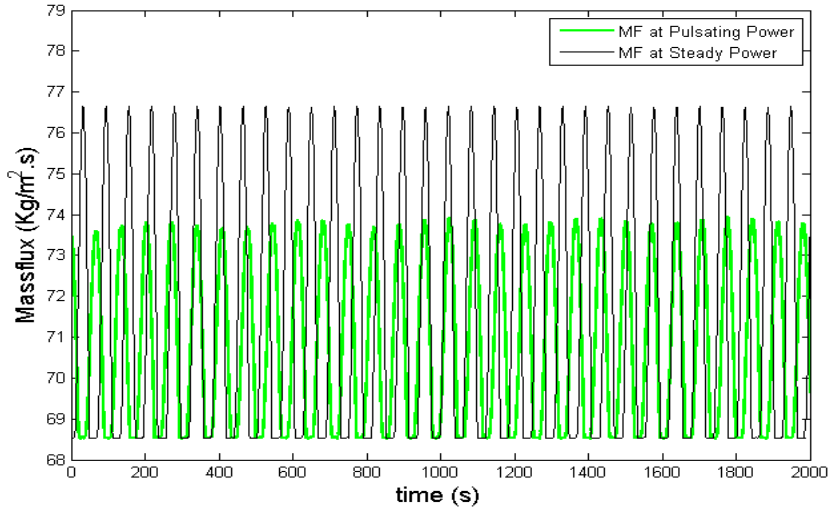

(B) Time series of mass flux under constant power vs pulsating power

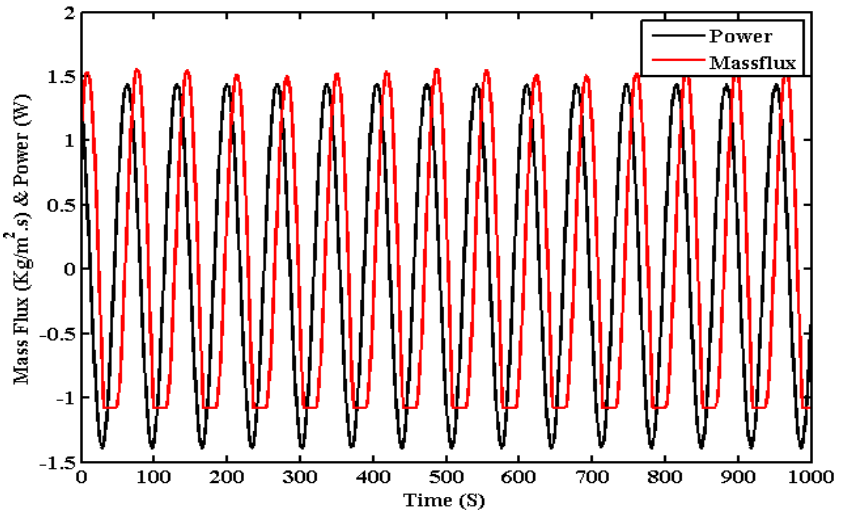

(C) Time series of mass flux and pulsating power

Figure 34: *System dynamics for base input power of 700W at 7% amplitude and frequency ratio 0.90*

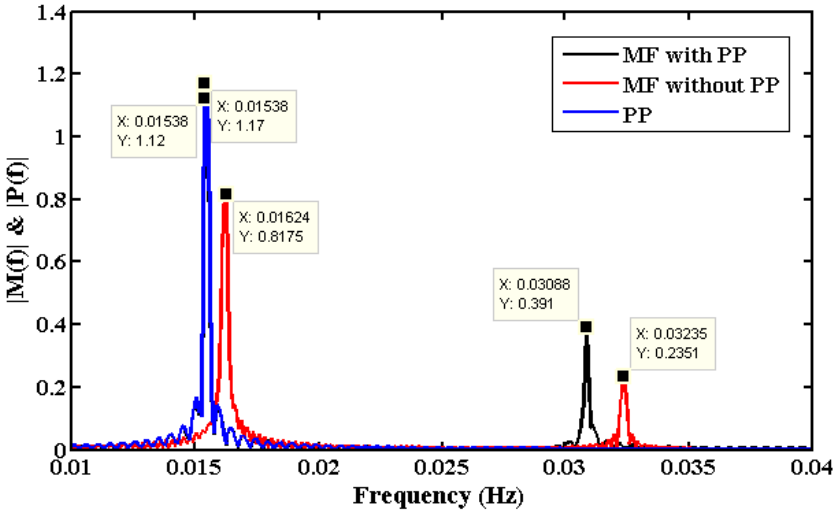

(A) FFT plot

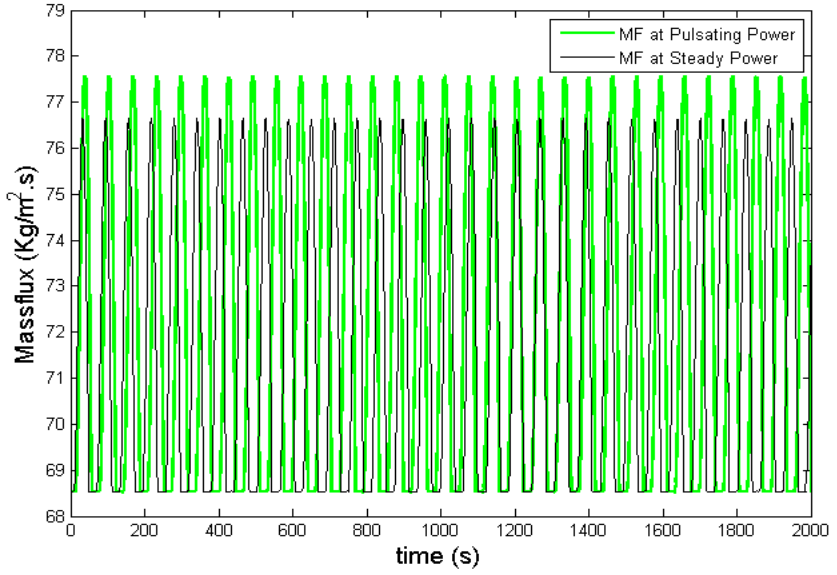

(B) Time series of mass flux under constant power vs pulsating power

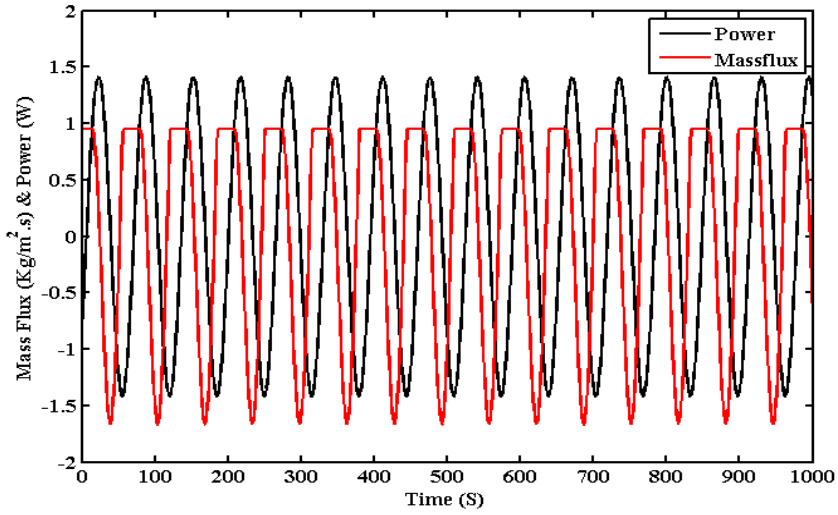

(C) Time series of mass flux and pulsating power

Figure 35: *System dynamics for base input power of 700W at 7% amplitude and frequency ratio 0.95*

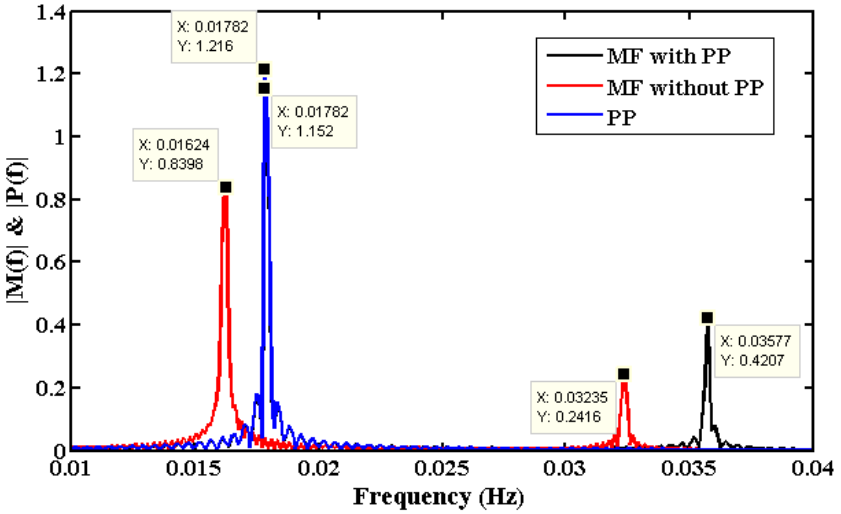

(A) FFT plot

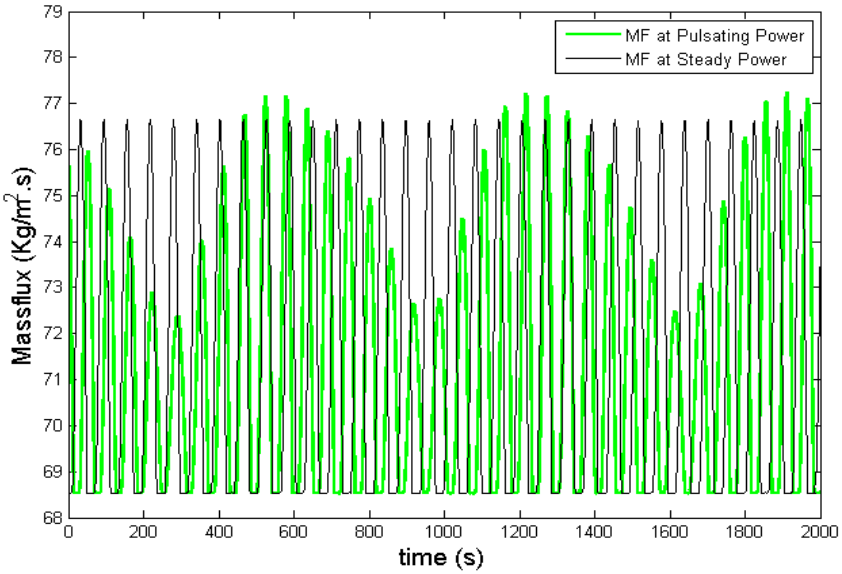

(B) Time series of mass flux under constant power vs pulsating power

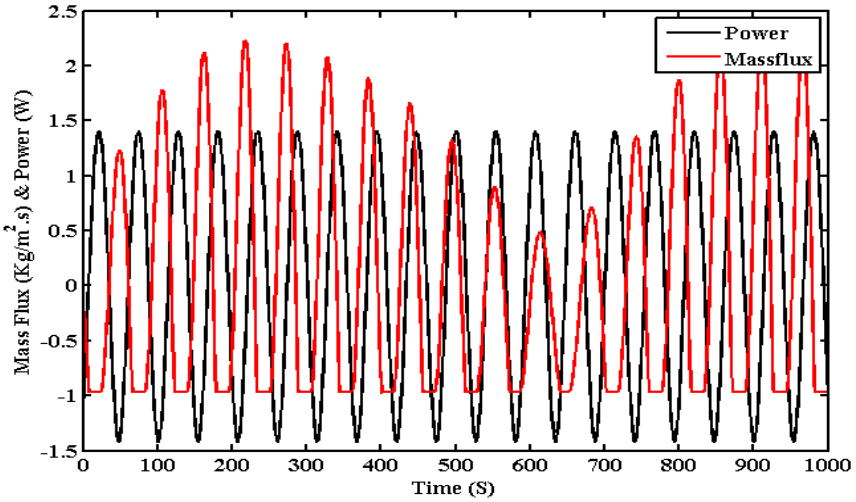

(C) Time series of mass flux and pulsating power

Figure 36: *System dynamics for base input power of 700W at 7% amplitude and frequency ratio 1.10*

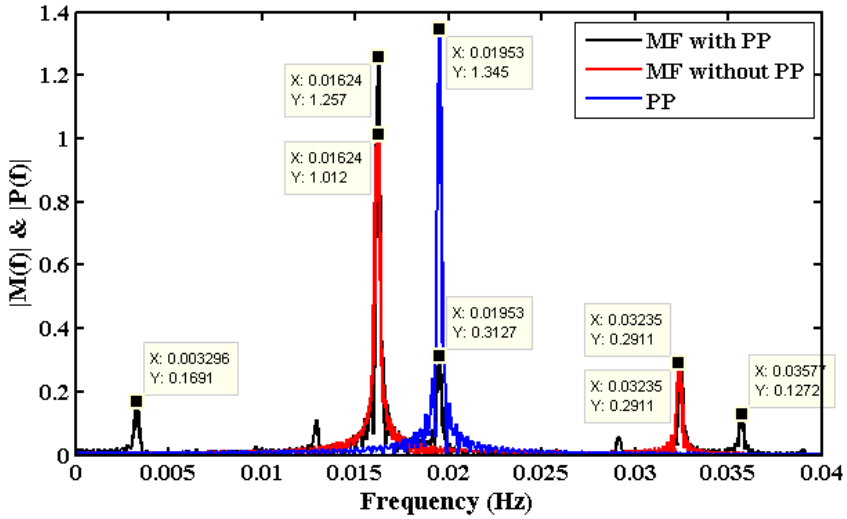

(A) FFT plot

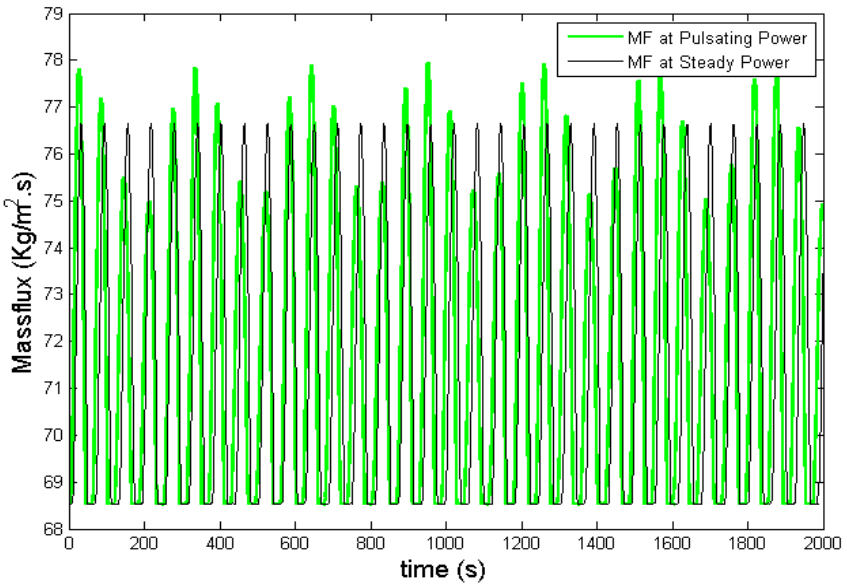

(B) Time series of mass flux under constant power vs pulsating power

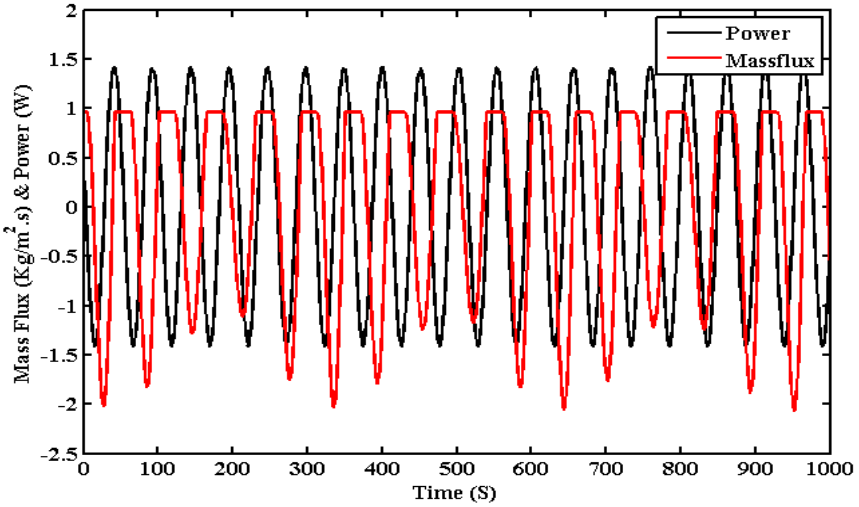

(C) Time series of mass flux and pulsating power

Figure 37: *System dynamics for base input power of 700W at 7% amplitude and frequency ratio 1.20*

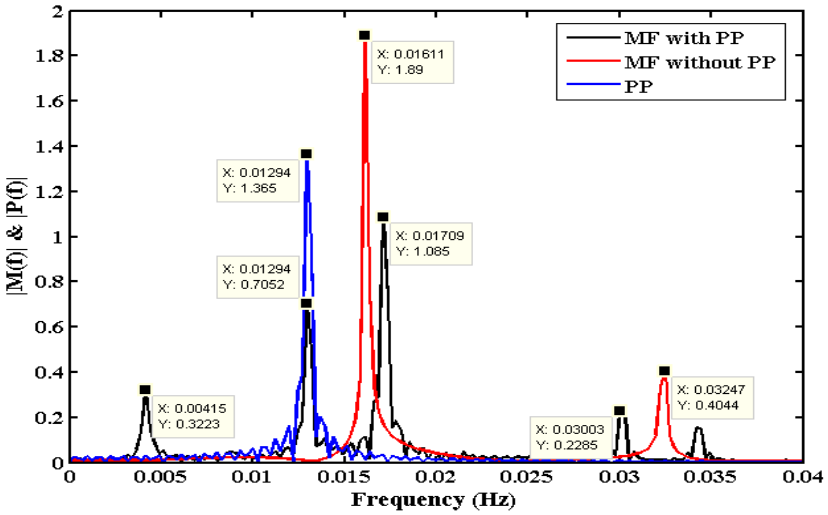

(A) FFT plot

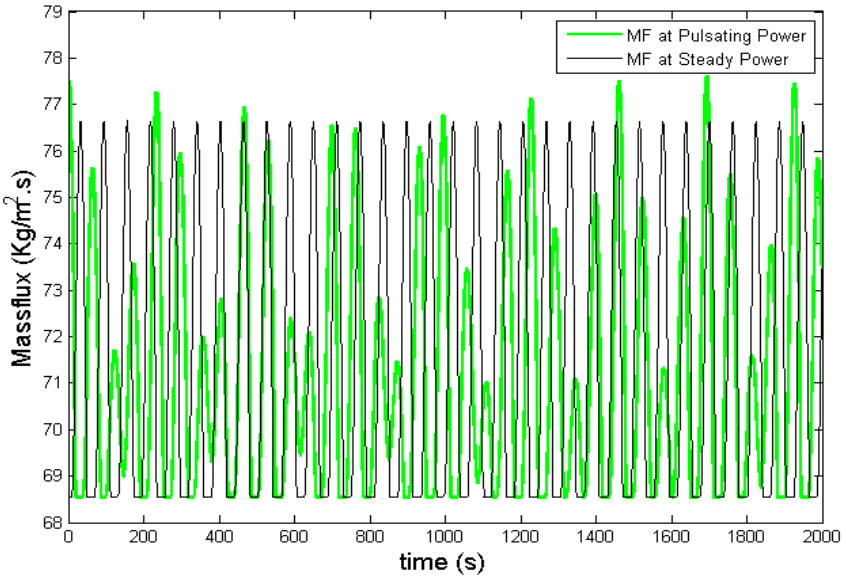

(B) Time series of mass flux under constant power vs pulsating power

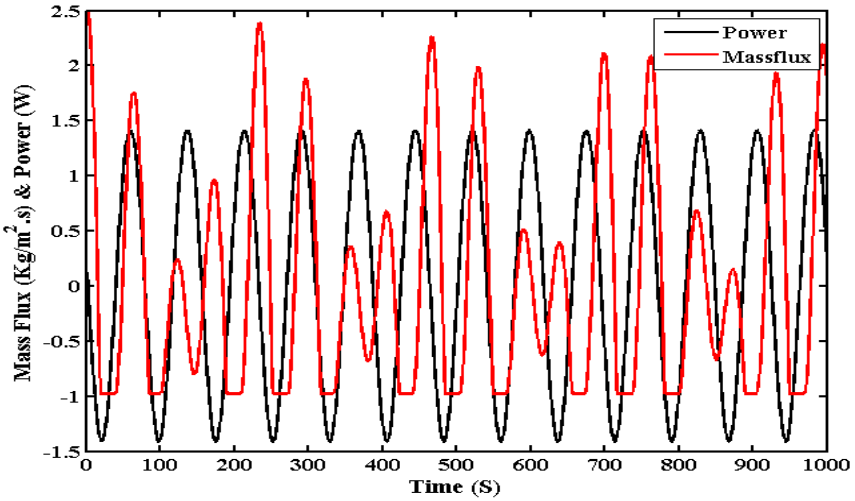

(C) Time series of mass flux and pulsating power

Figure 38: *System dynamics for base input power of 700W at 10% amplitude and frequency ratio 0.80*

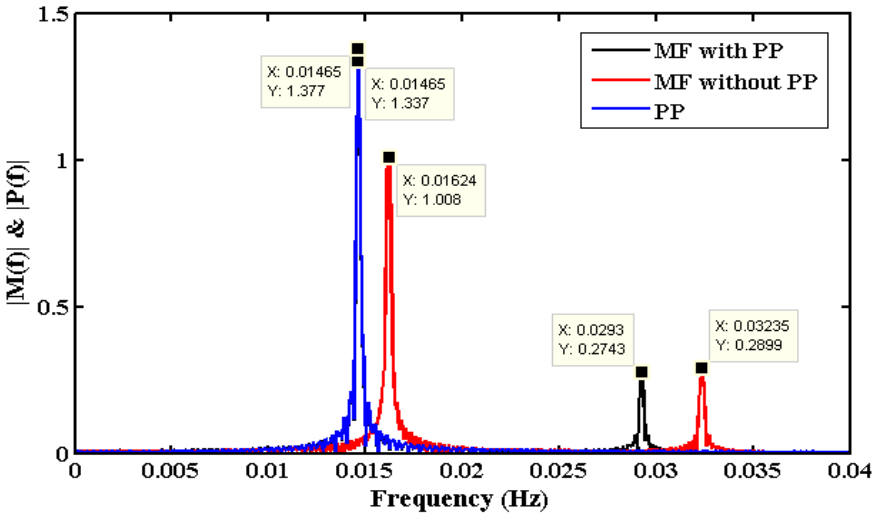

(A) FFT plot

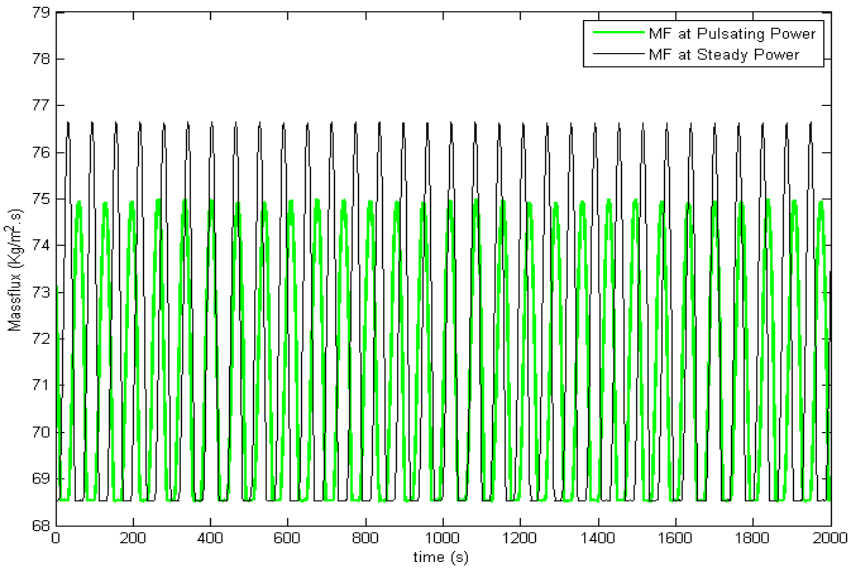

(B) Time series of mass flux under constant power vs pulsating power

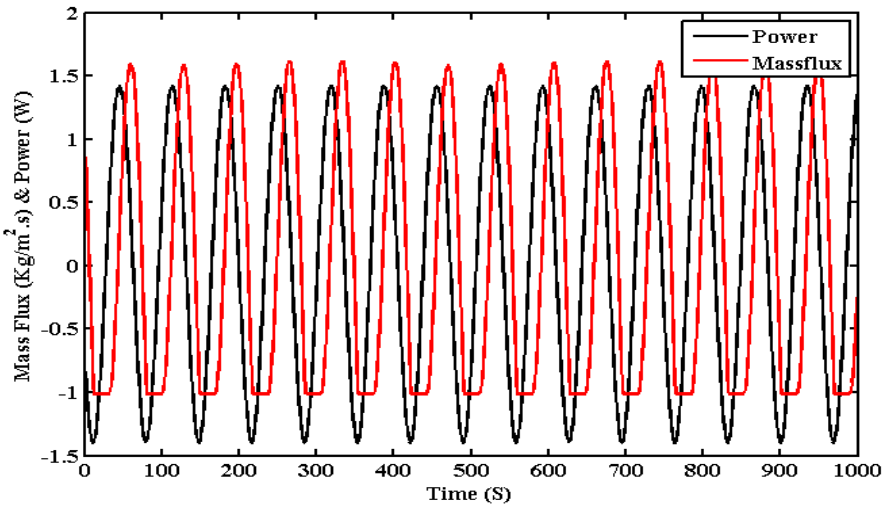

(C) Time series of mass flux and pulsating power

Figure 39: *System dynamics for base input power of 700W at 10% amplitude and frequency ratio 0.90*

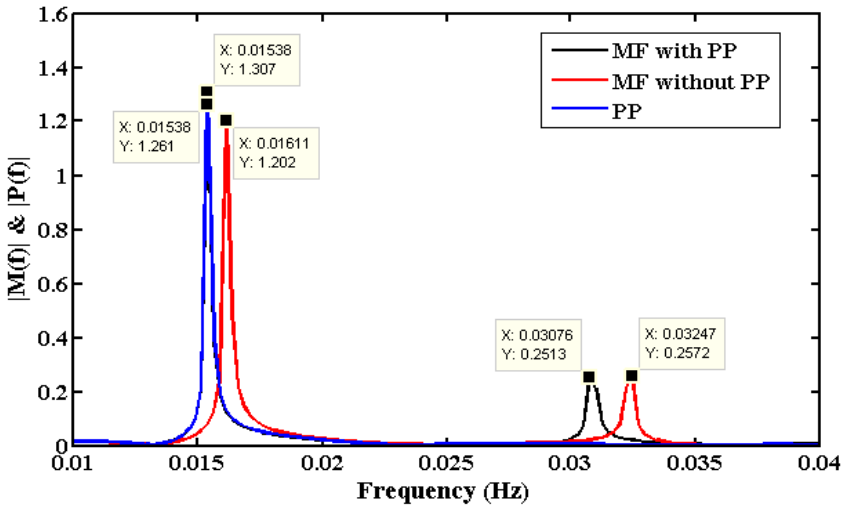

(A) FFT plot

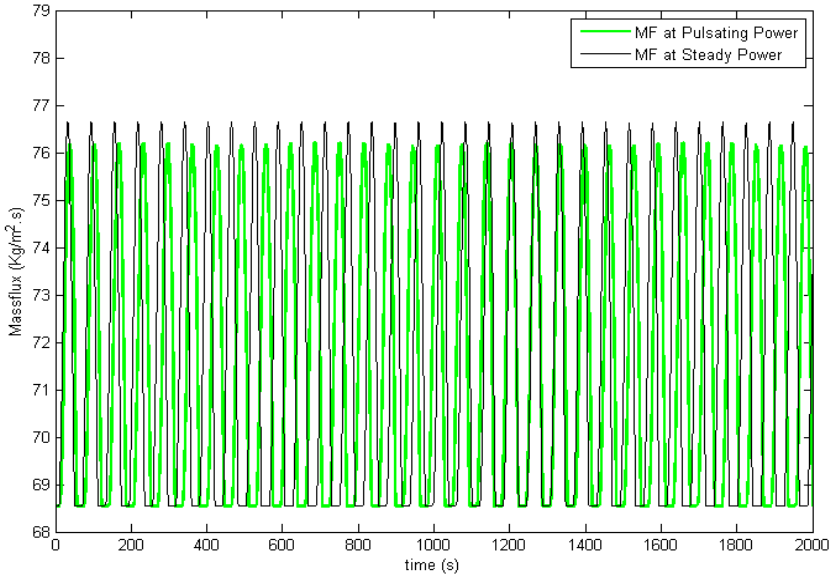

(B) Time series of mass flux under constant power vs pulsating power

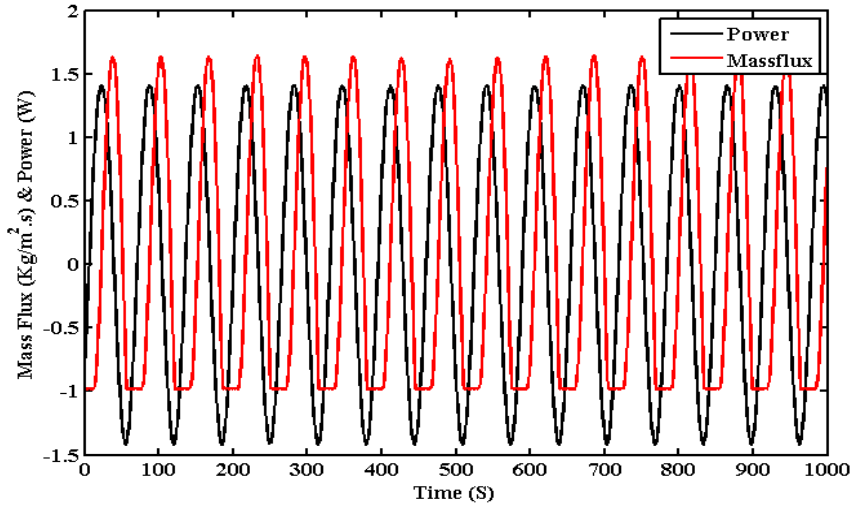

(C) Time series of mass flux and pulsating power

Figure 40: *System dynamics for base input power of 700W at 10% amplitude and frequency ratio 0.95*

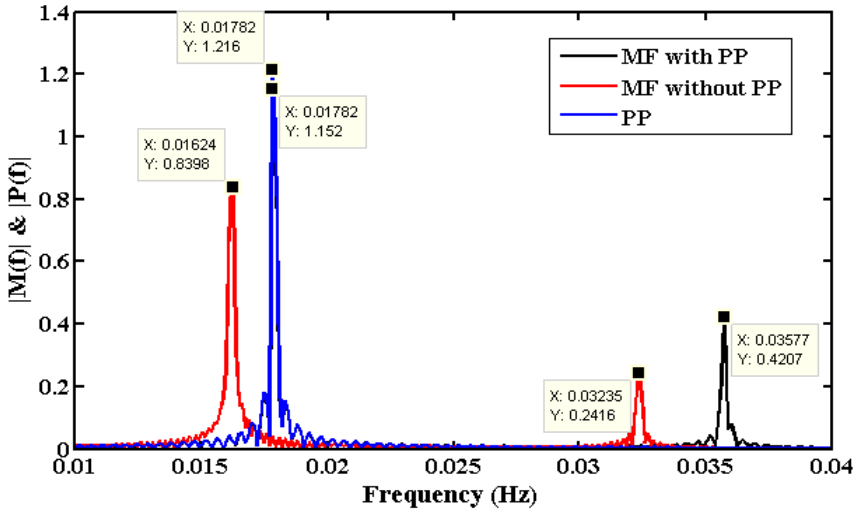

(A) FFT plot

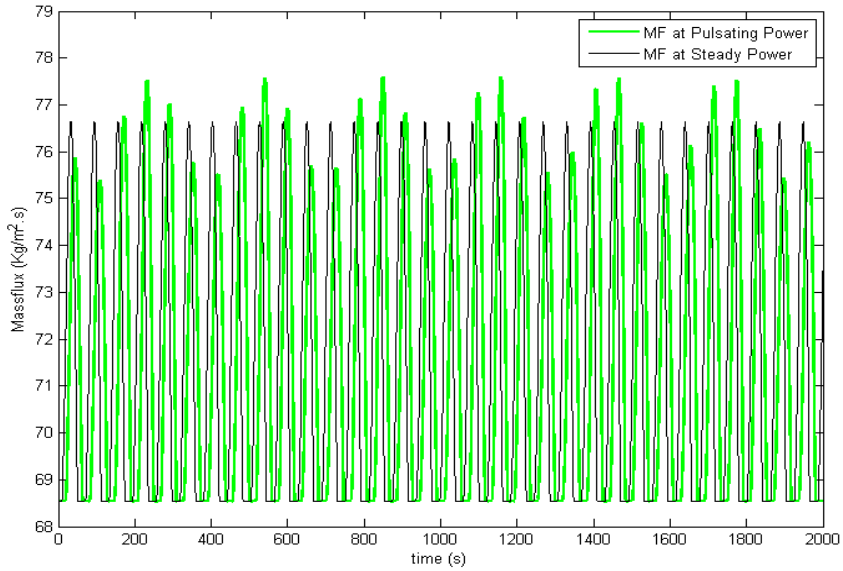

(B) Time series of mass flux under constant power vs pulsating power

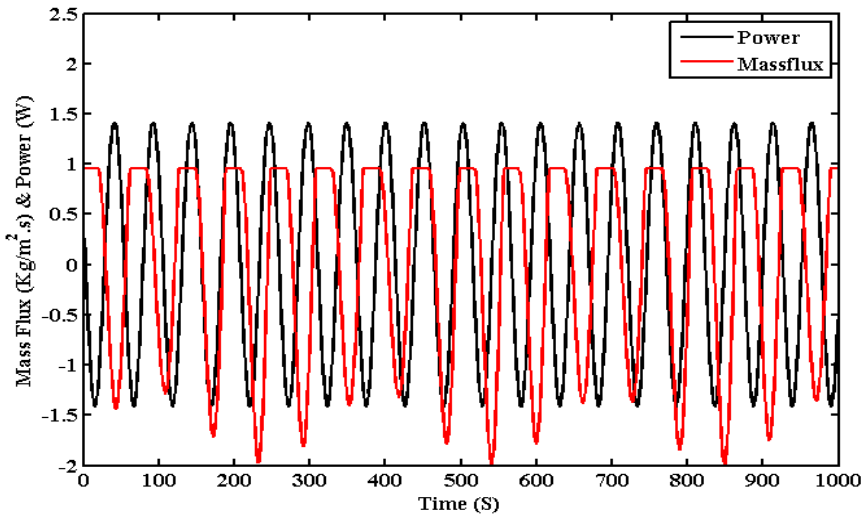

(C) Time series of mass flux and pulsating power

Figure 41: *System dynamics for base input power of 700W at 10% amplitude and frequency ratio 1.10*

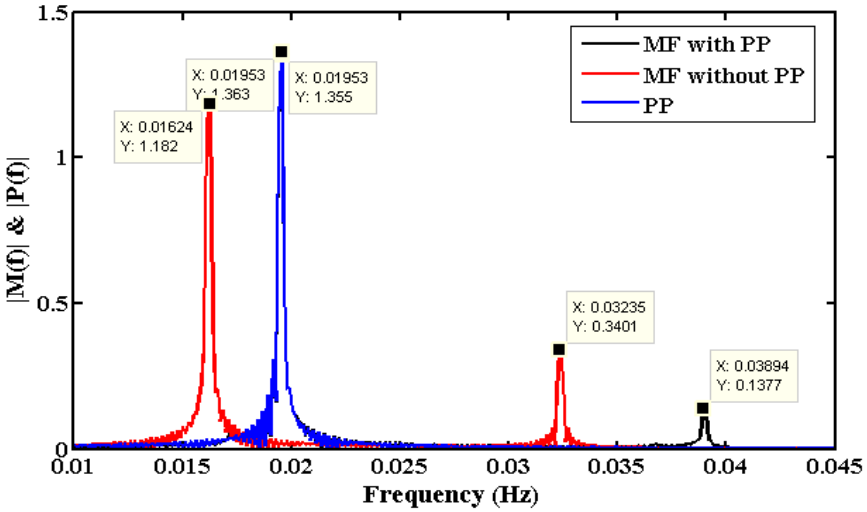

(A) FFT plot

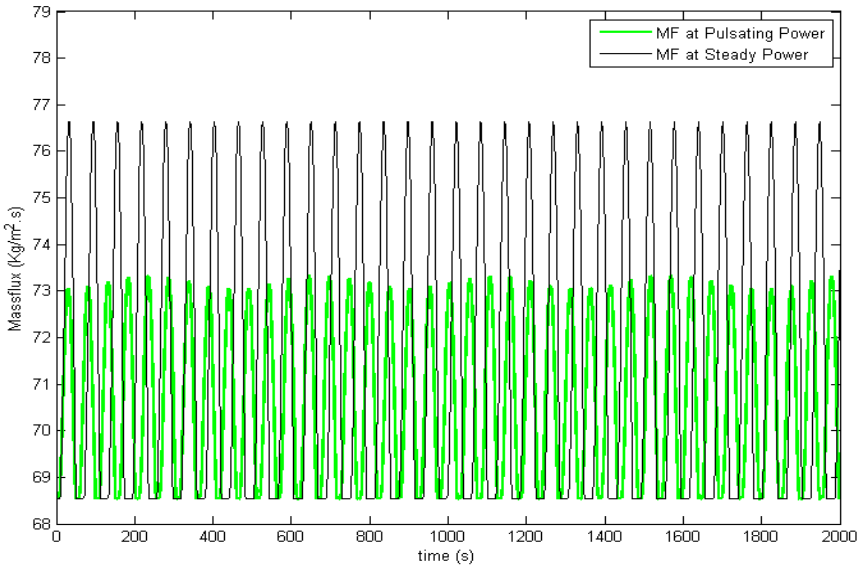

(B) Time series of mass flux under constant power vs pulsating power

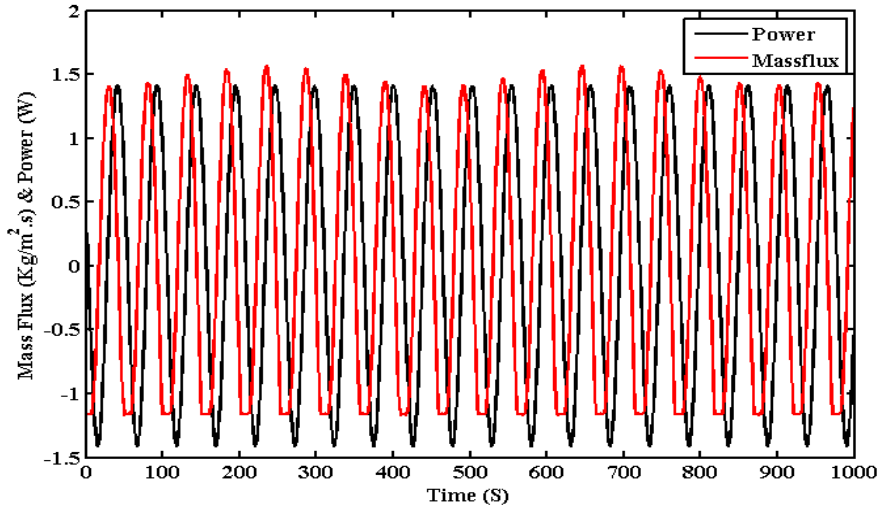

(C) Time series of mass flux and pulsating power

Figure 42: *System dynamics for base input power of 700W at 10% amplitude and frequency ratio 1.20*

When the amplitude of the external forcing is increased, the phase locking regime extends as we see the system showing synchronous behaviour at further values of forcing frequency both less than and more than the natural frequency. The system shows frequency locking for forcing frequency ratio as low as 0.45 and as high as 1.50 for 675 W input power applied at 10% fluctuation as seen in Fig 23 and Fig 26. This might be because at low input power level, an external forcing oscillator having significantly high forcing amplitude can influence the dynamics of an oscillator easily for a larger range of forcing frequency around the natural frequency of the system.

The observed dynamics of the mass flux oscillation can be presented in a 1:1 forced synchronous map by changing the forcing frequency ratio and amplitude of power perturbation.

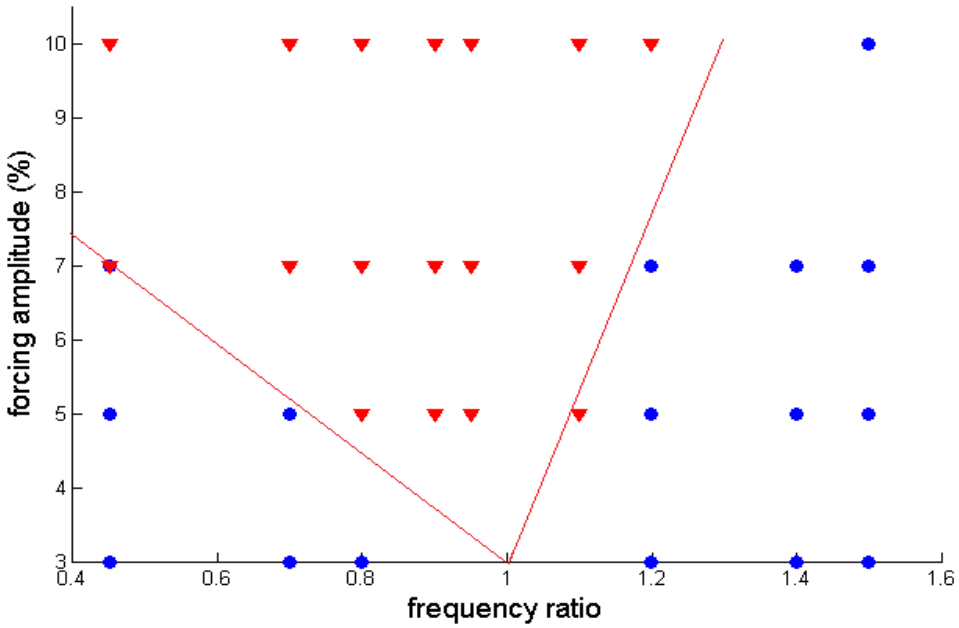

Figure 43: *Forcing amplitude vs frequency ratio plot for input power of 675W*

In Fig 43 and Fig 44 we get a V-shaped map, centred on the natural frequency known as the Arnold tongue in synchronization theory for 675 W and 700 W input power respectively. The red points indicate phase locked condition of the system where we see synchronous behaviour of the system, while the blue points indicate the non-synchronous condition. This map gives a clear idea of the extent of the phase locking regime with respect to the forcing amplitude and frequency where a system shows synchronous behaviour. On comparing both Fig 43 and Fig 44, we see the V shape generated by the synchronous regime is steeper for 700W input power than that of 675

W. This shows that the increase in the range of the forcing frequency around the natural frequency within the phase lock regime, with increase in the forcing amplitude, is higher for systems operating at lower input power.

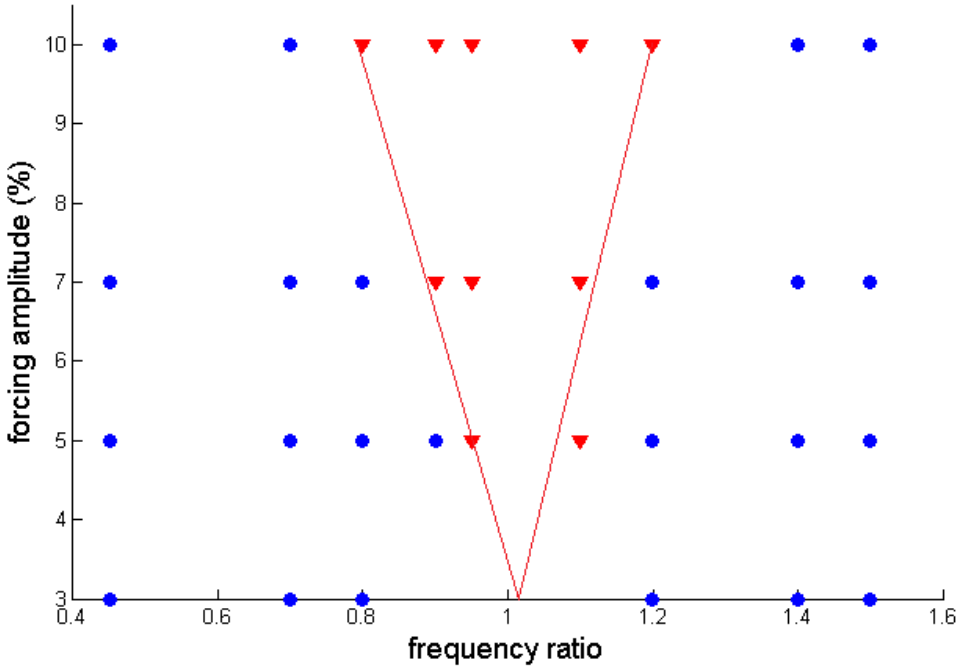

Figure 44: *Forcing amplitude vs frequency ratio plot for input power of 700W*

The external forcing also has an effect on the amplitude of the mass flux oscillation of the system. For input power of 675 W, we see an initial reduction in the amplitude during phase locking at frequency ratio of 0.45 for 7% and 10% fluctuating amplitude in Fig 20 and Fig 24, but a sudden jump in the oscillation as the forcing frequency reaches significantly close to the natural frequency, for frequency ratio equal to 0.95 and 1.20 as seen in Fig 21, Fig 22, Fig 25 and Fig 26.

The initial reduction of the amplitude of oscillations during the onset of synchronization occurs due to a phenomena identified as synchronous quenching. Within the phase locked regime, the forced oscillation amplitude demonstrates a gradual increase as the forcing frequency ratio approaches value close to 1. However, the sudden increase in oscillations occur due to resonance amplification because of close proximity of the external frequency to the natural frequency of the system, in this case almost equal to frequency ratio 0.95 to 1.10. However such observations are not recorded for 700 W input power which might indicate the requirement of higher forcing parameters to achieve similar effects at higher input power level.

CONCLUSION

The behaviour of a single-phase square NCL under an external power perturbation was studied in the current work. The observations and analysis of the results obtained showed that the system, when subjected to an external forcing behaved in agreement to the theory of synchronisation of oscillators. The region of influence of the external oscillator was predicted in the study and the variation of the dynamics with forcing amplitude and frequency was also shown. The nature of the response dynamics determined through numerical investigation of the MATLAB based Simulink model of the single-phase NCL were found to be similar to the observations reported in previous works related to synchronization of various systems.

It could be concluded from the results that systems operating at lower input power levels are easily influenced by external forcing, however, to achieve similar results regarding phase locking and modification of the response frequency or mass flux oscillation amplitude for higher input power, the operating parameters of the external forcing must be stronger as compared to lower power levels. This can be due to higher stability or robustness of the internal dynamics of a system with increasing power level.

This study hopes to create a pathway to solve the problems of instabilities in a natural circulation system using external forcing through synchronization to regulate the nature and magnitude of oscillations produced within the system, for improved application of the system.

FUTURE SCOPE

Further studies can be conducted related to the application of pulsating power on NCL especially the nature of the response dynamics when external forcing is applied to a chaotic system which might address many real-life challenges in the application of such a system. The effects of the power perturbation can also be studied by changing operating parameters, orientation and components of the loop to get an overall idea of the behaviour of the natural circulation system.

REFERENCES

1. M. Misale, (2014, May). Overview on single-phase natural circulation loops. In *Proc. of the Intl. Conf. on Advances In Mechanical And Automation Engineering–MAE,* **Vol. 2014**.
2. S. M. Seyyedi, N. Sahebi, A. S. Dogonhi, M. Hasemi-Tilehnoee, (2018). Numerical and experimental analysis of a rectangular single-phase natural circulation loop with asymmetric heater position. *International Journal of Heat and Mass Transfer* **130**,1343-1357.
3. L. Wu, Y. Liu, H. J. Jia, J. Wang, (2017). Innovative flow-resistance performance in the single-phase natural circulation loop and relevant experiment verification. *International Journal of Heat and Mass Transfer* **107**, 66-73.
4. L. Luzzi, M. Misale, F. Devia, A. Pini, M. T. Cauzzi, F. Fanale, A. Cammi (2017), Assessment of analytical and numerical models on experimental data for the study of single phase natural circular dynamics in a vertical loop, *Chemical Engineering Science* **162,** 262-282.
5. P. K. Vijayan, H. Austregesilo (1994), Scaling laws for single-phase natural circulation loop, *Nuclear Engineering and Design* **152**, 331-347.
6. B. T. Swapnalee, P. K. Vijayan (2011), A Generalised flow equation for single-phase natural circulation loops obeying multiple friction laws, *International Journal of Heat and Mass Transfer* **54**, 2618-2629.
7. D. N. Basu, S. Bhattacharyya, P. K. Das (2013), Dynamic response of a single-phase rectangular natural circulation loop to different excitations of input power, *International Journal of Heat and Mass Transfer* **65**, 131-142.
8. D. N. Basu, S. Bhattacharyya, P. K. Das (2008), Effect of geometric parameters on steady-state performance of single-phase NCL with heat loss to ambient, *International Journal of Thermal Sciences* **47**, 1359–1373.
9. R. Saha, K. Ghosh, A. Mukhopadhyay, S. Sen (2018), Dynamic Characterization of a single phase square natural circulation loop, *Applied Thermal Engineering* **128**, 1126-1138.

10. N. Goudarzi, S. Talebi (2018), Heat removal ability for different orientations of single-phase natural circulation loops using the entransy method, *Annals of Nuclear Energy* **111**, 509-522.
11. H. Cheng, H. Lei, C. Dai (2017), Heat Transfer of a single-phase Natural Circulation Loop With Heating and Cooling Fluids, *Energy Procedia* **142**, 3926-3931.
12. M. Misale (2016), Experimental study on the influence of power steps on the thermohydraulic behaviour of a natural circulation loop, *International Journal of Heat and Mass Transfer* **99**, 782-791.
13. P. K. Vijayan, H. Austregesilo, V. Teschendorff (1995), Simulation of unstable oscillatory behaviour of single-phase natural circulation with repetitive flow reversals in a rectangular loop using computer code ATHLET, *Nuclear Engineering and Design* **155**, 623-641.
14. L. K. B. Li, M. P. Juniper (2013), Lock-in and quasiperiodicity in hydrodynamically self-excited flames, *Proceedings of the Combustion Institute* **34**, 947-954.
15. E. M. Dewan (1972), Harmonic Entrainment of van der Pol Oscillations: Phaselocking and Asynchronous Quenching, *IEEE Transactions on Automatic Control,* Vol. **AC-17,** No 5.
16. M. Čercek, T. Gyergyek, M. Stanojević (1996), On the non-linear dynamics of an instability in front of a positively biased electrode in a magnetised plasma, Nuclear Society of Slovenia 3rd Regional Meeting, 19th September, 531-538.
17. Y. Guan, V. Gupta, K. Kashinath, L. K. B. Li (2019), Open loop control of periodic thermoacoustic oscillation: Experiments and low order modelling in a synchronization framework, *Proceedings of the Combustion Institute* **37**, 5315-5323.
18. M. Murugesan, Y. Zhu, L. K. B. Li (2019), Complex network analysis of forced synchronization in a hydrodynamically self-excited jet, *International Journal of Heat and Fluid Flow* **76**, 14-15.
19. Y. Guan, M. Murugesan, L. K. B. Li (2018), Strange nonchaotic and chaotic attractors in a self-excited thermoacoustic oscillator subjected to external periodic forcing, *Chaos* **28**, 093109 1-12.

20. K. Kashinath, L. K. B. Li, M. P. Juniper (2018), Forced synchronization of periodic and aperiodic thermoacoustic oscillations: Lock-in, bifurcation and open-loop control, *Journal of Fluid Mechanics* **838**, pp 690-714.

21. S. Mondal, S. A. Pawar, R. I. Sujith (2019), Forced synchronization and asynchronous quenching of periodic oscillations in a thermoacoustic system, *Journal of Fluid Mechanics* **864**, pp 73-96.

22. R. Saha, S. Sen, S. Mookherjee, K. Ghosh, A. Mukhopadhyay, D. Sanyal, (2015). Experimental and Numerical Investigation of a Single-Phase square Natural Circulation Loop, *Journal of Heat Transfer* Vol **137**, 121010-1-121010-8.

23. D. N. Basu, S. Bhattacharya, P. K. Das, (2014). A review of modern advances in analyses and applications of single-phase natural circulation loop in nuclear thermal hydraulics, *Nuclear Engineering and Design* **280**, 326-348.

24. S. Mondal, V. R. Unni, R. I. Sujith, (2017). Onset of thermoacoustic instability in turbulent combustors: an emergence of synchronized periodicity through formation of chimera-like states, *Journal of Fluid Mechanics* **881**, pp 659- 681.

25. P. K. Vijayan, & A. K. Nayak, (2005). Natural circulation systems: advantages and challenges. *Natural Circulation in Water Cooled Power Plants*..

26. A.Pikovsky, M. Rosenblum, J. Kurths, (2002). Synchronization: a universal concept in nonlinear science.

27. A. Balanov, N. Janson, D. Postnov, O. Sosnovtseva, (2008). Synchronization: from simple to complex, *Springer Science & Business Media.*

28. R. C. Hilborn, (2000). Chaos and nonlinear dynamics: an introduction for scientists and engineers, *Oxford University Press on Demand.*

29. R. Saha, (2013). Experimental and numerical study of a single phase square natural circulation loop, M. E. thesis, Jadavpur University, India.